The 10th Seoul International Symposium on Polar Sciences

RECENT APPROACHES IN POLAR EARTH SCIENCE

October 21-23, 2003
Songdo Beach Hotel, Incheon, Korea

Editors : Yeadong Kim
Jong Ik Lee
Jae Il Lee

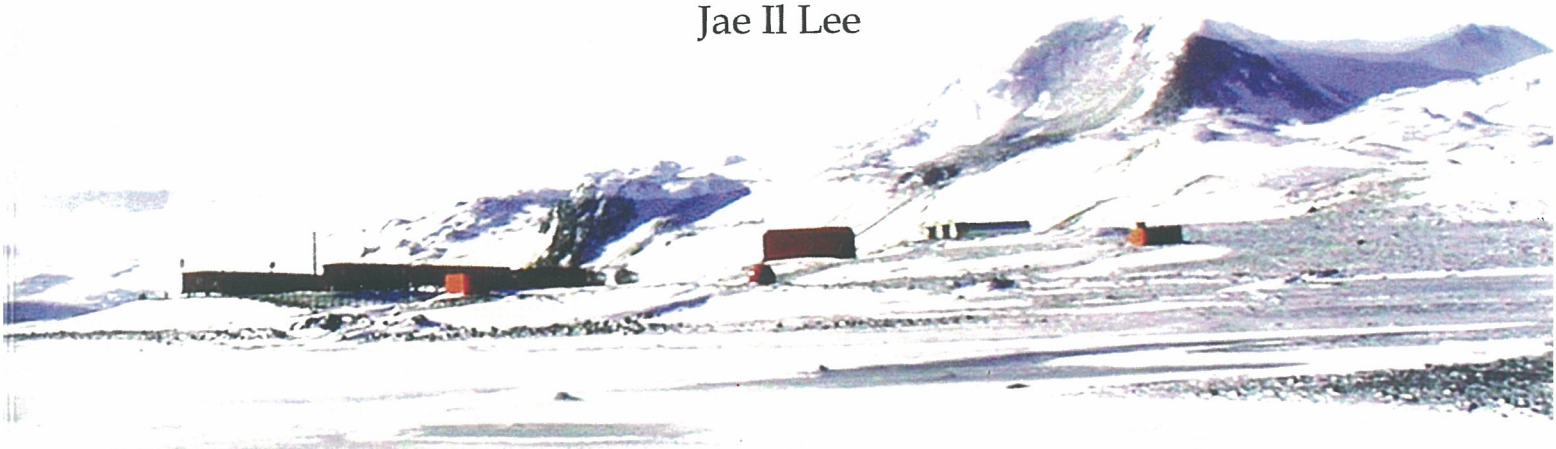

Organized by Korea Polar Research Institute, KORDI
Sponsored by Incheon Metropolitan City

The 10th Seoul International Symposium on Polar Sciences

RECENT APPROACHES IN POLAR EARTH SCIENCE

October 21-23, 2003
Songdo Beach Hotel, Incheon, Korea

Editors : Yeadong Kim
Jong Ik Lee
Jae Il Lee

Organized by Korea Polar Research Institute, KORDI
Sponsored by Incheon Metropolitan City

SCHEDULE AND CONTENTS

October 21, 2003

09:00-10:00	**Registration**		
10:00-10:30	**Opening Ceremony** (welcome speeches: Minister of Maritime Affairs and Fisheries, Major of Incheon Metropolitan City, President of KORDI)		
10:30-11:00	**Keynote Speech**		
	Byong-Kwon Park*	Polar sciences and global environmental change	1
11:00-11:15	*Coffee Break*		
Session 1: Atmospheric Science		*Chairs: Dr. Katsutada Kaminuma and Dr. Yong Il Lee*	
11:15-11:40	Niciejewski, R.J.* and Won, Y.-I.	The Sun Earth connection: thermodynamics of the terrestrial atmosphere during geo-effective events	4
11:40-12:05	Won, Y.-I*., Niciejewski, R.J., Espy, P., Chung, J.-K. and Lee, B.Y.	Observations of atmospheric waves in the high-latitude	8
12:05-12:30	Nasaruddin Rahman*, Salleh Mohd Nor and Azizan Abu Samah	Malaysian Antarctic Research Program	12
12:30-13:40	*Lunch*		
Session 2: Petrology and Sedimentology		*Chairs: Dr. Diedrich Fritzsche and Dr. Moon Young Choe*	
13:40-14:05	Lee, M.J.*, Williams, C.T., Lee, J.I. and Kim, Y.	Compositional variation in pyrochlore from the Sokli phoscorite-carbonatite comlex, Kola Peninsula, Arctic	14
14:05-14:30	Motoyoshi, Y.*, Hokada, T. and Shiraishi, K.	U-Th-Pb electron microprobe datings on the Rayner Complex, East Antarctica	18
14:30-14:55	Hur, S.D.*, Lee, J.I. and Hwang, J.	Geochemical variation during hydrothermal alteration of basaltic andesite at Barton Peninsula, King George Island, Antarctica	22
14:55-15:20	Kim, S.B.*, Sohn, Y.K. and Choe, M.Y.	The Paleocene-Eocene volcanic sucession in the Barton Peninsula, King George Island, Antarctica: lithofacies, eruption styles and depositional processes	23
15:20-15:35	*Coffee break*		
Session 3: Paleoceanography and Paleoclimatology		*Chairs: Dr. Xiaohan Liu and Dr. Sungmin Hong*	
15:35-16:00	Khim, B.K.*, Lee, K., Yoon, H.I. and Kang, C.Y.	Holocene paleoclimate in Antarctic Lake Langer (King George Island)	27
16:00-16:25	Hald, M.*, Ebbesen, H., Forwick, M., Korsun, S., Vorren, T.O., Khomenko, L. and Godtliebsen, F.	Holocene paleoceanography and paleoclimate of the West Spitsbergen area, Euro-Arctic margin	28
16:25-16:50	Yoon, H.I.*, Park, B.-K., Kim, Y., Kang, C.Y. and Kang, S.-H.	Origins and paleoceanographic significance of layered diatom ooze interval from the Bransfield Strait in the northern Antarctic Peninsula around 2500 yrs BP	32
16:50-17:15	Tatur, A*., del Valle, R., Barczuk, A., and Martinez-Macchiavello, J.	A record of Holocene environmental changes in terrestrial sedimentary deposits on King George Island, Antarctica	33
17:15-17:40	Lee, Y.I.*, Lim, H.S. and Yoon, H.I.	Geochemistry of soils of King George Island, South Shetland Islands, West Antarctica: implications for pedogenesis in cold polar regions	37
19:00-	**Welcome party (sponsored by Incheon Metropolitan City)**		

October 22, 2003

09:00-09:30	**Registration**		
Session 4: Geophysics and Gas Hydrate		*Chairs: Dr. Yoich Motoyoshi and Dr Young Keun Jin*	
09:30-09:55	Nogi, Y.* and Koizumi, K.	Seafloor structure around the epicenter of the great Antarctic Plate earthquake	42
09:55-10:20	Kanao, M., Miyamachi, H., Toda, S., Murakami, H., Tsutsui, T., Matsushima, T., Takada, M., Watanabe, A., Yamashita, M., Yoshii, K., Kaminuma, K.* and SEAL Geotransect Group	Multidisciplinary surveys by 'Structure and Evolution of the East Antarctic Lithosphere' : SEAL-2000, -2002	44
10:20-10:45	Kaminuma, K.* and Kanao, M.	Local seismic activity around Syowa Station, East Antarctica	46
10:45-11:00	*Coffee break*		
11:00-11:25	Kim, K.J.*, Jin, Y.K., Nam, S.H., Lee, J.H. and Kim, Y.	Morphological characteristics of the intersection between Phoenix Ridge and the Hero Fracture Zone	47
11:25-11:50	Shoji, H.*	Visual observation experiments to investigate the formation processes of globular gas hydrate	51
11:50-12:15	Jin, Y.K.*, Nam, S.H., Kim, Y., Kim, K.J. and Lee, J.H.	Gas Hydrate BSR-derived heat flow variation on the South Shetland continental margin, Antarctic Peninsula	54
12:15-13:40	*Lunch*		
Session 5: Glaciology		*Chairs: Dr. Morten Hald and Dr. Ho Il Yoon*	
13:40-14:05	Li Y.*, Tan, D., Pan, Z., Dong, Z., Sun, B. and Wen, J.	Introduction to ice core drilling program on Amery Ice Shelf in the 2002/2003 Antarctic summer season	58
14:05-14:30	Fritzsche, D.*, Schütt, R., Meyer, H., Miller, H., and Wilhelms, F.	724m deep ice core from Akademii Nauk ice cap Severnaya Zemlya (Russian Arctic) - electrical conductivity measurements and isotopic record	60
14:30-14:55	Qin, X.*, Qin, D. and Ding, Y.	Introduction of the Chinese Polar Cryospheric Database System (CPCDS)	62
14:55-15:10	*Coffee break*		
15:10-15:35	Hong, S.*, Lee, K.H., Boutron, C.F., Ferrari, C.P., Petit, J.R., Barbante, C., Rosman, K. and Lipenkov, V.Y.	Natural variations in lead, cadmium, copper and zinc concentrations and their sources in Vostok Antarctic ice from 65,000 to 240,000 years BP	63
15:35-16:00	Liu, X.*, Kong, P., Huang, F., Li, X. and Fang, A.	Fluctuation of ice sheet elevation in East Antarctica since the Late Pliocene	66
Poster Session		*Chairs: Dr. Jong Ik Lee and Dr. Jae Il Lee*	
16:00-17:30	Lee, B.Y.*, Cho, H.-K., Lee, Y.-G. and Won, Y.-I.	Variations of total ozone amount and erythemal ultraviolet radiation at King Sejong Station in West Antarctica	67
	Lee, J.-S.*, Kwon, T.-Y., Lee, B.Y., Yoon, H.I. and Kim, J.-W.	Variability of regional atmosphere circulation related with recent warming in the Antarctic Peninsula	72
	Lee, K.-T.*, Jee, J.-B., Lee, W.-H., Kim, Y.-J., Lee, B.Y. and Won, Y.-I.	The Surface UV-A and erythemal UV-B radiation changes at King Sejong Station of West Antarctica	75
	Kwak, Y.-S.* and Ahn, B.-H.	Climatological characteristics of the polar ionosphere based on the Sondrestrom and Chatanika Incoherent Scatter radar measurements	77

	Jeong, G.Y. and Lee, B.H.*	Chemical weathering of glacial debris and volcanic ash in King George Island, Antarctica	135
	Fang, A., Liu, X.*, Li, X., Lee, J.I., Ju, Y. and Huang, F.	The Cenozoic sedimentary records found in the Grove Mountains, East Antarctica and their climatic implications	137
	Fang, A., Liu, X.*, Li, X., Ju, Y. and Wang, W.	The pollen assemblages in the Cenozoic sedimentary rocks in Grove Mountains, East Antarctica	139
17:00-18:30	**KONPOR (Korea National Committee on Polar Research) meeting**		
19:00-	**Farewell Party (sponsored by KORDI)** **Celebration on the occasion of the 15th anniversary of the King Sejong Station**		

The 10th Seoul International Symposium on Polar Sciences
October 21-22, 2003, Incheon, Korea

KEYNOTE SPEECH:

POLAR SCIENCES AND GLOBAL ENVIRONMENTAL CHANGES

Byong-Kwon Park

Chairman, Korea Research Council of Public Science and Technology
1376-1 Seocho 2-dong, Seocho-gu, Seoul 137-072, Korea [bkpark@korp.re.kr]

Good morning! Ladies and gentlemen!

I am very honored to have this opportunity to share some of my thoughts on 『Polar Sciences and Global Environmental Changes』 at this 10th International Seoul Symposium on Polar Sciences. Last year, in addition to 『King Sejong』 Antarctic station, the 『DASAN』, Korean Arctic Station was established at Ny-Ålesund on the high Arctic island of Spitsbergen, part of the Svalbard Archipelago, and the Arctic Research Program was launched to increase our understanding on this complexity of this earth through studies on both polar systems.

I believe KARP, now appropriately abbreviated for the Korea Antarctic and Arctic Research Program, has contributed much in the polar sciences community including publishing numerous papers on various polar subjects as well as expanding scientific knowledge on past, present and possible future global environmental changes.

However KARP needs to exert more of its strength and influence to expand and contribute to the international scientific community and tax payers in Korea as they become part of this global community. I believe this symposium is making a headway in this direction undertaking KARP's scientific spirit for discovering and sharing detailed scientific knowledge of polar frontier.

As we all know, the polar region was the target for human exploration activities in early days to satisfy human curiosity about unknown world. However, since IGY program was launched for Antarctica in 1957, the scientific activities accelerated resulting in many great scientific discoveries. Dr. Kaminuma of NIPR, noted in his book such discoveries as Antarctic meteorites, ozone hole and Vostok subglacial lake as some of great scientific results from Antarctic studies. And, these exploration and discovery still continues because as polar regions reveal their secrets to us, the scientists, our insatiable curiosity, especially our explorative scientific mind still want more from these wintry regions.

However, what about our tax payers and average citizens? Are they interested in scientific curiosity? May be, but mostly likely, they are more curious about nature itself. They want to see

how Antarctica and Arctic look. Average tax-paying citizens also want to satisfy their curiosity, curiosity toward unknown nature itself than scientific curiosity. They want to go to these polar regions. They want to see. They want to tour. And, as we all know, polar tourism industry is booming.

Here, we face issues and conflicts in conservation and preservation. But I believe that there is no such thing as exclusive science with support from our tax payers. We have to find a way to gratify out inquisitive tax payers in order to satisfy our scientific curiosity. Because, polar regions do not exist exclusively for scientists. They are part of common heritage of humankind.

I believe, time has come to seriously consider how these two can exist collectively. Collect existence in the polar regions is possible through joining science with tourism instead of excluding each other. Tourism can be used to help science. If average citizens visit polar regions in managed way, they probably go back to their homeland with much understanding in importance of polar region. And then, we can confidently demand their understanding and support. Therefore, we have to find a way to submerge polar tourism into science.

We are living in unusual time where the twentieth century was dominated by universal warming. However, the data obtained through modern instruments are very limited in temporal perspective and provide only a glimpse on present climate. How unusual was the twentieth century compare to longer-term context of climate in the past centuries or last millennia?

Records of climate variability and forcing mechanisms of recent uniformitarian past can help scientists to establish how the climate system varied under natural conditions before significant anthropogenic effect. And, the natural forcing mechanisms will be a undeniable part of future climate variation, so, regardless of human impact on climate, it is essential to understand the truth about underlying background story of forcing and responding climate system.

Major sources of information on the climate for the last millennium include historical documentary records, tree rings, ice cores, corals, varved lake and marine sediments.

These examples are all paleoclimate, especially polar-related proxies often providing continuous records with annual to decal resolution. Other information may be obtained from sources that are not time continuous and have less strict chronological control, such as geomorphological evidence and macrofossils.

As you have seen many times, greenhouse gas level is rapidly increasing and is now much higher than they have been for at least 420,000 years. In addition, modern global average temperature surpasses anything seen in the last thousand years. And, the evidence is now strong enough that much of this rapid change is the result of human activities. But these changes are superimposed on underlying natural variations. And, as I have briefly mentioned before, climate

changes are also driven by external factors such as variation in solar output and internal factors like volcanic eruptions.

Then, how can we distinguish the human impact from the natural changes? What changes would wait for the future of mankind as population pressure grows, as fossil fuel consumption increases and as land cover is altered? How would climate respond? What about the polar regions? And, would mankind acclimate to these changes fast enough to adapt to survive and prosper?

Such questions are compelling as survival of mankind depend on them. And the need for answers is urgent. But the search for answers will only be successful when we have developed insight and detailed scientific knowledge into the full range of natural variability of the climate system and its control factors. The range is illustrated by the events of the past, and it is only by unravelling these events that we will be able to predict and prepare for the future with some confidence.

In conclusion, global environmental change research program, especially paleoclimatic research based on polar proxies, has revealed an astonishing picture of past changes in the earth system. Over the last 2 million years, climate has varied widely from ice ages to warm interglacials. All of these studies remind us that our modern perspective on the climate system provides a totally inadequate perspective on its real variability. The message from the paleorecords is that change is normal and the unexpected can happen.

The issue of climate variability and change, the level and potential affects of human contributions to these issues, and how we adapt and manage our response is a capstone issue for our generation and those to follow.

The 10th Seoul International Symposium on Polar Sciences
October 21-22, 2003, Incheon, Korea

THE SUN EARTH CONNECTION: THERMODYNAMICS OF THE TERRESTRIAL ATMOSPHERE DURING GEO-EFFECTIVE EVENTS

R.J. Niciejewski[1] and Y.-I. Won[2]

[1] Space Physics Research Laboratory, The University of Michigan, Ann Arbor, MI 48109, USA
[niciejew@umich.edu]
[2] Korea Polar Research Institute, Korea Ocean Research & Development Institute, Ansan 425-170, Korea

INTRODUCTION

Over the past several decades, it has become increasingly clear that solar storms have had an impact on human activity, especially those activities related to technology and orbital space resources. A particularly egregious example involves the events surrounding the March 1989 storm (Allen et al., 1989). On March 6, 1989, a large and complex sunspot group that had rotated into Earth view produced the first of several very powerful X-ray flares. From March 6 to March 19, this sunspot group produced 11 large X-class X-ray flares and 48 M-class flares with many associated terrestrial consequences. Aurora was observed at unusual locations: the Tropic of Capricorn in Australia, Grand Cayman Island in the Caribbean Sea. A long lasting 'Polar Cap Absorption' event occurred as well as a significant decrease in the cosmic ray flux, a Forbush event. The terrestrial ionosphere was greatly disturbed, resulting in one of the most magnetically disturbed periods since record keeping began in the mid-nineteenth century.

In terms of societal consequences, there were many problems with operational satellites. The solar events heated the terrestrial upper atmosphere, increasing the density at high altitudes, which caused orbital perturbations for many satellites due to increased drag. The NASA SMM satellite was reported to have dropped three miles during the disturbed period. Many navigation systems failed and there were many problems with telecommunications. There were concerns relating to the launching of the shuttle Discovery during March 1989.

The currents generated by the aurora associated with the storms on March 13/14, 1989, caused serious power failures. The electrical power grid in Quebec Canada failed affecting six million subscribers for nine hours during the morning rush hour. There were also failures in Scandinavia. There were increased concerns regarding pipeline corrosion due to these currents. Geophysical exploration survey work was disrupted. A magnetic declination change of six degrees was reported, affecting aircraft navigation systems. Finally, microchip production facilities in northeastern USA

were forced to curtail operation several times due to the enhanced auroral storming.

As society continues to rely more on advanced electronics and satellite technology, the susceptibility to major impacts on systems and the human population due to solar storms increases. It is important that the global community learn to live with the sun and its associated solar storming. A major component of this strategy is to be able to monitor space weather and to understand the effects of the geo-effectiveness of the sun on the Earth. The upper atmosphere is the most sensitive region of the Earth to solar modulations and is the region that will be affected first. In particular, the terrestrial magnetic field is oriented such that the upper atmosphere at high latitudes is open to solar forcing. This paper will describe research performed by the University of Michigan and the Korea Ocean R & D Institute to better understand the polar upper atmosphere.

FACILITIES

The University of Michigan has monitored the Earth's upper atmosphere since rockets became available to scientists following the end of the Second World War. Swapping out explosive payloads for scientific experiments in captured German V-2 rockets provided the earliest opportunities to explore the ionosphere and upper thermosphere. These early results indicated that the electron temperature greatly exceeded the neutral temperature at high altitudes, a highly controversial result at that time (Brace et al., 1963). Recent experiments have been primarily devoted to documenting and understanding the thermodynamics in the various temperature regimes of the upper atmosphere: the stratosphere (~10 to 50 km), the mesosphere (~50 to 80 km), and the

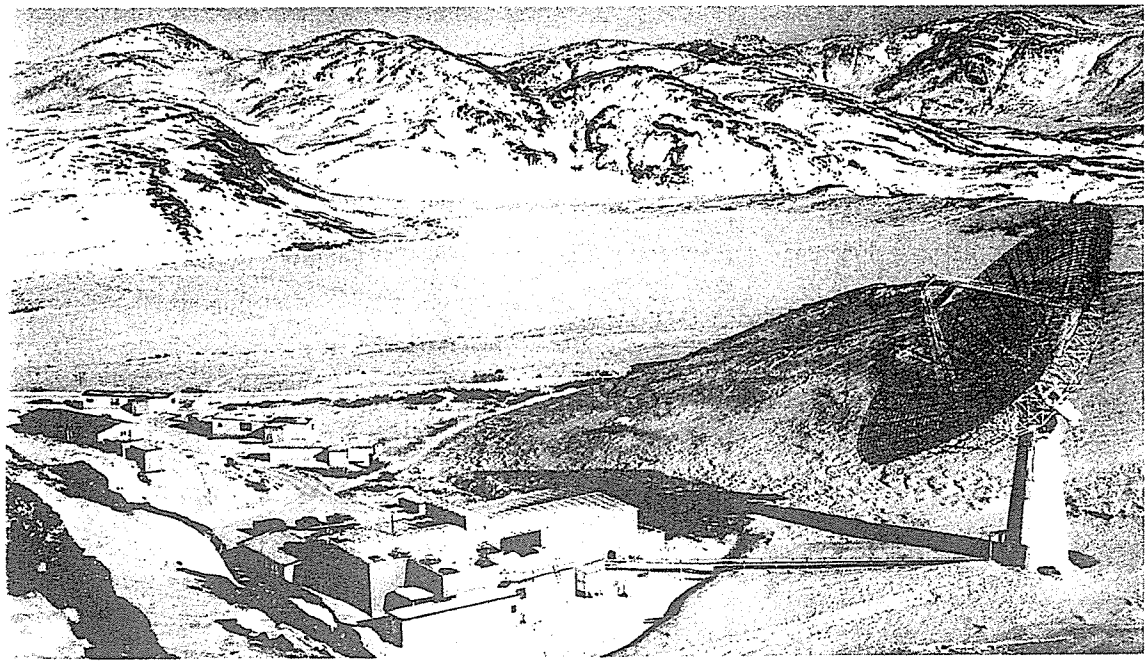

Figure 1. The NSF aeronomy laboratory at Kangerlussuaq, Greenland

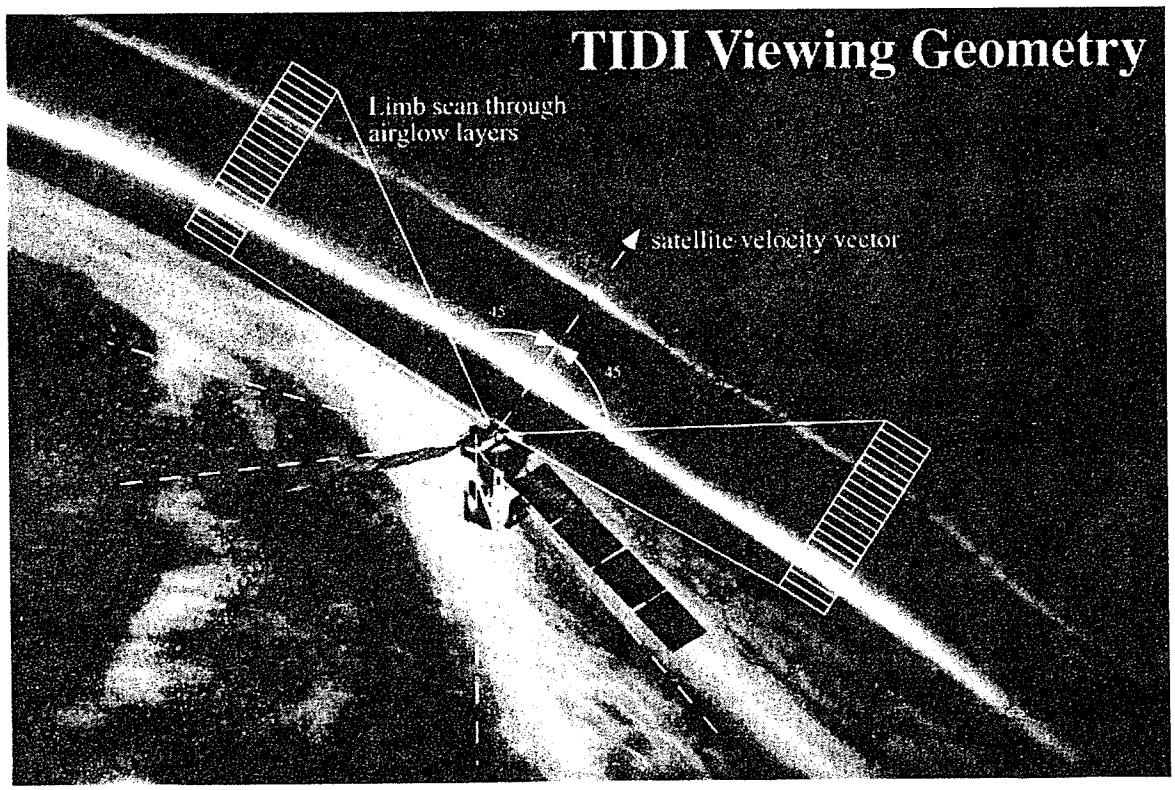

Figure 2. The viewing geometry of the TIDI instrument aboard the TIMED satellite.

thermosphere (above ~80 km).

Figure 1 provides a view of the aeronomical observatory at Kangerlussuaq, Greenland. The observatory is located at 67 degrees N, 50 degrees W in western Greenland, near the Arctic Circle. The main instrument at the observatory is an incoherent scatter radar that is used primarily to monitor the Earth's ionosphere. The large building to the left of the radar houses a full complement of optical diagnostic devices that monitor the Earth's neutral atmosphere. The University of Michigan has maintained a Fabry Perot interferometer (Niciejewski et al., 1994) at the observatory since its inception in 1983. This experiment measures the winds and temperatures in the lower and upper thermosphere. Other instruments that have been deployed in Greenland at Kangerlussuaq and at other sites include a Michelson interferometer to observe the mesosphere, an all-sky imager to monitor airglow and auroral morphology and spectrometers and photometers to monitor auroral emissions.

The University of Michigan has monitored the upper atmosphere from space for several decades. The most recent experiment is shown in Figure 2, which provides a view of the TIDI instrument aboard the TIMED satellite.

TIMED was launched on December 7, 2001, into a 74 degree inclination circular orbit with an altitude of 625 km. The TIDI (Thermosphere Ionosphere Doppler Interferometer) instrument observes limb airglow emissions with extremely high spectral resolution (Killeen et al., 1999). The

experiment measures simultaneously the line of sight neutral winds and temperatures at four limb positions, at orthogonal directions 45 degrees away from the satellite velocity vector. By combining fore and aft views, horizontal wind vectors may be constructed. The field of view is roughly rectangular, 2.5 by .05 degrees, with the long axis coincident with the limb. Altitude scanning is accomplished by moving each of four telescopes over tangent limb heights from 60 to 180 km, choosing the appropriate airglow filter for different altitude regions. The high inclination orbit allows TIDI to observe the upper atmosphere over all latitudes from north pole to south pole.

This paper will describe the capabilities of these instruments and new measurements from space and from ground dealing with the thermodynamics of the upper atmosphere. Since the launch of TIMED, there have been several moderate geo-effective storms which have impacted the Earth, specifically the period around April 20, 2002, and the period near May 29, 2003. The first event has been the subject of intense study within the aeronomical community (Niciejewski et al., 2003) and continues to be a model for the NASA Sun-Earth Connection project, the complete specification of a geo-effective solar storm from its eruption on the sun, its travel through interplanetary space, and finally to its consequences on Earth.

REFERENCES

Allen, J., L. Frank, H. Sauer, and P. Reiff, Effects of the March 1989 solar activity, EOS, 70, 1479, 1989.

Brace, L. H., Spencer, N. W., and Carignan, G. R., Ionosphere electron temperature measurements and their implications, J. Geophys. Res., 68, 5397, 1963.

Killeen, T. L., W. R. Skinner, R. M. Johnson, C. J. Edmonson, Q. Wu, R. J. Niciejewski, H. J. Grassl, D. A. Gell, P. E. Hansen, J. D. Harvey, and J. F. Kafkalidis, TIMED Doppler Interferometer (TIDI), SPIE, 3756, 289, 1999.

Niciejewski, R., T. L. Killeen, and M. Turnbull, Ground-based Fabry-Perot interferometry with a bare charge-coupled device: remote field site deployment, Opt. Eng., 33, 465, 1994.

Niciejewski, R., and the TIDI/MF and Meteor Radar Team, Neutral wind observations during the April 2002 storm period, spring AGU, Nice, April, 2003.

The 10th Seoul International Symposium on Polar Sciences
October 21-22, 2003, Incheon, Korea

OBSERVATIONS OF ATMOSPHERIC WAVES IN THE HIGH-LATITUDE

Y.-I. Won[1], R.J. Niciejewski[2], P. Espy[3], J.-K. Chung[1] and Bang Yong Lee[1]

[1] Korea Polar Research Institute, Korea Ocean Research & Development Institute, Ansan 425-170, Korea
[yiwon@kordi.re.kr]
[2] Space Physics Research Laboratory, The University of Michigan, Ann Arbor, MI 48109, USA
[3] British Antarctic Survey, Cambridge, CB3 0ET, UK

INTRODUCTION

The principal dynamic features of the lower thermosphere and upper mesosphere (MLT) regions are the tides and gravity waves. These oscillations, excited in the troposphere, stratosphere, and lower mesosphere, mostly propagate upwards and their amplitudes grow exponentially until they reach an altitude where dissipation starts to play a dominant role. The internal gravity waves are known to break near and below this atmospheric layer, resulting in large energy deposition (Andrews et al., 1987). Until recently, this region, between roughly 80-150 km altitudes, was the least understood of all atmospheric regions due, in part, to its inherent complexity and due, in part, to the difficulty of carrying out in-situ measurements at this altitude. The complexity and the variability come from a mixture of propagating tides, gravity waves of multiple origin, planetary waves within this region, and in-situ forcing from solar heating. The lower thermosphere and upper mesosphere region is too high for balloon measurements and too low for in-situ observations by long-lived satellites without on-board propulsion, therefore the data base is exceptionally sparse.

Recently, there has been a marked improvement in the techniques for measuring the MLT region by observing a number of airglows emitted from various atmospheric species, such as OH, O_2, O and Na. The mesospheric OH nightglow emission rate and temperature fluctuations induced by tides and gravity waves have been the subject of numerous theoretical and experimental investigations (Smith et al., 2000; Walterscheid and Schubert, 1995; Walterscheid et al., 2001).

INSTRUMENT

The Polar Sciences Laboratory at KORDI has been involved in performing ground-based optical observations of terrestrial nightglow emission using a FTS (Won et al., 2001). The FTS system (MR 160) was obtained from Bomem Inc., and employs a thermoelectrically cooled InGaAs detector with maximum sensitivity in the wavelength region 1.0 to 1.65 μm. For our study,

temperature measurements were determined from three rotational features of the Meinel OH (3-1) and OH(4-2) bands. The instrument could not resolve the lambda doublets, but these are not essential to the analysis.

The system provides 5 choices of spectral resolution that can be selected manually. Increasing the spectral resolution compromises temporal resolution: for the current study, we chose 8 cm^{-1} as the unapodized spectral resolution, sufficient to resolve individual rotational P-lines. With this resolution, the interferometer records an interferogram every 5 seconds. Co-addition of interferograms (50) was used to increase the signal-to-noise ratio. The composite interferogram was then apodized using a simple cosine-apodization function in order to reduce the ringing (Gibbs phenomenon) associated with the Fourier transform. The relative spectral response of the detector is determined by calibration with a low brightness source that is integrated with the experiment. This source has been calibrated against an intensity standard permitting absolute intensity determinations of atmospheric emissions.

Rotational temperature was retrieved from a least squares fit to the calibrated intensity distribution of three rotational lines. The rotational lines were assumed to have intensities that conform to a Boltzmann distribution of excited OH amongst the rotational levels of a vibrational state. The analysis also provides the intensity of the vibrational level. The detailed procedure for the analysis of OH rotational temperature and band intensity was based on Hecht et al. (1987).

RESULTS

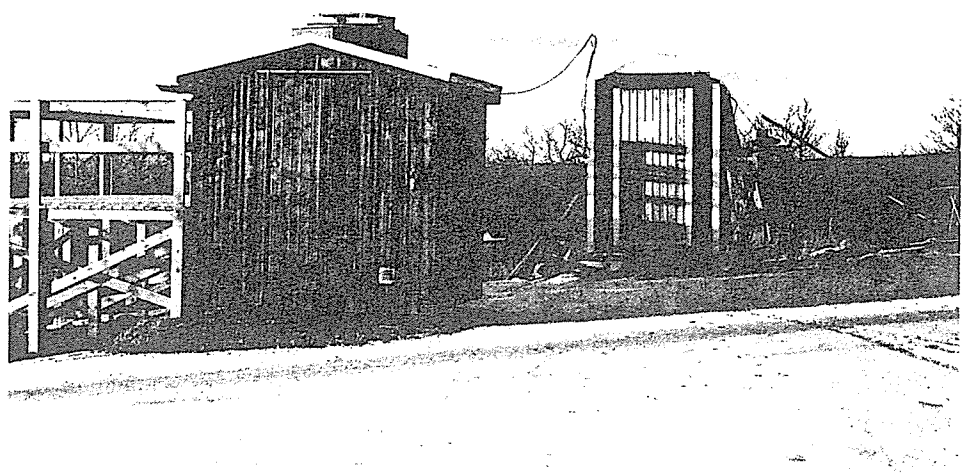

Figure 1. The Optical Observatory housing IR Spectrometer at Esrange, Kiruna, Sweden.

Upper mesospheric rotational temperatures have been derived from measurements of the hydroxyl nightglow emissions using the ground-based near IR spectrometer. The Spectrometer has been operated in King Sejong station for two year period from 1999 and after a brief modification for automatic and remote operation, was moved to Kiruna, Sweden (67.90°N, 21.10°E) in 2001 (Figure 1). During this system upgrade, the system was tested in Chungwon (36.6° N, 127.3° E), Korea for several months.

Figure 2 shows an example of the measured data on the night of May 17, 2001 at Chungwon, Korea. The composite plot shows a coherent variation both in the temperature and intensity, suggesting the modulation of OH chemical and dynamical processes around the mesopause. Various waves were observed from the observed temperature and airglow intensity variation and some of results will be presented in this paper.

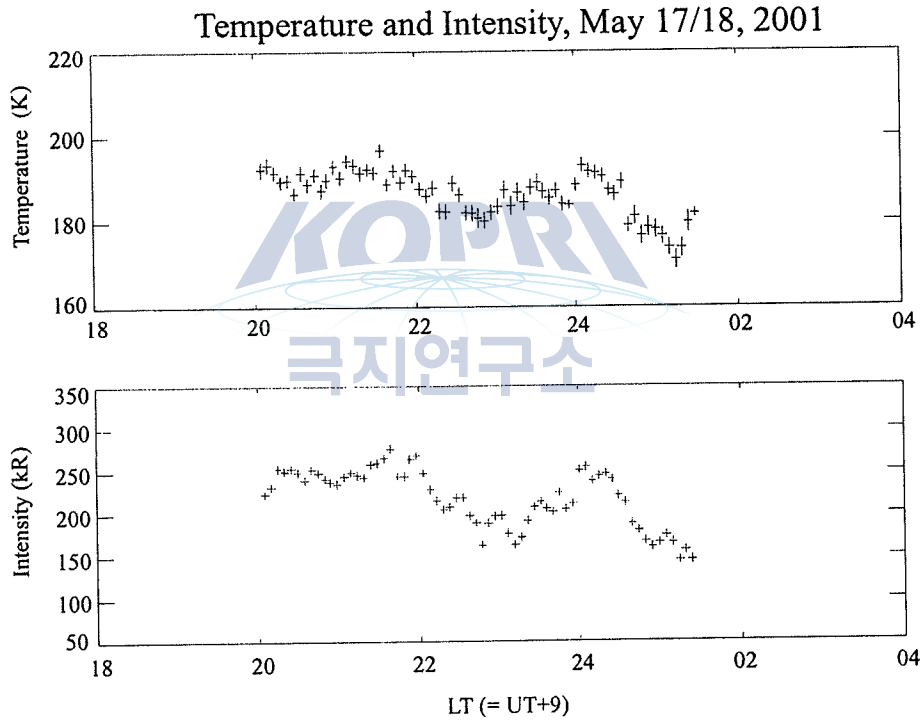

Figure 2. A composite plot of rotational temperatures and intensities measured on the night of May 17, 2001, with error bars superimposed.

REFERENCES

Andrews, D. G., J. R. Holton, and C. B. Leovy, 1987: Middle Atomosphere Dynamics, Academic Press

Hecht, J. H., R. L. Walterscheid, G. G. Sivjee, A. B. Christensen, and J. B. Pranke, Observations of Wave-

Driven Fluctuations of OH Nightglow Emissions From Søndre Strømfjord, Greenland, *J. Geophys. Res.*, 92, 6091, 1987.

Smith, S. M., M. Mendillo, J. Baumgardner, and R. R. Clark, 2000: Mesophspheric gravity wave imaging at a subauroral site: First results from Millstone Hill, J. Geophys. Res. 105, 27119-27130

Walterscheid, R. L., and G. Schubert, 1995: Dynamical-chemical model of fluctuations in the OH airglow driven by migrating tides stationary tides, and planetary-waves, J. Geophys. Res., 100 (A9), 17443-17449

Walterscheid, R. L., G. Schubert, and D. G. Brinkman, 2001: Small-scale gravity waves in the upper mesosphere and lower thermosphere generated by deep tropical convection, J. Geophys. Res., 106, 31825-31832

Won, Y.-I., Y.M. Cho, and R. J. Niciejewski, and J. Kim, 2001: Observations of OH(3,1) airglow emission using a michelson interferometer at 62°S, Adv. Space Res. 25, 1165-1170

MALAYSIAN ANTARCTIC RESEARCH PROGRAM

Nasaruddin Rahman[1], Salleh Mohd Nor[2] and Azizan Abu Samah[3]

[1] Scientific Officer, Academy of Sciences Malaysia, Kuala Lumpur [nasa@akademisains.gov.my]
[2] Chairman of the Academy of Sciences Malaysia Task Force on Antarctica
[3] Technical Coordinator, Malaysian Antarctic Research Program

This paper outlines the development of the Malaysian Antarctic Research Program with emphasis on the research interest and its management since the first expedition of the Malaysian scientists to Antarctica in 1999.

In 1997, the Malaysian Cabinet approved for Malaysia's involvement in scientific research in Antarctica. The Academy of Sciences Malaysia (ASM) was given the task to coordinate and plan Malaysia's research in Antarctica and it was decided that the Program should concentrate its research on two fields namely Atmospheric Sciences and Biological Sciences. The first team of Malaysian scientists left for Scott Base, Antarctica in October, 1999 to study the long range transport of biomass burning aerosols : characterization of particulates in the atmosphere.

Since the first research expedition, the Program has made good progress and in the 8th Malaysian Plan (2001-2005), an allocation of RM 5 million was approved by the Government of Malaysia. In 2000/2001 summer season, the Program undertook two scientific expeditions, one in Scott Base and one in Casey Station. In 2001/2002 summer season, two scientific expeditions on atmospheric sciences and sea ice were undertaken in Scott Base and one expedition on biological sciences was made to Casey Station. In the summer season of 2002/2003, Malaysian scientists took part in seven scientific expeditions. Up to 2002, 12 scientific research projects proposed by Malaysian scientists were approved by the Australian Antarctic Research Council, the New Zealand Antarctic Research Council and the Instituto Antarctico Argentino. These 12 projects are now funded by the Program. The projects are as follows :

1. Atmospheric Sciences
    - i. Role of Gravity Waves in the Dynamics of the Stable Boundary Layer in the Ross Ice Shelf
    - ii. Modeling and Observational Studies of Antarctic Katabatic
    - iii. Remote Sensing and Modeling of Sea Ice in the Ross Sea
    - iv. Polar Atmospheric Water Vapour/Ionospheric Sensing Using GPS
2. Biological Sciences

i. Microalgal Diversity
ii. Occurrence of Fungi in Extreme Environment
iii. Diversity of Metabolic Abilities of Antarctic Bacteria
iv. Antarctic Microbial Genomics
v. Evolution and Diversity of Antarctic Periphytic Algae
vi. Biodiversity of the Benthic Invertebrate Fauna in Antarctic Marine Ecosystem
vii. Understanding of Adaptive Mechanism Through Gene and Enzyme Studies of Antarctic Microbes
viii. Bacteria Biodegradation and Bioremediation of Hydrocarbon in Antarctic

These projects are at various stages of implementation and for each project, there is a project leader and team members who comes from various universities. To foster greater interest among Malaysian scientists and to strengthen present networking, the Program also organized international seminar on Antarctica. The next seminar will be held on 3-5 May, 2004 in Penang, Malaysia jointly organized by the Academy of Sciences Malaysia and the Universiti Sains Malaysia. The Malaysian Antarctic Research Centre was also established in August, 2002. This Centre acts as a focal point and resource centre for the Program activities. The Program has been given an observer status in the Scientific Committee on Antarctic Research (SCAR) meeting since 2000. The Academy of Sciences Malaysia has also submitted application to be associate member of SCAR which will be decided during the next SCAR Meeting in Bremerhaven next year. Due to the Program's interest and research activities, the Antarctic Treaty Consultative Parties invited Malaysia to observe the 25th and the 26th Antarctica Treaty Consultative Meetings.

Apart from research projects, the Program is now examining the Antarctica Treaty System with respect to the national stand on Antarctica. Being aware of the need to sustain Malaysia's involvement, the Program encourages young scientists to join the Program through the post-graduate scholarship. The current management structure of the Program consists of a Task Force which is chaired by Vice President of the Academy of Sciences Malaysia. The Academy serves as the secretariat. A researcher from the University of Malaya acts as the National Technical Coordinator as well as Coordinator for Atmospheric Sciences and another researcher from Universiti Sains Malaysia, the Coordinator for Biology assists the National Technical Coordinator.

Overall the Program is still at initial stage and more needs to be done to develop the national capacity and experience of doing research under different and challenging environment, thus it is crucial at this stage for Malaysia to have assistance from other countries. The Program is therefore looking at expanding its research collaboration with more countries and we would welcome collaboration with the Korean Antarctic Research Program. The expansion proposal has been submitted to the Government of Malaysia and it is likely that additional funding of RM 5 million will be approved for the Program.

The 10th Seoul International Symposium on Polar Sciences
October 21-22, 2003, Incheon, Korea

COMPOSITIONAL VARIATION IN PYROCHLORE FROM THE SOKLI PHOSCORITE-CARBONATITE COMPLEX, KOLA PENINSULA, ARCTIC

Mi Jung Lee[1], C. Terry Williams[2], Jong Ik Lee[1] and Yeadong Kim[1]

[1] Korea Polar Research Institute, KORDI, Ansan P.O. Box 29, Seoul 425-600, Korea [mjlee@kordi.re.kr]
[2] Department of Mineralogy, Natural History Museum, Cromwell Road, London SW7 5BD, U.K.

INTRODUCTION

The Sokli complex is a member among more than 24 alkaline complexes that make up the Paleozoic Kola Alkaline Province (KAP). It is located in the eastern Finish Lapland (67°48′N, 29°27′E) and intruded into an Archean Belomorian group rocks at about 360 Ma (Kramme et al., 1993). A characteristic feature of the Sokli carbonatites is spatial and temporal association with phoscorites (magnetite-apatite-forsterite-calcite rocks). Like many carbonatite complexes of the KAP, phoscorites and carbonatites at Sokli are emplaced within a plug surrounded by ultramafic rocks (Kukharenko et al., 1965; Borodin et al., 1973; Yegorov, 1993; Kogarko et al., 1995; Verhulst et al., 2000). Ultramafic rocks of the Sokli complex are largely transformed by hydrothermal processes, and their relic mineralogies suggest they should be mostly pyroxenites.

The Sokli phoscorite-carbonatite complex (PCC) is made up of several sequences of carbonatites and phoscorites. Five intrusive groups are distinguished: the first three comprise both phsocorites, referred to as P1 to P3, and their paired calcite carbonatites, C1 to C3, the last two comprise only dolomite carbonatites D4 and D5. Paired phoscorites and carbonaties share their specific mineral assemblage and chemistry.

Pyrochlore from the Sokli PCC occurs as a late-crystallizing mineral and crystallizes from stage 2 (P2C2 rocks) to the latest D5 rocks. It tells us little about the early stages directly, but it bears a lot of information about evolution of the Sokli PCC, and also segregation mechanisms between phoscorites and paired carbonatites because it is the main host for High Field Strength (HFS) elements shch as Nb, Ta, Th and U of which inter-element variation can provide important clues to trace an evolution of alkaline complexes.

We report here on the detailed mineralogy and chemistry of pyrochlore from phoscorites and carbonatites in the Sokli complex, to document the overall trend of evolution of the Sokli PCC, and to investigate the genetic relationships between the phoscorites and associated carbonatites.

COMPOSITIONS OF PYROCHLORES

Pyrochlore has the general formula A2-mB2O6-wY1-n·pH2O (where includes Na, Ca, Sr, Ba, REE, Th and U; B includes Nb, Ta, Ti, Zr and Fe; Y=O, OH or F). From the phoscorites and carbonatites at Sokli, the mineral chemistry of pyrochlore has been studied in detail, with >600 electron microprobe analyses, which have included several high resolution traverses on zoned grains.

Figure 1 illustrates the most significant chemical variations in fresh pyrochlores, from P2C2 to D5.

Early type I pyrochlore is red brown and enriched in U and Ta (up to 0.4 and 0.33 apfu). It commonly shows compositional zoning with decreasing U, Ta, Ti and increasing Th, LREE towards margins. Type I pyrochlore is found as enhedral crystals in C2 carbonatite or relic cores mantled by U-Ta poor and Th-rich (type II) pyrochlore in P2 phoscorite. Type II pyrochlore is yellow to grey, much richer in Th and LREE relative to Type I pyrochlore and still shows substantial zoning towards Ta-U depleted and Th enriched margins. This is a dominant one in P2 phoscorite, where it forms large crystals having amiboidal outlines. It may be found also in C3 carbonatite as smaller and more euhedral crystals and in the cores of pyrochlores from P3 phoscorite. The majority of pyrochlore in P3 phoscorite is a grey, turbid and nearly euhedral variety (type III) with strongly depleted in Ta-U (10-2 apfu.), but still rich in Th. Composition of the latest pyrochlore (type IV and V) is very homogeneous and close to that of an ideal pyrochlore of formula (Ca, Na)2Nb2O6(F,OH). It has the lowest contents in U, Ta and Th.

F and Sr contents continuously increase along the sequence from P2C2 to D5. La and Ce contents follow trends similar to that of Th, but the maximum enrichment is reached in type IV (D4) rather than in type III (P3).

Compared with the pyrochlores from phoscorites, the pyrochlores from paired calcite carbonatites are generally depleted in A-site cations (U and Na). This depletion is reflected in a large A-cation deficiency, which is related with abundant internal fractures and a pattern of patch alteration, clearly observed in secondary electron images. These A-site cation deficient parts occasionally have high Ba content (up to 22 wt % BaO) that corresponds to visibly altered parts of the grain. The low totals obtained from such grains suggest an extensive hydration. The late stage pyrochlores are usually less altered, and thus the deficiency of the A-site cations is lower.

DISCUSSION AND CONCULSIONS

In the Sokli complex, the compositional changes of host rocks from stage to stage are well reflected in those of pyrochlores; F and Sr contents, and Nb/Ta ratio of pyrochlore increase with

evolution. The evolution trends of pyrochlores in phoscorites and calcite carbonatites from stage to stage are broadly similar with each other. However, the pyrochlore compositions between the phsocorite and calcite carbonatite in a given stage show a little difference: pyrochlore from the phoscorite has higher Ti and lower Nb, Zr and Fe and it always has the more evolved composition compared to those of the same stage carbonatite. This may imply that the pyrochlore in phoscorite began to crystallize earlier and continued to later stage (two stage crystallization) under a long temperature interval, whereas its crystallization in calcite carbonatites finished only in the early stage, because of difference of the bulk compositions of their host rocks. The significantly higher amount and larger compositional variation of pyrochlore in phoscorites may support the above hypothesis. Moreover, the fact that the pyrochlore from the phoscorite usually shows a low deficiency of A-site cations compared to that of paired calcite carbonatite is considered to be related with the later stage additional crystallization of pyrochlore in the phoscorite, which may prevent hydration of early crystallized pyrochlore in the phoscorite from hydrothermal alteration.

The different chemistry of pyrochlore from the phoscorite and paired carbonatite suggests an important clue for the segregation mechanism of the two rocks. The hypothesis that the phoscorite crystallizes from a cumulate, whereas the carbonatite represents the residual liquid of the parental magma, can be easily discarded because the most evolved mineral composition, which would be crystallized from the liquid, found in the phoscorite. In the opposite case, the idea that the phoscorite is viewed as a liquid, does not fit easily with the mineralogical equivalence observed in the early crystallizing mineral from phoscorite and paired carbonatite (Lee, 2002). The chemical contrast between the phoscorite and carbonatite may be explained by liquid immiscibility involving calcite accumulation from the carbonated silicate parental magma.

REFERENCES

Borodin, L.S., Lapin, A.V. & Kharchenkov, A.G., 1973, Rare-metal bearing camaforites. Nauka, Moscow 176p (in Russian).

Kogarko, L.N., Kononova, V.A., Orlova, M.P. & Woolley, A.R. (eds.), 1995, Alkaline rocks and carbonatites of the World : Part 2. Former USSR. Chapman and Hall, London, 225 p.

Kramm, U., 1993, Mantle components of carbonatites from the Kola alkaline province, Russia and Finland: A Nd-Sr study. Eur. J. Mineral., 5, 985-989.

Kukharenko, A.A., Orlova, M.P., Bulakh, A.G., Bagdasarov, E.A., Rimskaya-Korsakova, O.M., Nefedov, E.I., Ilinskiy, G.A., Sergeev, A.S. & Abakumova, N.B., 1965, The Caledonian ultramafic alkaline rocks and carbonatites of the Kola Peninsula and Northern Karelia. Nedra Press, Moscow, 772 p. (in Russian).

Lee, M.J., 2002, Mineralogy, petrology and geochemistry of the phoscorite-carbonatite association of the Sokli alkaline complex, Finland. Thesis, Ecole des Mines de Saint Etienne, France, 233p.

Verhulst, A., Balaganskaya, E., Kirnarsky, Y. & Demaiffe, D., 2000, Petrological and geochemical (trace

elements and Sr-Nd isotopes) characteristics of the Paleozoic Kovdor ultramafic, alkaline and carbonatite intrusion (Kola Peninsula, NW Russia). Lithos, 51, 1-25.

Yegorov, L.S., 1993, Phoscorite of the Maymecha-Kotuy, ijolite-carbonatite association. Int. Geol. Rev., 35, 346-358.

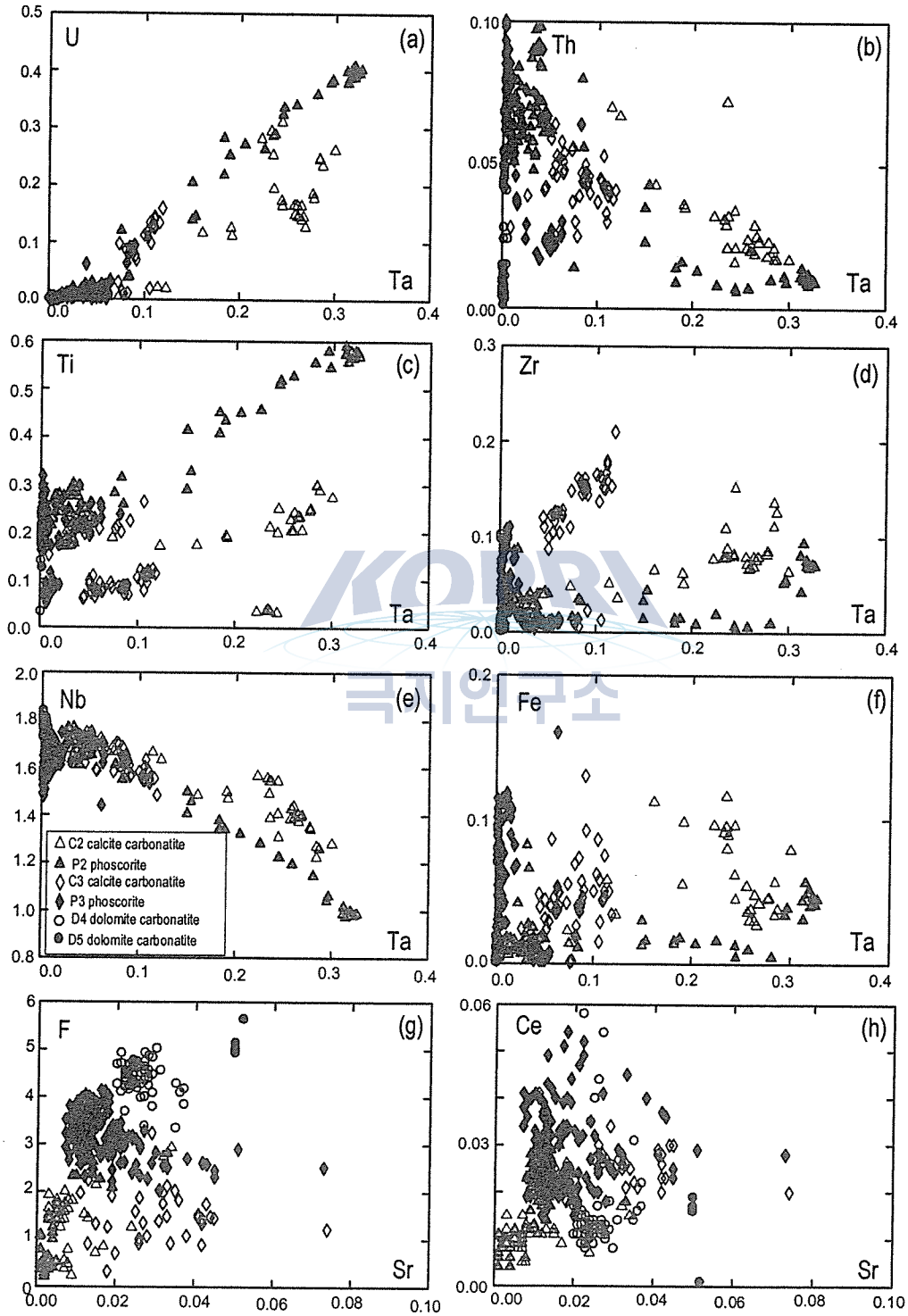

Figure 1. Atomic plots of compositional variations in pyrochlores from the Sokli phoscorite-carbonatite complex.

The 10th Seoul International Symposium on Polar Sciences
October 21-22, 2003, Incheon, Korea

U-Th-Pb ELECTRON MICROPROBE DATINGS ON THE RAYNER COMPLEX, EAST ANTARCTICA

Yoichi Motoyoshi, Tomokazu Hokada and Kazuyuki Shiraishi

National Institute of Polar Research, 1-9-10 Itabashi, Tokyo 173-8515, Japan [motoyosi@nipr.ac.jp]

INTRODUCTION

The Rayner Complex in Enderby Land, East Antarctica, has been considered to be a late Proterozoic (~1000Ma) mobile belt after the reworked portion of the Archean Napier Complex, and such isotopic ages as 1000-1400Ma, 770Ma, 520-550Ma and 480Ma, *etc.* have been summarized by Sheraton *et al.* (1987). Shiraishi *et al.* (1997) conducted U-Pb zircon dating by SHRIMP, and they reported at least two distinct ages within the Rayner Complex; one is 522-537Ma at the western coastal region including Forefinger Point and Mt. Vechernyaya, and the other is 907Ma,

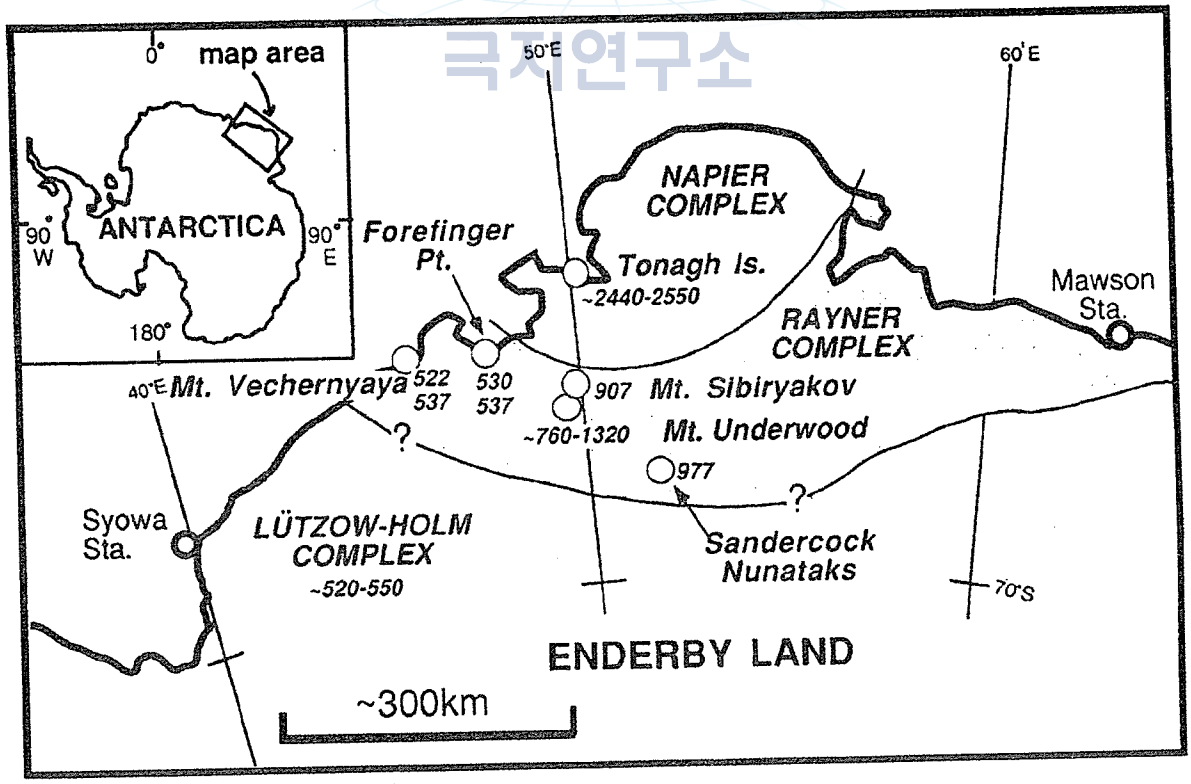

Figure 1. Location of the Rayner Complex and results of U-Pb SHRIMP datings by Shiraishi et al. (1997). (*This figure is a reproduction of Fig. 1 therein).

977Ma and ~760-1320Ma at the inner part including Mt. Sibiryakov, Sandercock Nunataks and Mt. Underwood (Fig. 1). They also reported that ~1800-2400Ma inherited zircon cores were detected from both areas.

This study reinvestigates the geochronology on the Rayner Complex with chemical datings on monazite and zircon from Forefinger Point and Sandercock Nunataks by means of an electron microprobe (EMP) to compare age data with those by SHRIMP, and tries to discuss their significance in relation to the areal extent of the Pan-African event.

PETROGRAPHY

The Forefinger Point rocks used in this study (Sp. 93022209, 93022222, 93022225) are all metapelitic granulites characterized by outstanding reaction textures suggesting substantial isothermal decompression such as,

Opx + Sil + Qtz = Crd,
Grt + Qtz = Opx + Crd,
Grt = Spr + Opx + Crd

depending on the mineral assemblages (Harley *et al.*, 1990; Motoyoshi *et al.*, 1994, 1995). Such reactions textures are not distinctive in the Sandercock Nunataks rocks (Sp. 45121501, 45121503), and they should be generally referred to as orthogneisses.

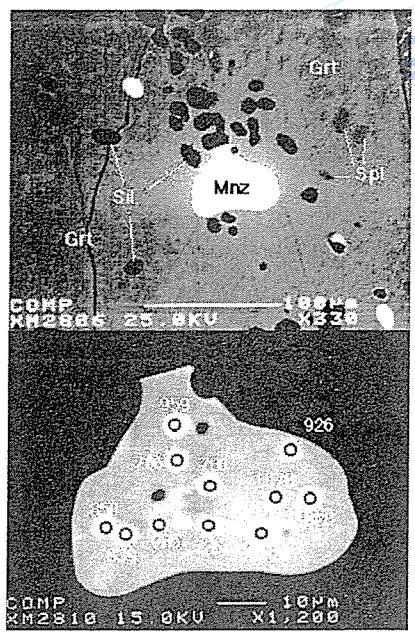

Figure 2. (above) Representative BSE images of monazite with age data (Sp. 93022209).
Figure 3. (below) Monazite inclsion in garnet with aga data (Sp. 93022225).

EMP ANALYSES AND RESULTS

All monazite and zircon in a sigle thin section were analyzed with an electron microprobe analyzer JEOL JXA-8800 at NIPR. UO_2, ThO_2 and PbO were analyzed along with other REE, SiO_2, CaO, P_2O_5, ZrO_2 and HfO_2, with the intensity date being adjusted with $\phi(\rho Z)$ correction method. Analyses with PbO>0.02wt% were selected as data source for further dating analyses.

1. Forefinger Point

Monazite occur generally in the matrix being associated with cordierite, sapphirine and biotite which are reaction products due to decompression. They yielded around 500Ma (Fig. 2). One of the monazites (Mnz6 in 93022222)

preserves an inner core with older ages 750~960Ma being surrounded by 500Ma rim. Monazite inclusion in garnet (Mnz12 in 93022225) yielded ~1000Ma without 500Ma rim, whereas monazite in the matrix of the same sample yielded 500Ma (Fig. 3). Zircon included in prismatic sillimanite yielded extremely older ages than 2000Ma, but because of its large error, the significance of these data is uncertain.

2. Sandercock Nunataks

Monazite ages from Sandercock Nunataks are concentrated around 1000Ma. The isochron ages for two samples (45121501 and 45121503) yielded 981Ma and 1005Ma, respectively (Fig. 4). It is noted that 500Ma are not detected in monazite. The results of EMP datings on monazite are quite consistent with 977Ma SHRIMP dating by Shiraishi et al. (1997).

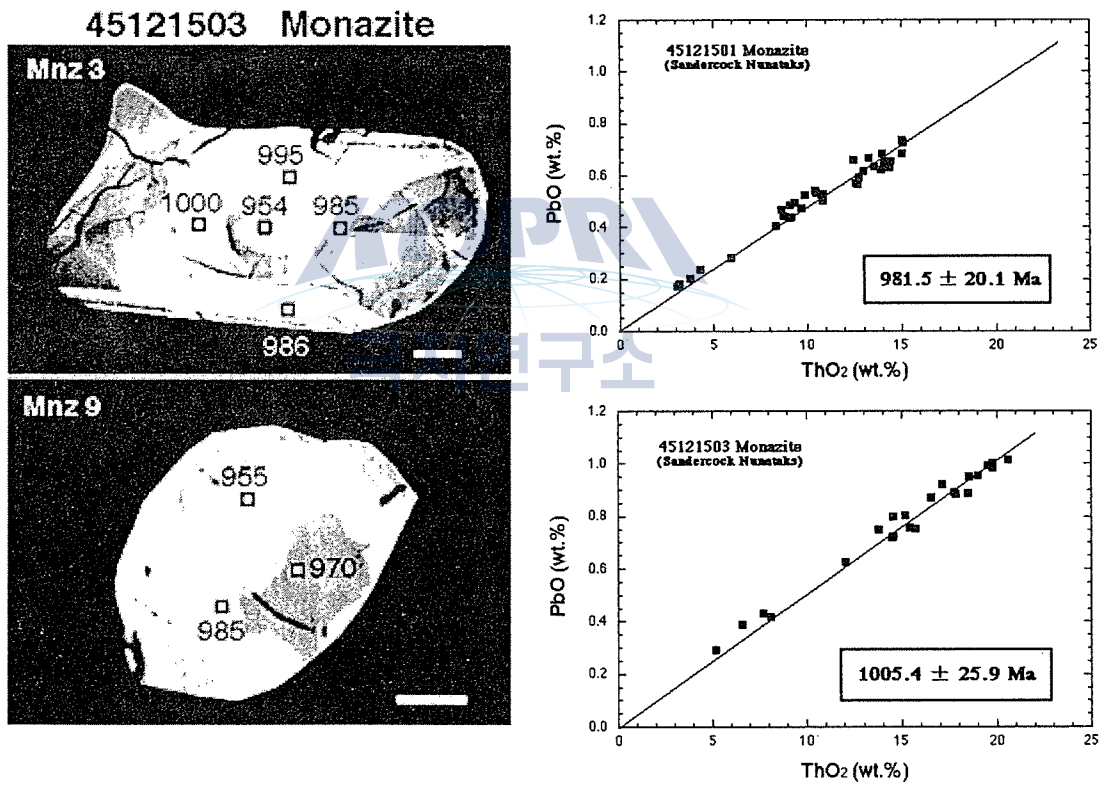

Figure 4. BSE images of monazite with age data (left). Scale bar – 100μm. ThO_2 *vs.* PbO isochron diagrams (right).

SUMMARY AND DISCUSSION

On the basis of SHRIMP datings by Shiraishi *et al.* (1994, 1997) and EMP datings in this study, it is highly probable that Forefinger Point granulites have been subjected to Pan-African event at

~500Ma. Moreover, they have also preserved ~1000Ma event during the evolution. On the contrary, no 500Ma ages were detected in the Sandercock Nunataks rocks, and they have been obviously metamorphosed at ~1000Ma (or even an age of plutonic intrusion?). Although it is uncertain at this stage as to whether the Rayner Complex is geochronologically heterogeneous, or it can be divided into several units with different origin and evolution, a part of the complex has been overprinted with Pan-African orogeny along with the neighbouring Lützow-Holm Complex.

REFERENCES

Harley, S.L. *et al.* (1990), *J. metamor. Geol.*, **8**, 591-613.

Motoyoshi, Y. *et al.* (1994), *Proc. NIPR Symp. Antarct. Geosci.*, **7**, 90-100.

Motoyoshi, Y. *et al.* (1995), *Proc. NIPR Symp. Antarct. Geosci.*, **8**, 121-129.

Sheraton, J. W. *et al.* (1987), *BMR Bulletin*, **223**, 51pp.

Shiraishi, K. *et al.* (1994), *J. Geol.*, **102**, 47-65.

Shiraishi, K. *et al.* (1997), *The Antarctic Region: Geological Evolution and Processes*, 79-88.

The 10th Seoul International Symposium on Polar Sciences
October 21-22, 2003, Incheon, Korea

GEOCHEMICAL VARIATION DURING HYDROTHERMAL ALTERATION OF BASALTIC ANDESITE AT BARTON PENINSULA, KING GEORGE ISLAND, ANTARCTICA

Soon Do Hur[1], Jong Ik Lee[1] and Jeong Hwang[2]

[1] Polar Environment Research Division, Korea Polar Research Institute, Korea Ocean Research and Development Institute, Ansan P.O. Box 29, Seoul 425-600, Korea [sdhur@kordi.re.kr]
[2] Department of Geosystem Engineering, Daejeon University, Taejon 300-716, Korea

Pervasive hydrothermal alteration of basaltic andesite in Barton Peninsula occurred during the intrusion of granodiorite. Hydrothermally altered rocks in Barton Peninsula can be divided into three categories based on alteration indices: least-altered rock, sericitized- or chloritized-rock, and slilcified rock. Least-altered rocks, and sericitized/chloritized rocks and silicified rocks show different features in mass change during hydrothermal alteration. While trace element during hydrothermal alteration in least-altered rocks was almost immobile so that almost no mass change in trace element happened, both sericitized- or chloritized- rocks and silicified rocks experienced mass change. While Fe, As, Cu, Rb, Pb, Mo, Co, and W are enriched, Ca, Hf, Sr, Ba, Nb, and Y are depleted in sericitized- or chloritized- rock. In silicified rocks, Si, K, Ba, As, Nb, U, Mo, Hf, and Ni are enriched, whereas Ca, Fe, Sr, Sn, and V are depleted. Al and Ti behaved as an immobile element during hydrothermal alteration so that no change occurred in altered rocks. Mass change during hydrothermal alteration is not remarkable from the least-altered rocks. In the sericitized- or chloritized rocks, mass of major element decreased due to loss of Ca and Na, whereas gain of As, Co, Cu, Ni, Pb, Rb, V, Zn increased mass of trace element. Notable increase in Si amount compared to small decrease in Fe, Mg, and Ca amount in the silicified rocks resulted in net gain in major element. Increase in As, Ba, Ni, Pb, Rb, Th, W, and Zr, but decrease in Co, Cu, Sr, V, Zn, and Sc caused only small mass change of trace element in the silicified rocks. The pattern of rare earth element in both least-altered rocks and sericitized- or chloritized- rocks seems to be similar to that in the fresh rocks, whereas silicified rocks exhibit enrichment in light rare earth elements compared to the fresh rocks. Enrichment in light rare earth element of the silicified rocks is thought to be caused by active formation of complex ions with hydrochloric acid and fluoric acid under the lower PH and higher temperature environment.

The 10th Seoul International Symposium on Polar Sciences
October 21-22, 2003, Incheon, Korea

THE PALEOCENE-EOCENE VOLCANIC SUCCESSION IN THE BARTON PENINSULA, KING GEORGE ISLAND, ANTARCTICA: LITHOFACIES , ERUPTION STYLES AND DEPOSITIONAL PROCESSES

Seung Bum Kim[1], Young Kwan Shon[2] and Moon Young Choe[1]

[1] Korea Polar Research Institute, KORDI, Ansan P.O. Box 29, Seoul 425-600, Korea [sbkim@kordi.re.kr]
[2] Department of Earth and Environmental Sciences, Gyeongsang National University, Jinju 660-701, Korea

INTRODUCTION

The volcanic succession in the Barton Peninsula, King George Island, Antarctica, has been regarded as a stratiform complex formed in an island-arc setting. It consists of a lower volcaniclastic succession (Sejong Formation, 100–200 m thick) and an upper succession (ca. 200–300 m thick) of basaltic-andesite lava flows interlayered with rare welded tuffs (Tokarski 1988, Birkenmajer 1998, Lee et al. 2002). Recovered plant fossils indicate deposition of the formation during the Late Paleocene to Eocene (Chun et al. 1994). Previous studies have centered on the structures, petrology and geochemistry of the volcanic rocks, but paid little attention to the responsible, eruptive and depositional processes and environments (Yoo et al. 2001). This study focuses on the Sejong Formation and attempts to reconstruct volcano-sedimentary evolution based on detailed facies analysis and field mapping. A revision on the stratigraphy is proposed; the basaltic rocks that have been attributed as late-stage intrusion (dikes or plugs) are reassessed as lava/agglutinate complexes at the base of the Sejong Formation and are designated as Chottae Member.

LITHOFACIES AND FACIES ASSOCIATIONS

Based on composition, texture (coherent vs clastic) and grain size, nine lithofacies are identified in the Sejong Formation: basaltic lava (lithofacies BL), basaltic agglutinate (BA), basaltic tuff breccia (BTB), basaltic lapilli tuff (BLT), andesitic lava (AL), andesitic tuff breccia (ATB), andesitic lapilli tuff (ALT), reworked conglomerate (C), and sandstone/siltstone couplets (S/Z). These volcanic rocks can be grouped into three facies associations based on the constituent facies, facies sequences, and their field relationships. Each facies association records formation in distinct eruptive and/or depositional environments: (1) spatter/cinder cones (Facies Association (FA) I), (2)

volcaniclastic apron (FA II), and (3) distal apron to floodplain (FA III).

1. Facies Association I

FA I comprises basaltic rocks that form semi-circular patches in map view. The rocks have been regarded as late-stage intrusions (dikes or plugs) but the lack of distinctive discordant contact and thermal metamorphism between the adjacent volcaniclastic rocks negates an intrusive origin. Identification of gradational transition from central massive/vertically jointed lava (lithofacies BL) to fringing agglutinates (lithfacies BA) through a zone of locally brecciated, either blocky or fluidally, compound lavas (lithofacies BL) in this study rather suggests intact preserved spatter/cinder cones. This inference is further supported by the fact that the outermost basaltic agglutinates are conformably overlain by the volcaniclastic rocks of the Sejong Formation. The basaltic lava/agglunate complexes can be therefore designated as a new stratigraphic unit, i.e., Chottae Member that occupies the base of the Sjeong Formation.

The central coherent basalt is most fresh and hardened, forming a distinctive edifice and shows vertical to subhorizontal joints arrayed in a fan-shaped fashion. This suggests emplacement of the basalt as vent-filling lava pond or plug. The adjacent piles of compound lava flows dip outward away from the central massive basalt. Each flow unit is slightly vesicular, particularly at the top. In situ breccia is locally associated that comprises either slabby, flow foliated clasts with jagged margins or blocky glassy clasts with curviplanar margins, both with no matrix material. This suggests an autobrecciation and a transitional rheology of the lava flows between aa and pahoehoe types. The outermost agglutinates are characterized by flattened and stretched non- or very slightly vesicular, dense basaltic spatters between aerodynamically shaped, slightly vesicular bombs and moderately vesicular, angular blocks. This indicates near-vent accumulation of spatters and bombs. The sequential relationships among ponded lavas, lava flows and agglutinates of FA I suggest Hawaiian, fire-fountaining to Strombolian eruptions and formation of discrete spatter/cinder cones. The lateral persistence of the basaltic agglutinate may indicate a spatter rampart at the initial stage of the eruption. Endogenous dome-like emplacement is unlikely because there is no evidence of large-scale disruptions or brecciations indicative of mechanical compressions due to succeeding magma pulses. There is also no evidence of water influence: neither pillows nor hyaloclastites are associated. On the other hand, the development of autobreccia and agglutinated texture suggest subaerial emplacement of the FA I deposits.

2. Facies Association II

FA II comprises the bulk of the Sejong Fomation. It is conformably underlain by FA I and is

interlayered with sandstone/siltstone couplets (lithofacies S/Z) of FA III. It consists dominantly of very thick, tabular beds of andesitic to basaltic, either welded or non-welded, lapilli tuffs and tuff breccias (lithofacies BTB, BLT, ATB and ALT), and rare intervening lava flows (lithofacies AL). Each volcaniclastic unit is rather irregularly bedded and is characterized by ungraded and disorganized fabric. Clasts are either fluidally shaped or subordinately angular blocky shaped, showing various degree of vesicularity. Clast margins are either smooth and curviplanar or occasionally rugged. Matrix materials consist predominantly of glass particles with subordinate amount of crystal fragments. Lithic particles are scarce. Welded texture is common in andesitic lapill tuffs (lithofacies ALT). At the base of a very thick bedded tuff breccia, a unique thin-bedded granular andesitic lapilli tuff occurs and shows inversely graded fabric. Andesitic lava flow (lithofacies AL) shows an abrupt lobate termination.

The common welded features, together with the presence of crystal fragments in the matrix and the rarity of lithic particles, suggest a primary pyroclastic origin of the FA II deposit, contrary to the previous attributions to secondary resedimentation (Yoo et al., 2001). The coexistence of rounded clast with irregular outlines and angular blocky clasts and the large grain size (common block-size clasts) suggest specifically explosive magmatic eruptions (Vulcanian?). The thick-bedded nature, the lack of stratification and channel incision, and the ungraded and disorganized fabric collectively indicate mass-flow-like emplacements, i.e., laminar pyroclastic-flow origin. On the other hand, the virtual lack of ash fall deposits and pedogenic alteration features suggest near-vent accumulation. The FA II deposit is therefore interpreted as slope aprons extending from summit crater of a stratovolcano.

3. Facies Association III

FA III occurs in fault contact with FA I or intercalated with FA II deposits. It consists mainly of sandstone/siltstone couplets (lithofacies S/Z) locally with resedimented conglomerates (lithofacies C). The sandstone/siltstone couplets are characteristically diffusely bounded and are upward graded from sandstone-dominant base to mudstone-dominant top. Siltstone layers are mostly homogeneous, red to brown in color and locally bioturbated (vertical burrows). Abundant plant fossils are recovered in some horizons. Sandstone layers are generally thin bedded with occasional scours at the base. Each layer is either ungraded or normally graded with an upward increase in silt content. Cross-stratification is relatively rare. The couplets are commonly deformed and distorted with flame structures. Resedimented conglomerates are typically irregularly bedded with downtruding and protruding clasts. Each unit is inversely graded with large amounts of boulder-size clasts near the top. Clasts range in size from pebble to boulder grade; mostly rounded to suangular. Matrix comprises extremely poorly sorted coarse sandstone.

The color, texture, structure and bedding features of the sandstone/siltstone couplets collectively

suggest a predominance of suspension settling from rapidly waning floods. Ephemeral shallow channels are indicated by the scours and rare cross-stratification of sandstone layers. The scarce pedogenic structures suggest rapid accumulation rate deposition likely due to high flood frequency. The resedimented conglomerates are interpreted as debris flows based on the prominent inverse grading, irregular bedding and the presence of protruding clasts. Intimate association of debris flow deposits in suspension settled flood deposits is indicative of relative proximity to the source area, i.e., mountain slope. FA III is therefore interpreted as floodplains developed in low lands extending from lower slopes of the stratovolcano of FA II. The floodplains must have developed during inter-eruptive periods, while which hydrologic remobilization processes were active during and in the immediate aftermath of the eruptions.

CONCLUSIONS

Based on detailed facies analysis and field mapping, volcano-sedimentary evolution of the Sejong Formation is reconstructed. Initial stage is marked by the basalt/agglutinate complexes (FA I, Chottae Member) that form discrete semi-circular patches in map view. They represent spatter-cinder cones due to Hawaiian, fire-fountaining to Strombolian eruptions. Second stage is represented by repetitive emplacement of ignimbrite sheets and attendant lava flows complexes (FA II), which suggests onset of explosive and effusive eruptions (Vulcanian?) of more evolved (intermediate) magmas from the summit crater. On the flanks of the stratovolcano, hydrologic remobilizations were active during and in the immediate aftermath of the eruptions, resulting in the interlayered fluvial deposits of FA III. The overall characteristics of individual lithofacies and facies associations suggest subaerial magmatic eruptions for the Sejong Formation. The change in eruption styles from effusive Hawaiian to explosive types may reflect compositional differentiation of parental magma.

REFERENCES

Birkenmajer, K., 1998, Bull. Pol. Acad. Sci., Earth Sci. 46: 191-209.

Chun, H.Y., Chang, S.G. & Lee, J.I., 1994, J. Paleontol. Soc. Kor. 10: 69-84.

Lee, J.I. et al., 2002, Geological map of the Barton & Weaver peninsulas. KORDI.

Tokarski, A.K.. 1988, Stud. Geol. Pol. 105: 53-63.

Yoo, C.M., Choe, M.Y., Jo, H.R., Kim, Y. & Kim, K.H., 2001, Ocean Polar Res. 23: 97-108.

The 10th Seoul International Symposium on Polar Sciences
October 21-22, 2003, Incheon, Korea

HOLOCENE PALEOCLIMATE IN ANTARCTIC LAKE LANGER (KING GEORGE ISLAND)

B.K. Khim[1], K. Lee[2], H.I. Yoon[3] and C.Y. Kang[3]

[1] Department of Marine Science, Pusan National University [bkkhim@pusan.ac.kr]
[2] Department of Life Science, Catholic University
[3] Korea Polar Research Institute, KORDI

The Antarctic Peninsula represents a possible linkage between marine and terrestrial transition areas sensitive to climatic and environmental change. King George Island, one of South Shetland Islands, is characterized by several lakes formed during the postglacial period. A variety of approaches (sediment facies, magnetic susceptibility, sediment and geochemical properties, carbon isotopic composition, and diatom abundance) were conducted on the lake sediments drilled from the Langer See (King George Island) for the purpose of reconstructing the evolution of Holocene paleoclimate. Core sediments are divided into two lithologic facies, the upper part of fine-grained sediments and the lower part of mixed sediment with dominant gravel and sand. The sediment and geochemical properties provide the postglacial paleoclimate evolution in King George Island, indicating the prominent paleoproductivity events, in which the level of paleoproductivity is supported by the abundance of diatom species. The ^{14}C-dated lithologic transition at about 5,000 yr BP seems to correspond to the complete retreat of glacier and the initiation of lake formation, which corresponds to the climatic transition in Maxwell Bay. In particular, interesting is the late Holocene characterized by the unstable local (or regional) climatic system. Thus, the lake sediments of Langer See in King George Island preserves the potential evidence of unstable climatic variation during the last 5,000 years.

The 10th Seoul International Symposium on Polar Sciences
October 21-22, 2003, Incheon, Korea

HOLOCENE PALEOCEANOGRAPHY AND PALEOCLIMATE OF THE WEST SPITSBERGEN AREA, EURO-ARCTIC MARGIN

Morten Hald[1], Hanne Ebbesen[1], Matthias Forwick[1], Sergei Korsun[2], Tore O. Vorren[1], Liza Khomenko[2] and Fred Godtliebsen[3]

[1] Department of Geology, University of Tromsoe, Norway [Morten.Hald@ig.uit.no]
[2] Department of Biology, St. Petersburg University, Russia
[3] Department of Mathematics and Statistics, University of Tromsoe, Norway

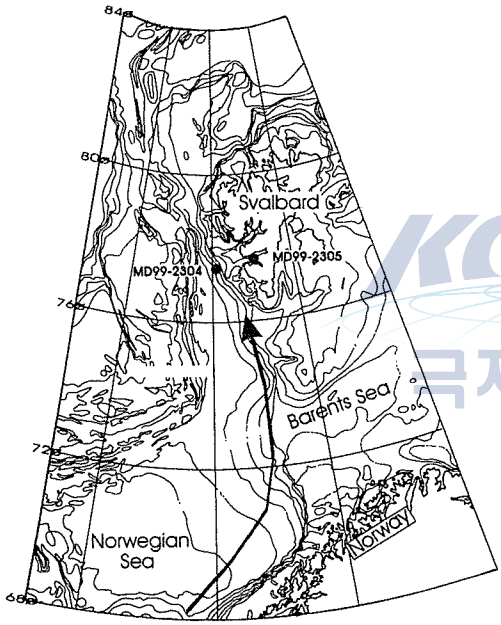

Figure 1. Location map. Arrow indicates direction of the Norwegian Current – West Spitsbergen Current.

Two sediment cores from the West Spitsbergen area, Euro-Arctic Margin, MD99-2304 and MD99-2305, retrieved during the IMAGES cruise in 1999, have been investigated for paleoceanographic proxies (Fig. 1).

CORE MD99-2305 VAN MIJENFJORD WEST SPITSBERGEN (FIG. 2)

MD99-2305 is 18 m long and located in the Van Mijenfjord. This fjord is 50 km long and 10 km wide with three tide water glaciers and a sill in the outer part. The fjord is normally covered by sea-ice 8-9 months per year. The core is located in the outer part of the fjord, about 10 km in fjord from the sill Akseløya at 115 meter water depth. The uppermost 16 m of the core contain a Holocene mud, and the lowermost 2 m consist of glaciomarine mud and diamictons, the latter interpreted to be a basal till. A total of 10 AMS ^{14}C dates have been obtained (another 12 are in progress) and an age model in calendar years BP has been produced. The boundary between till and the Holocene mud is dated to c. 11 000 cal. years BP, (corresponding to 9800 ^{14}C years BP). Holocene mud represents the last 11 000 cal. years BP. A proxy record of this part of the stratigraphy, including benthic foraminifera, IRD counts from X-radiographs (statistically tested by SiZer technique), and stable oxygen and carbon isotopes, has been established . The Younger Dryas/Preboreal transition is characterized by

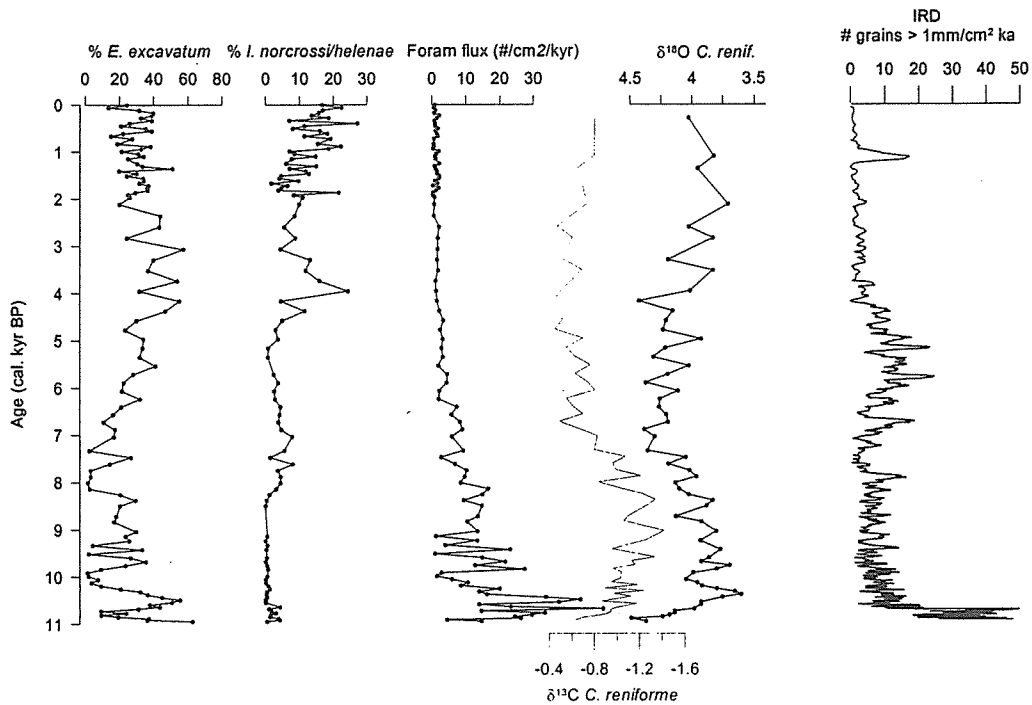

Figure 2. The Van Mijenfjord proxy record, core MD99-2305

a marked depletion in both δ ^{18}O and δ ^{13}C (measured on the benthic foraminiferal species *Cassidulina reniforme*). The structure of the δ ^{18}O curve is similar to that of the IRD curve. Relatively low δ ^{18}O corresponds to a minimum in IRD and a reduction in the ice proximal species *C. reniforme* and *Elphidium excavatum*. During this period there is a high flux of foraminifera and high content of bivalve molluscs. A broad maximum in both δ ^{18}O and IRD is found between 7000 and 5000 cal. years BP. During this period there is a rise in the ice proximal foraminifera. The last 4000 cal. years BP are characterized by low IRD (except from one surge-event at 1300 AD), depletion in δ ^{18}O, decline in bivalve molluscs and foraminiferal flux.

CORE MD99-2304 WEST SPITSBERGEN CONTINENTAL SLOPE (FIG. 3)

CoreMD99-2304 is located on the upper continental margin 77° 37 26' N and 09° 56 90' E, at 1315 m water depth under the axis of the West Spitsbergen Current transporting relatively warm, saline Atlantic Water northwards along the continental margin and into the Arctic Ocean (Fig. 1). The upper c. 1, 5 meter of the core was investigated for this study. Dominant sediment type is homogenous clay with scattered IRD clasts. The chronology is based on eight AMS ^{14}C dates performed on foraminiferal shells and molluscs. A proxy record including planktic foraminiferal fauna and planktic δ ^{18}O and δ ^{13}C has been established. The foraminiferal fauna shows a characteristic decline in subpolar species and rise in polar species around 8300 cal. years BP. The δ ^{18}O shows a declining trend from 8300 to 6500 cal. Years BP. The δ ^{13}C depicts fairly low values

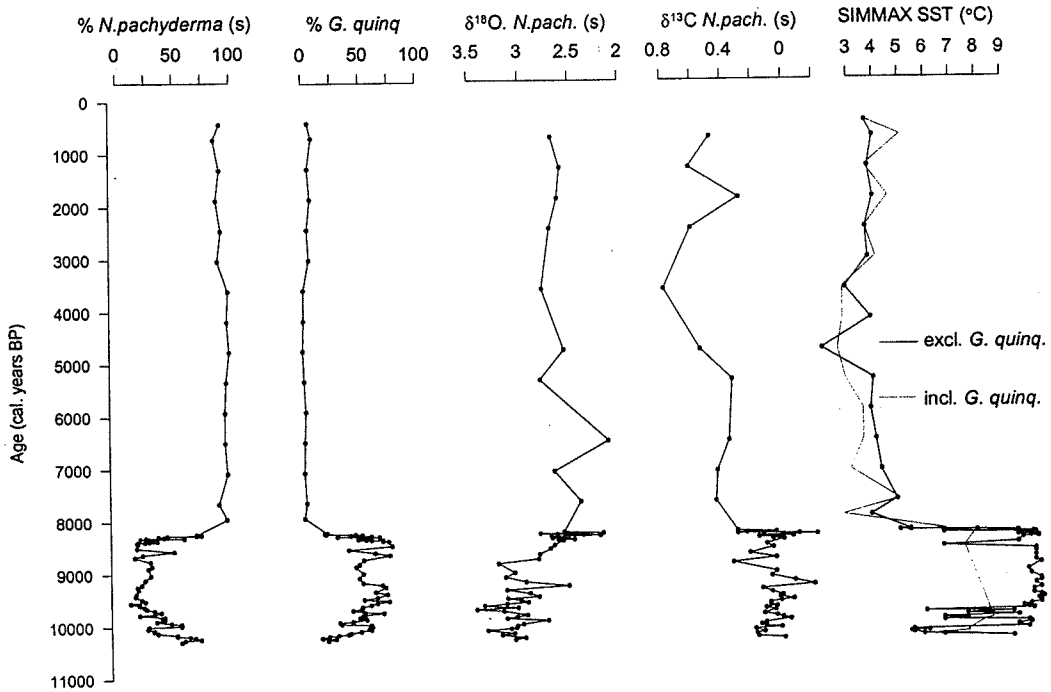

Figure 3. The West Spitsbergen margin proxy record, core MD99-2304

until 8300 cal. years BP, followed by a rise.

PRELIMINARY INTERPRETATION

Core MD99-2304 mainly reflects changes in the flux of Atlantic Water in the West Spitsbergen Current. The foraminiferal fauna as well as the $\delta^{18}O$ suggest a stronger influx of Atlantic Water on the Euro-Arctic margin between 10 000 and 8300 cal. years BP, compared to the last 8300 years. The faunal and isotopic shifts around 8300 cal. years BP indicate increasing dominance of Arctic Water. An attempt to reconstruct summer sea surface temperatures (SST) was made using the SIMMAX method (Pflaumann et al., 1996) both including and excluding the species. *G. quinqueloba* (Fig. 3). Both reconstructions depict a very marked cooling step of > 4 ^{o}C between 8280 and 8260 cal. years BP. Due to a more protected location of the Van Mijenfjord, its record contains more of a "continental" climate signal. By comparing the two proxy records (Figs. 2 & 3) the following preliminary interpretation of the climatic/paleoceanographic conditions is suggested: Early Holocene had a stronger influx of Atlantic Water than today and was relatively warm. Glacial activity on Svalbard was reduced. Mid Holocene (7000-5000 cal. years BP) appears to have experienced increased glaciation indicated by the IRD record in the van Mijenfjord (Fig. 2). This compares well to the marked cooling on the continental margin after 8300 cal. years BP (Fig. 3). A broad maximum in $\delta^{18}O$ in the fjord record between 7000 and 5000 cal. years BP, may be due to

increased oceanic flux or due to slight cooling.The gradual depletion of $\delta^{18}O$ on the continental margin may indicate a weak increase of Arctic Water, thus supporting cooling. Upper Holocene reflects relatively stable, cool conditions on the continental margin (Fig. 3). However, the fjord record probably reflects a more local signal due to a progressing isolation resulting from the postglacial isostatic rebound of the fjord sill. The low IRD content the last 4000 cal. years BP (Fig. 2) represents conditions similar to that of the modern fjord. The depletion in $\delta^{18}O$ during the last 4000 years BP in the fjord record may reflect increased sea ice formation bringing light isotopic water to the fjord bottom by brine formation.

REFERENCE

Pflaumann, U., Duprat, J., Pujol, C. and Labeyrie, L.D., 1996. SIMMAX: A modern analogue technique to deduce Atlantic sea surface temperatures from planktonic foraminifera in deep-sea sediments. *Paleoceanography, 11(1):* 15-35.

ORIGINS AND PALEOCEANOGRAPHIC SIGNIFICANCE OF LAYERED DIATOM OOZE INTERVAL FROM THE BRANSFIELD STRAIT IN THE NORTHERN ANTARCTIC PENINSULA AROUND 2500 YRS BP

Ho Il Yoon, Byong-Kwon Park, Yeadong Kim, Cheon Yun kang and Sung-Ho Kang

Korea Polar Research Institute, Korea Ocean Research and Development Institute, Ansan, P.O. Box 29, Seoul 425-600, Korea [hiyoon@kordi.re.kr]

Diatom and pore water data from two piston cores from the central sub-basin and one from the western sub-basin of Bransfield Strait in the northern Antarctic Peninsula were used to elucidate the depositional mechanism of a layered diatom ooze unit observed in all three cores. The diatom ooze unit, formed by the alternation of diatom ooze layers and terrigenous layers, is enriched in organic carbon, biogenic silica, sulfide sulfur content and depleted in pore water sulfate concentration. This depletion of pore water sulfate in the diatom ooze interval is indicative of development of reducing micro-environment in which bacterially mediated sulfate reduction occurred. The negative relationship between the organic carbon and sulfate contents, however, indicates that sulfate reduction was taking place but does not control organic carbon preservation in the diatom ooze interval. Rather, the overwhelming dominance of intact *Chaetoceros* resting spores in the diatom ooze layer indicates rapid sedimentation of the diatom spores as a result of repetitive late summer blooms at the sea-ice margin on the Bransfield shelf at around 2500 yrs BP when persistent sea-ice margin might have existed on the shelf and/or shelf break. During the cold period, underflows were probably caused by cooling of Bransfield shelf water, and these flows probably played an important role for concentrating the summer diatom blooms to produce the diatom ooze layer recorded in the sub-basins of the Bransfield Strait. Intervening terrigenous layers were mostly deposited during the winter and represent the input of reworked detrital clay by stronger bottom flows in non-bloom conditions under the sea ice.

The 10th Seoul International Symposium on Polar Sciences
October 21-22, 2003, Incheon, Korea

A RECORD OF HOLOCENE ENVIRONMENTAL CHANGES IN TERRESTRIAL SEDIMENTARY DEPOSITS ON KING GEORGE ISLAND, ANTARCTICA

A. Tatur[1], R. del Valle[2], A. Barczuk[3], J. Martinez-Macchiavello[4]

[1] Department of Antarctic Biology, Polish Academy of Sciences, Ustrzycka 10/12, 02-141 Warszawa, Poland. [tatura@interia.pl]
[2] Instituto Antartico Argentino, Cerrito 1248,10-10 Buenos Aires, Argentina
[3] Department of Geology, Warsaw University, Zwirki i Wigury 91, 02-089 Warszawa, Poland
[4] Museo Argentino de Ciencas Naturales, Av. Angel Gallardo 470-C C 220, 14-05 Buenos Aires, Argentina

INTRODUCTION

Numerous geological evidences permit to reconstruct global scenario of events during transition from the Late Pleistocene to Holocene. Sudden melting of shelf ice in the polar regions caused global rise of seawater in the ocean following by glacio-isostatic uplift of land continuing till present times. However, a local progress of Holocene deglaciation as well as climate dependent development and stability of terrestrial ecosystems on ice-free patches of land in the maritime Antarctic are still the questions that need further discussion. Since the South Shetlands lie close to boundary between maritime and continental climatic modes therefore one may suspect its sensitive response to any regional climate fluctuations. Thus the question arises whether we may use sedimentary record from this area for reconstruction of past Holocene climate. As a background for discussion we wish to present our (Argentine-Polish) data and hypotheses inferred from paleolimnological and peleontological investigations and confront them with the knowledge in being.

IMPORTANT PROFILES INVESTIGATED BY THE ARGENTINE-POLISH TEAM

Long Lake is located in abandoned melt-water channel on Fildes Peninsula, behind raised beach 16 m. asl. Core of bottom sediment 2.3 m. long was taken from the water depth 4 m.

The profile represents local Holocene prograding sequence of marine - estuarine - lacustrine sediments and consists of upward finning and thinning sediment cycle formed at the mouth of a meltwater stream during regional isostatic uplift, which followed Early Holocene deglaciation and

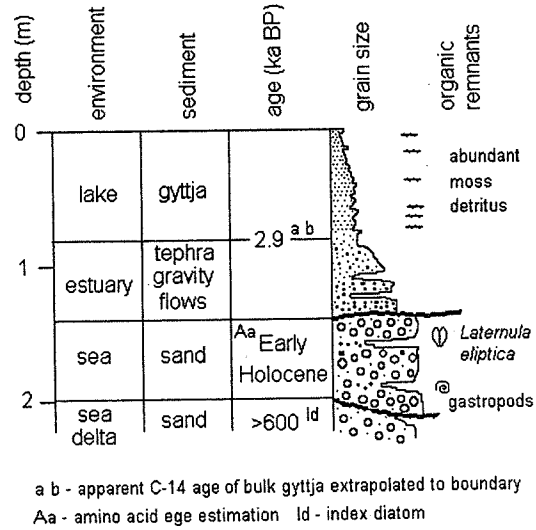

Figure 1. Core of bottom sediments from Long Lake.

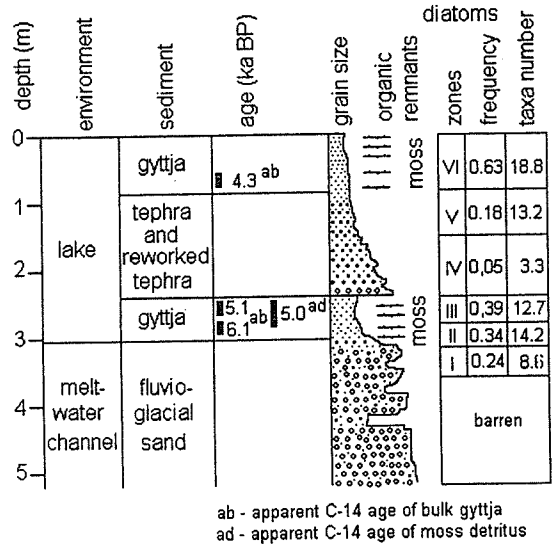

Figure 2. Core of bottom sediments from Hotel Lake

marine inundation events. The sequence begins in the lower Holocene with sublittoral sand (marine diatoms and abundant molluscs) overlying (a transgressive base) the deltic (?) clastic sediments marking probably one of the pre-Holocene interglacial periods (index diatom *Actinocyclus ingens* suggests an age >0.62 Ma). The lower Holocene marine sand was truncated by middle Holocene gravity flows, carrying volcanic ash. They were deposited in a high-energy estuarine environment (brackish diatoms). The beach was subsequently formed and separated the estuary from the sea, changed it into a freshwater lake. Accumulation of moss gyttja, containing a freshwater diatom assemblage, marks the final late Holocene stage of this coastal sedimentary sequence, which can be considered as typical for the maritime Antarctic. For details see Martinez-Macchiavello *et al.* 1996.

Hotel Lake is located at an altitude 40-45 m., on the edge of an extensive, flat erosional surface in an abandoned subglacial, meltwater channel. Therefore, barren fluvioglacial clastics form the base of Holocene sediment deposited in the lake environment since about 7-6 ka apparent C-14 years BP. Gyttja sediments rich in moss detritus are divided into upper and lower part by tephra fallout (about 4-5 ka apparent age BP) followed by gravity flows of reworked tephra sediments washed down with delay from the catchment area to the lake. Tephra horizons of Deception Island volcano were found in lacustrine sediments on Fildes Peninsula, Potter Peninsula and Bransfield Strait. Changes of diatom assemblages in sediment core of Hotel Lake mark the evolution of the lake ecosystem and strongly suggest that tephra fallout should be considered as an important factor disturbing biota. Increasing biodiversity (number of species) and trophy (frequency of diatoms) of lake just after its formation, was highly reduced due to sudden tephra fallout. Recovery of biodiversity and trophy took place later, however, the species composition of new assemblages changed significantly. Several new species substituted the former dominants at the same ecological

functions. This example indicates that succession and stress from tephra fallout might be considered as the driving factor commonly changing biota of lakes on King George Island and might overlap every response of the lake ecosystem to climate changes. For details see Tatur *et al.* (1991), and Tatur *et al.* (1999a,b).

SCENARIO OF HOLOCENE EVENTS ON KING GEORGE ISLAND

The oldest Holocene organic remnants represent shells of marine molluscs or wedges deposited in beach, littoral and sublitoral environment during early Holocene inundation event. Often these marine sediments contain also much older reworked material. Sea level, marked by traces of raised beaches, was at that time 55-65 m. higher than today, sea entered inland and stopped on mountain glaciers much thicker than today. There are no any important evidences proving deglaciation of land until a middle Holocene climatic optimum, when glacio-isostatic movement raised the land and relative sea level fell down finally to the recent latitude about 16 m. asl. The oldest Holocene terrestrial deposits bearing organic remnants (moss detritus) were found at the base of some lacustrine sediment. These lakes are situated in the largest ice-free part of land on King George Island (Fildes Peninsula), now far away from the glaciers. According to the suggestions of authors based on radiocarbon dating of bulk gyttja samples, deglaciation might have started even 9 ka before present. However, taking into account highly limited reliability of radiocarbon dating (particularly bulk gyttja samples) in that environment (Björk *et al.* 1991), one might suppose much later beginning of deglaciation. Anyway, it certainly started before 5-6 ka BP, when wide bands of 16 m. raised beaches were formed along coastline already free of ice. Soon after 16 m. raised beach formation, possibly 5-4 ka BP, important tephra fallout after Deception volcano eruption took place. Thick tephra horizon probably occurs in all older lakes on the island (and in the cores of marine sediments) and may be considered as chronostratigraphic marker. Although, some authors interpret reworked tephra material as epiclastic in origin and marking wetter climatic condition. Moreover, it can not be excluded that much younger tephra fallout that is slightly marked in our profile, might be much more important in quite young lakes with watershed covering also large part of glacier in time of volcanic eruption. There are only a few peat banks on the island. The oldest ones probably post-dated (4950 y BP, Birkenmajer *et al.* 1985) 16 m. raised beaches formation and fallout of tephra. At more or less the same time or a little earlier large parts of coast got widely accessible for sea animals breading on land. The oldest traces of breading rookery of penguins on King George Island were dated to about 5 ka BP (Tatur *et al.* 1997).

CONCLUSIONS

Collected evidences let to propose coherent sequence of events during the Holocene on King George Island. However, the timing of these events is uncertain: radiocarbon dating contains mixture of reliable and misleading results, tephro-chronological pattern is not documented sufficiently.

Glacial features from King George Island delivered several examples of past climate fluctuations during Holocene, whereas, there are no clear records of such fluctuations in the lake sediments, peat banks and abandoned ornithogenic soils. Common indicators of past climate changes are useless here. Pollen record is extremely poor. Mosses composition in few saved banks is poorly diversified. Determination of lacustrine diatoms in sediment cores is not comparable among authors and probably much more constrained by succession process and tephra fallout or eutrophication than by climate changes. Interpretations of geochemical and mineralogical records are not synchronised among several authors, and according to our knowledge may be heavily disturbed by tephra fallout. Moreover, most of the natural terrestrial archives of the past history (peat banks, guano, and subfossil bones) have been strongly eroded and disappeared.

Therefore, any future attempt of past climate reconstruction in this area should take into consideration new unconventional scientific tools or ideas, since habitually used biological and geochemical markers are inefficient in that case.

REFERENCES

Birkenmajer, K., R. Ochyra, I. Olsson, K. Stuchlik. 1985. Mid-Holocene radiocarbon dated peat at Admiralty Bay, King George Island (South Shetland Islands, West Antarctica). Bull. PAS, ser.Sci. de la Terre 38, 17-24.

Björk, S., S.C. Hjort, O. Ingolfsson, G. Skog. 1991. Radiocarbon dates from the Antarctic Peninsula Region - problems and potential. Quat. Proc. 1, 55-65.

Tatur, A., R. del Valle, M. Pazdur. 1991. Lake sediments in maritime Antarctic zone. A record of landscape and biota evolution. Proc. of SIL Conf. München 1989. Verh. Für Internat. Verein. Limnol., 24, 3022-3024.

Martinez-Macchiavello, J.C., A. Tatur, S. Servant-Vildary and R. del Valle. 1996. Holocene environmental changes in a marine-estuarine-lacustrine sediment sequence, King George Island, South Shetland Islands. Antarctic Sci. 8,4, 312-322.

Tatur, A., A. Myrcha, J. Niegodzisz. 1997. Formation of abandoned penguin rookery ecosystems in the maritime Antarctic. Polar Biol. 17, 405-417.

Tatur, A., , R. del Valle and A. Barczuk. 1999a. Discussion on the uniform pattern of Holocene tephrochronology in South Shetland Islands, Antarctica. Pol. Polar Stud., 26 Polar Symposium, Lublin 1999, 303-321.

Tatur, A., J.C. Martinez-Macciavello, J. Niegodzisz and R. del Valle. 1999b. A record of Holocene environmental changes in sediment core of Hotel Lake, King George Island, Antarctica. Pol. Polar Stud., 26 Polar Symposium, Lublin 1999, 379-389.

The 10th Seoul International Symposium on Polar Sciences
October 21-22, 2003, Incheon, Korea

GEOCHEMISTRY OF SOILS OF KING GEORGE ISLAND, SOUTH SHETLAND ISLANDS, WEST ANTARCTICA: IMPLICATIONS FOR PEDOGENESIS IN COLD POLAR REGIONS

Yong Il Lee[1], Hyoun Soo Lim[1] and Ho Il Yoon[2]

[1] School of Earth and Environmental Sciences, Seoul National University, NS 80, Seoul 151-747, Korea [lee2602@plaza.snu.ac.kr]
[2] Korea Polar Research Institute, Korea Ocean Research and Development Institute, Ansan P.O. Box 29, 425-600, Korea

INTRODUCTION

Chemical compositions of soils vary as a function of various soil-forming processes. To interpret the soil-forming processes and factors operating at the soil site properly one needs to test parent-material uniformity. One source of nonuniformity is the influence of allogenic materials, which may be important where physical weathering is more significant than the chemical weathering such as in Arctic and Antarctic regions as well as cold desert regions. These areas are characterized by strong wind activity, resulting in mixing of in situ soils with eolian input materials. The proportion of the eolian additions in the soils depends on the wind speed or direction.

Chemical characteristics of soils in the offshore islands of the maritime Antarctic region have not been studied before although this region has a higher potential for chemical weathering because of its warmer and more humid climate than other parts of Antarctica (e.g., Campbell and Claridge, 1987). Instead of studying total changes in the soil profile, this study intends to characterize the surface soils in this maritime Antarctica. Soils in this region are suggested to have formed since the last deglaciation, *ca.* 9500-6000 yr BP. By studying geochemical characteristics of the reactive finer-grained soil fractions we try to determine the degree of chemical weathering, and the contribution of allogenic materials including eolian additions to the soils. The results of this study may contribute to the understanding of pedogenesis in cold polar regions.

MEHTODS

A total of 30 surface soil samples were collected from the uppermost 10 cm of the active layer in the soil on the Barton Peninsula (Fig. 1). Soils on altered bedrocks were avoided. Soil samples

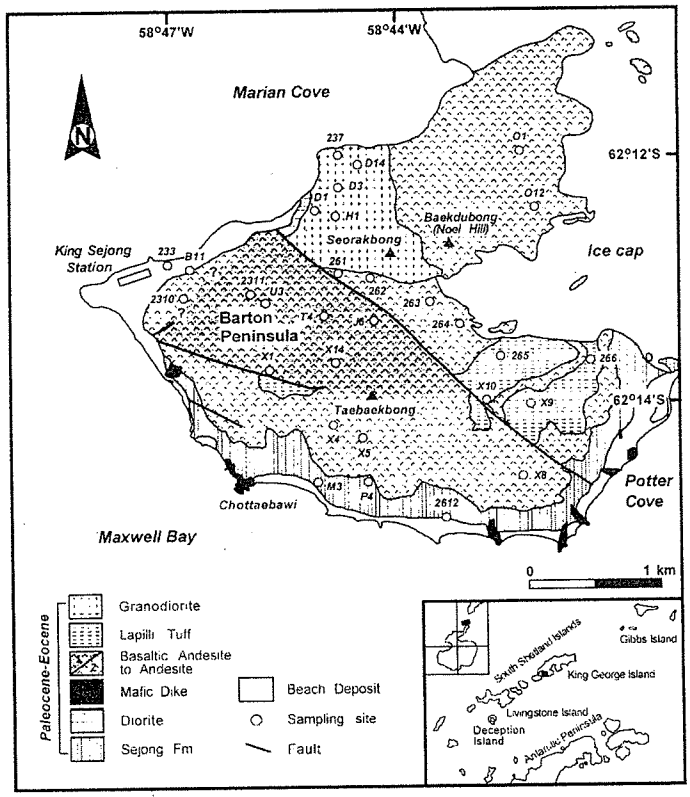

Figure 1. Geological map of the Barton Peninsula, King George Island, West Antarctica. The inset shows the location of King George Island. The numbered open circles in the geological map represent the soil sampling sites.

were dried and impregnated with epoxy under vacuum and thin sections were made. Soil samples were subdivided into two parts by a 230-mesh sieve, and finer fractions (<sand size) and coarser rock debris were separately powdered in an agate motar and fused-glass beads were prepared for major element analysis by a Philips PW244 model X-ray fluorescence spectrometer. Total Fe content is reported as Fe_2O_3. Loss on ignition (LOI) was measured by weighing before and after 1 hr of calcinations at 1000°C. Trace elements and rare earth elements concentrations were determined using a Jobin Yvon 138 Ultrace inductively coupled plasma atomic emission spectrometer (ICP-AES) and a Perkin Elmer Elan 6100 inductively coupled plasma mass spectrometer (ICP-MS). All major, trace, and rare earth elements were analyzed at the Korea Basic Science Institute.

SOIL MICROSTRUCTURE

Soils are unsorted and composed of mineral and rock fragments derived from the bedrock (Late Paleocene and Eocene) and volcanic ashes. The ash particles are mostly pumice glass shards both unaltered and altered, having a basaltic andesite and partly basalt composition. Petrographic observation shows that pumice shards in the soils are most abundant in the western region of the peninsula. Jeong and Yoon (2001) interpreted that they were blown from Deception Island located about 130 km southwest of King George Island (Fig. 1).

SOIL GEOCHEMISTRY

Based on bedrock type, Barton Peninsula soils are subdivided into four suites; soils on granodiorite (S-GD), soils on basaltic andesite (S-BA), soils on lapilli tuff (S-LT), and soils on the Sejong Formation (S-SJ). Soils on basaltic andesite are further subdivided into two subsuites, S-

BA1 developed on BA1 volcanic rocks having positive Eu anomaly and S-BA2 on BA2 volcanic rocks having negative Eu anomaly.

The ICV [ICV = $(Fe_2O_3 + K_2O + Na_2O + CaO + MgO + MnO + TiO_2)/Al_2O_3$; Cox et al., 1995] values of Barton Peninsula soils range between 1.00 and 1.44 with an average of 1.13 (Table 1). The ICV values of S-GD ranges between 0.9 and 1.3 (av. 1.1), S-BA1 between 0.8 and 1.4 (av. 1.2), S-BA2 between 0.9 and 1.3 (av. 1.1), S-LT between 1.0 and 1.2 (av. 1.1), and S-SJ between 1.0 and 1.4 (av. 1.2), indicating that the Barton Peninsula soils are compositionally immature and dominated by non-clay silicate minerals. All the ICV values of soils except for soils on the Sejong Formation are slightly lower than those of bedrocks. This implies that most of the Barton Peninsula soils are formed by physical disintegration of bedrocks and that components of chemical weathering product such as clay minerals are very minor, suggesting that the chemical weathering has not occurred significantly.

Chemical index of alteration (CIA; Nesbitt and Young, 1982) values of Barton Peninsula soils ranges between 49.6 and 77.3 with an average of 59.2. S-BA ranges between 49.6 and 77.3 (average 58.2; S-BA1 = 57.5, S-BA2 = 58.6) and S-GD between 51.7 and 63.7 (average 57.5). Average CIA values in the two soil suites are equal at 5% level of significance. Soil samples have generally higher CIA values than bedrocks. The high CIA values of soils may not indicate the chemical weathering of the bedrocks in the Barton Peninsula, but represent the results of mixing with eolian smectite-bearing pumice shards. Barton Peninsula soils have different oxide ratios (Y_2O_3/ZrO_2 and ZrO_2/TiO_2) from bedrocks. Also, these oxide ratios are different among soil samples. These results indicate nonuniformity of parent materials, attributing to varying degrees of mixing of allogenic components including eolian pumice shards as observed in soil microstructes. The result of this study suggests that the CIA value of soils for measure of chemical weathering degree should be used with caution.

The REEs of studied soils have slight different distribution patterns from those of respective bedrocks. Also, all soil samples have total REE contents about 30% higher than respective bedrocks. The REE enrichments in the studied soils compared to bedrocks would indicate some degrees of chemical weathering of bedrocks. Most soil samples show slightly fractionated distribution patterns than bedrocks except for S-BA1. The latter displays lesser fractionation than the bedrock [(La/Yb)n = 3.6 vs. 4.4]. In this study, REE mobility in surface soils is assumed to be negligible based on the low chemical weathering degrees as evidenced by slight changes in major elements compared to bedrocks. Homogeneous REE distribution patterns in each soil suite also suggest that the soil REEs were not affected much during weathering, but rather are controlled by source material characteristics. Thus, it is interpreted that mobilization and fractionation of REEs during the chemical weathering were relatively insignificant and that the REE characteristics are resulted from mixing of different source components. Considering that REEs are transferred to soils quantitatively from bedrocks during weathering the different REE distribution patterns of the

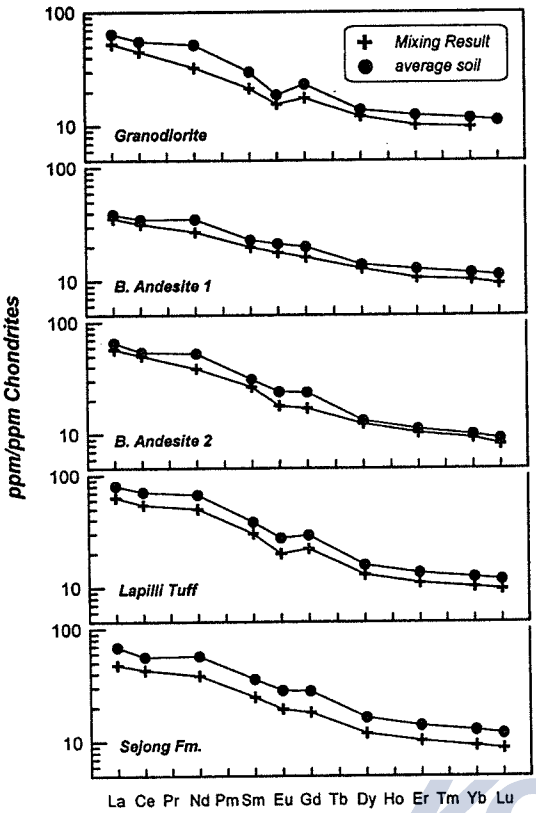

Figure 2. Chondrite-normalized results of REE mixing calculations compared to averages of the Barton Peninsula soil suites.

soils compared to corresponding bedrocks indicate that the REE characteristics of each soil suite were not solely inherited from the bedrocks, but may reflect the varying importance of extra materials, such as adjacent parent materials and eolian additions relative to contributions from the respective parent material.

Bedrocks in the Barton Peninsula soils are granodiorite, basaltic andesite, lapilli tuff, and the Sejong Formation. In addition to these bedrocks, eolian input is also considered as a potential contributor. As discussed above pumice shard from Deception Island constitutes an important eolian addition. As an additional eolian source it is well known from ice core studies in Antarctica that atmospheric transport of dust has been continuous and that dusts have been originated from Patagonia region of South America (Grousset et al., 1992; Basile et al., 1997).

Mixing calculations based on immobile REEs (Fig. 2) show that as expected bedrocks contributed major influence on the REE compositions of fine fractions of the overlying soils, with proportions ranging from 45% for S-BA1 to 75% for S-LT. The modeled mixes also show that significant amounts of externally derived materials were also mixed in the Barton Peninsula soils. Generally, the Patagonian dust proportion is estimated to be in the range between 5 and 15%, whereas pumice shard formed the significant contributor to the fine fraction of the soil in S-BA1 comprising about 40%. The latter contributed about 15% in S-GD, but its contribution to S-BA2, S-LT, and S-SJ is generally about 5%. The high pumice shard contribution to S-BA1 can be explained by the valley-like topography with gentle slope dipping to the southwest, the direction of the pumice shard source.

CONCLUSIONS

Fine fractions of soils in King George Island, South Shetlands Islands, West Antarctica have been studied texturally and geochemically to understand soil-forming process. We conclude the following from the data and the discussion presented here:

1) Soils are unsorted and composed of mineral and rock fragments derived from the bedrock and volcanic ashes. The presence of both unaltered and altered pumice shards seems to indicate the importance of eolian additions to the soil formation in the Barton Peninsula, King George Island. Soils are subdivided into five suites depending on the different lithology of bedrock.

2) Geochemistry of soils on the Barton Peninsula has been more influenced by eolian additions than the chemical weathering, as evidenced by rare earth element compositions. Fresh and altered volcanic ashes blown from Deception Island contributed much in the early deglaciated areas, the western part of the peninsula, which is followed by eolian dusts sourced from Patagonia, South America. The latter influence is well distributed in the whole peninsula. Also, mixing of soil materials from the neighboring bedrocks also controlled soil REE geochemistry.

3) Even in the warmer and humid climatic conditions in the maritime Antarctic region, the chemical weathering of bedrocks seems insignificant, probably due to the relatively short time exposure of about 6000 years since the last deglaciation. The result of this study suggests that the present soils in the maritime Antarctica are mostly composed of physically weathered mineral and rock fragments mixed with eolian additions of volcanic ashes and Patagonian dusts.

ACKNOWLEDGEMENTS: This research was supported by a grant from the Korea Ocean Research and Development Institute (Antarctic paleoclimatology and paleoceanography-PP03106). We thank Dr. G.Y. Jeong for providing some soil samples

REFERENCES

Basile, I., Grousset, F., Revel, M., Petit, J., Biscaye, P., and Barkov, N. (1997) Patagonian origin of glacial dust deposited in East Antarctica (Vostok and Dome C) during glacial stages 2, 4 and 6. *Earth Planet. Sci. Lett.* 146, 573-589.

Campbell, I. B. and Claridge, G. G. C. (1987) Antarctica: Soils, weathering processes and environment. Developments in soil sciences 16, Elsevier, Amsterdam, 368.

Cox, R., Lowe, D. R., and Cullers, R. L. (1995) The influence of sediment recycling and basement composition on evolution of mudrock chemistry in the southwestern United States. *Geochim. Cosmochim. Acta* 59, 2919-2940.

Grousset, F. E., Biscaye, P. E., Revel, M., Petit, J. R., Pye, K., Joussaume, S., and Jouzel, J. (1992) Antarctic (Dome C) ice core dust at 18 ky BP – isotopic constraint on origins. *Earth Planet. Sci. Lett.* 146, 573-589.

Jeong, G. Y. and Yoon, H. I. (2001) The origin of clay minerals in soils of King George Island, South Shetland Islands, West Antarctica, and its implications for the clay-mineral compositions of marine sediments. *J. Sed. Res.* 71, 833-842.

Nesbitt, H. W. and Young, G. M. (1982) Early Proterozoic climates and plate motions inferred from major chemistry of lutites. *Nature* 299, 715-717.

The 10th Seoul International Symposium on Polar Sciences
October 21-22, 2003, Incheon, Korea

SEAFLOOR STRUCTURE AROUND THE EPICENTER OF THE GREAT ANTARCTIC PLATE EARTHQUAKE

Yoshifumi Nogi[1] and Kin-ichiro Koizumi[2]

[1] National Institute of Polar Research, 1-9-10 Kaga, Itabashi, Tokyo 173-8515, Japan [nogi@nipr.ac.jp]
[2] Ocean Research Institute, University of Tokyo, 1-15-1 Minamidai, Nakano, Tokoy 164-8639, Japan

The March 25, 1998 great Antarctic plate earthquake is one of the largest oceanic intraplate strike-slip events ever recorded. The mainshock occurred far from the nearest plate boundary and nearest recorded earthquake (Fig. 1). The most of aftershock locations suggest E-W trending fault plane, which is almost perpendicular to the nearest fracture zones. However E-W trending structural lineaments have not been observed from marine gravity anomalies by Sandwell and Smith (1997) around the epicenter of the great Antarctic Plate earthquake and the driving force of that is still unknown. Detailed marine geophysical surveys of the area are needed to elucidate the cause of the earthquake.

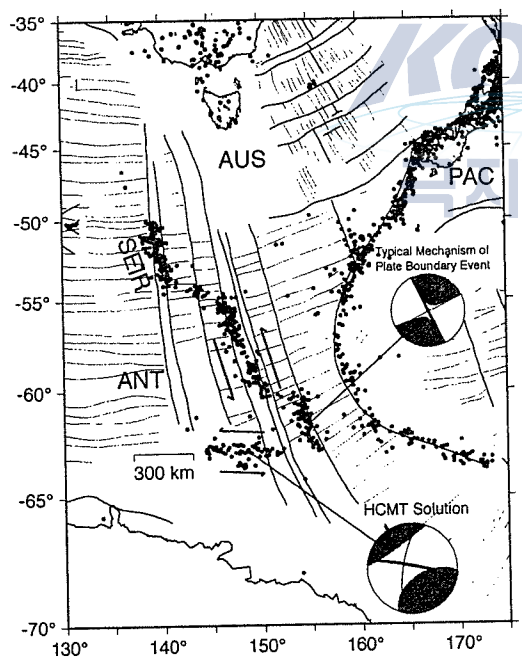

Figure 1. The epicenters around the study area (solid circles). Typical focal mechanism (middle right) and that of the great Antarctic Plate earthquake (lower right) are also indicated. Dashed and solid lined show the fracture zones and magnetic anomaly lineations, respectively. AUS: Australia Plate, PAC: Pacific Plate, ANT: Antarctic Plate, SEIR: South East Indian Ridge.

A detailed swath bathymetry survey had been conducted around the mainshock epicenter of the great Antarctic earthquake during Leg 2 of KH01-3 (R/V Hakuho-maru, Ocean research Institute, University of Tokyo) in January 2002. Swath bathymetry data had been obtained by SeaBeam 2120 along N-S oriented observation lines with intervals of about 7 km, and one E-W observation line, which just across the epicenter. The results of bathymetry data are shown in Figure 2. We found a seamount with almost E-W tending lineaments just in the south of the epicenter of the mainshock. The strike of the fault plane deduced from aftershocks almost coincides with the trend of lineaments in the seamount. These E-W trending lineaments are

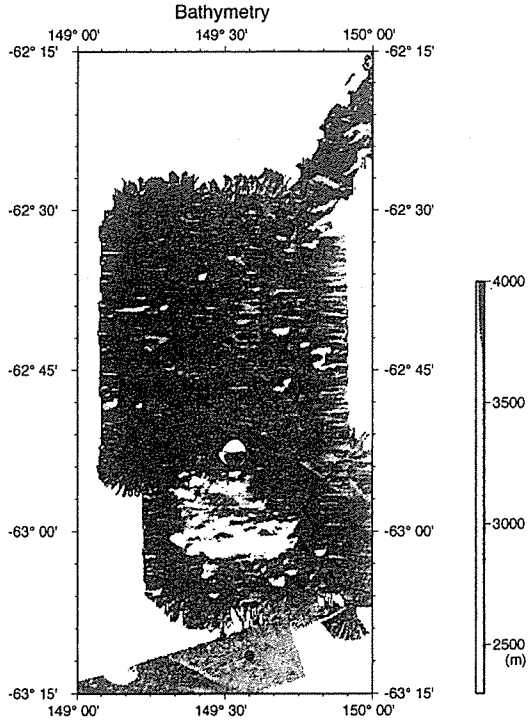

Figure 2. Bathymetry map obtained by SeaBeam surveys during Leg2 of KH01-3 cruise around the epicenter of the great Antarctic Plate earthquake. The focal mechanism of mainshock of the great Antarctic earthquake and the epicenters of the aftershock (solid circles) from ISC are also shown.

most likely preexisting structures and seem to be normal fault related to the initial rifting between Antarctica and Australia. The great Antarctic earthquake may occur along the same trending lineaments in the foot of the seamount covered by sediments.

The gravity and magnetic data had been also collected along the ship's track in the study area. Clear positive magnetic anomalies are observed in the north of the seamount, but prominent magnetic anomalies are not detected in the seamount. The depth of the seafloor in the south of the seamount gradually shallows toward the Antarctic continent. In the north of study area, NE-SW trending magnetic anomalies are also observed. The feature of the free-air gravity anomalies in the south are different from that in the north bounded by the NE-SW trending magnetic anomalies. These may indicate that the nature of oceanic crust where the mainshock and aftershocks occurred is different from that in the north of NE-SW trending magnetic anomalies.

REFERENCES

SANDWELL, D. T. and SMITH, W. H. F. (1997): Marine gravity anomaly from Geosat and ERS-1 satellite altimetry. Journal of Geophysical Research, 102, 10039-10054.

The 10th Seoul International Symposium on Polar Sciences
October 21-22, 2003, Incheon, Korea

MULTIDISCIPLINARY SURVEYS BY 'STRUCTURE AND EVOLUTION OF THE EAST ANTARCTIC LITHOSPHERE': SEAL–2000, -2002

M. Kanao[1], H. Miyamachi[2], S. Toda[3], H. Murakami[4], T. Tsutsui [5], T. Matsushima[6], M. Takada[7], A. Watanabe[6], M. Yamashita[8], K. Yoshii[9], K. Kaminuma[1] and SEAL Geotransect Group

[1] National Institute of Polar Resaerch, 1-9-10 kaga, Itabashi-ku, Tokyo 173-8515, Japan [kanao@nipr.ac.jp]
[2] Kagoshima University, Kagoshima 890-0065, Japan [miya@sci.kagoshima-u.ac.jp]
[3] Aichi Education University, Hirosawa 1, Inogatani-cho, Kariya 448-8542, Japan [shigeru@auecc.aichi-edu.ac.jp]
[4] Earthquake Observation Research Technology Center, Tennoudai 3-1, Tsukuba, Ibaraki 305-0006, Japan [mrkm@geo.bosai.go.jp]
[5] Akita University, Tegata Gakuen-cho 1-1, Akita 010-8502, Japan [tom@geophys.mine.akita-u.ac.jp]
[6] Kyushu University, 2-5643-29 Shin'yama, Shimabara, 855-0843, Japan [mat@sevo.kyushu-u.ac.jp, atsushi@geo.kyushu-u.ac.jp]
[7] Hokkaido University, Nishi 8, Kita 10, Kita-Ku, Sapporo 060-0810, Japan [takada@eos.hokudai.ac.jp]
[8] The Graduate University for Advanced Studies, 1-9-10 Kaga, Itabashiku, Tokyo, 173-8515, Japan [yama@nipr.ac.jp]
[9] Kyoto University, Gokasho, Uji, Kyoto, 611-0011, Japan [yoshii@rcep.dpri.kyoto-u.ac.jp]

Lithospheric evolution and deep structure viewed from East Antarctic Shield have significance in relating to the continental growth process in Earth's evolution. Here, we focus on the lithospheric structure of the early-Paleozoic crust of the Lützow-Holm Complex (LHC), Enderby Land, East Antarctica. LHC is considered to be one of the collision zones between the East- and the West-Gondwana during the formation of a paleo-supercontintnt when the Pan-African orogeny. The "Structure and Evolution of the East Antarctic Lithosphere (SEAL)" project has been carried out since 1996-1997 austral summer season in the framework of the Japanese Antarctic Research Expedition (JARE). Several geophysical studies and deep seismic refraction / wide-angle reflection surveys have been conducted in the LHC. The main target of the SEAL seismic traverse is to obtain a lithospheric imaging in several geological terrains from the eastern Archean (Napier Complex) to the early-Paleozoic ages (LHC & Yamato Mountains) between Western Enderby Land and Eastern Dronning Maud Land.

In the austral summer season in 2000, and 2002, deep seismic surveys were conducted on ice sheet in the northern Mizuho Plateau of the LHC by JARE-41, and –43, respectively. In both surveys, more than 170 plant-type 2 Hz geophones were installed on the Mizuho plateau totally 190 km in length. A total of 8,300 kg dynamite charges at the fourteen seismic shot points on the ice

sheet gave an enough information concerning the deep structure of a continental margin of the LHC. These surveys revealed that the Moho depth was more than 40 km with the velocity of the surface layer, middle crust, lower crust and mantle, about 6.2, 6.4, 6.7 and 7.9 km/s, respectively. Moreover, the clear reflections from the lower crustal depth and around the Moho discontinuity were observed on the record sections; which implies the existence of heterogeneity on the crust-mantle boundary beneath the Paleozoic orogenic zone of the LHC. Laminated layers around the Moho discontinuity could also be identified by the precise spectral analyses for the Moho reflection phases (PmP waves).

The 10th Seoul International Symposium on Polar Sciences
October 21-22, 2003, Incheon, Korea

LOCAL SEISMIC ACTIVITY AROUND SYOWA STATION, EAST ANTARCTICA

Katsutada Kaminuma and Masaki Kanao

Department of Earth Science, National Institute of Polar Resaerch, 1-9-10 kaga, Itabashi-ku, Tokyo 173-8515, Japan [kaminuma@nipr.ac.jp, kanao@nipr.ac.jp]

The observation of seismic monitoring at Syowa Station (69°S, 39°E: SYO), located on the continental margin of the Western Enderby Land, East Antarctica, was started in 1959. Phase readings of the earthquakes have been reported since 1967 and have been published from the National Institute of Polar Research once a year since1968, as one of the Data Report Series (e.g., Kanao 1999).

An observation of a tripartite seismic network had been carried out at SYO during three years of 1987-1990 (Akamatsu et al. 1989). Epicenters of local earthquakes were determined the first time by the array network during the three years. A many different type of earthquakes, such as a mainshock-aftershock type, twin earthquake, earthquake swarms, etc., were detected at that time. Since that period, local events around SYO can be detected empirically from their waveforms on the monitoring seismograms. The seismic activity during 1987-1990 was higher than that of the following a decade. Earthquake location at that period was concentrated along the coast area and the central part of the Lützow-Holm Bay (LHB).

In the period of 1990-1996, nine local earthquakes were recorded with many different types of events. The seismicity during the period was very low and the magnitudes ranged from 0.1 to 1.4. Some of the events were determined their locations by a single station method at SYO, by using particle motions of the initial phase and S-P times (Kaminuma et al. 1998).

Two local events were detected in 1998 and one event in 2001. The last event was recorded on February 21, 2001. The P-S time of the event was determined 10.8 s on the three-component seismogram of the short period seismograph (HES). The low seismic activity is still continued around 2000.

In this presentation, we discuss about the characteristics of time series for the local seismicity around the LHB region relating to the deglacial lithospheric uplift and the sea-level changes.

REFERENCES

Akamatsu, J., N. Ichikawa & K. Kaminuma, 1989, Polar Geosci.,3, 1-12.

Kaminuma, K., M. Kanao & A. Kubo, 1998, Polar Geosci.,11, 23-31.

Kanao, M., 1999, JARE Data Rep., 236 (Seismology 33), 1-65.

MORPHOLOGICAL CHARACTERISTICS OF THE INTERSECTION BETWEEN PHOENIX RIDGE AND THE HERO FRACTURE ZONE

Kyu Jung Kim, Young Keun Jin, Sang Heon Nam, Joo Han Lee and Yeadong Kim

Korea Polar Research Institute, KORDI, Ansan P.O. Box 29, Seoul 425-600, Korea [kjkim@kordi.re.kr]

ABSTRACT: The bathymetric data of the Phoenix Ridge show the characteristics of both slow- and intermediate-spreading ridges. A rift valley of the Phoenix Ridge and the Hero Fracture Zone represent the steep scarp and the deep valley, which are affected by the extension. The extinction of two directions would occur the oblique slip fault against the spreading direction, and form the discontinuous and hooked ridges in the southern domain. The abrupt decrease of the spreading rate effects the anomalous topographic feature. The last extension of the rift valley may occur the melting of magma beneath the axis, and then, the focused volcanism form the anomalous seamount.

INTRODUCTION

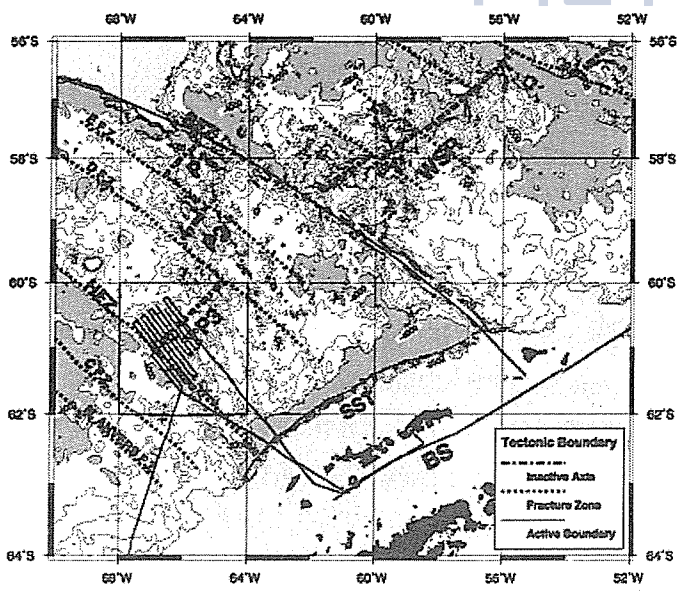

Figure 1. Tectonic boundary map and multibeam track chart over the bathymetry in Drake Passage predicted using satellite altimetry (Smith and Sandwell,1994).

Mid-Ocean Ridge apparently divided by morphological characteristics. Ridge Morphology is determined by mantle temperature and chemical heterogeneity in the upper mantle (Niu, *et al.*, 2001) governing ridge process. Large morphological characteristics in spreading ridges, classified the variation of topography along/across spreading axis, and the segmentation across the axes. These apparent topographic patterns are known to be intimate with spreading rates. The Phoenix Ridges are the youngest extinct ridges at 3.3 Ma (Livermore, *et al.*, 2000) and conserved the topography with a thin sediment cover

at the cessation of spreading, because of the strong Antarctic Circumpolar Current. The morphological variations along southernmost Phoenix Ridge (P3) reflect the complex tectonic history of Phoenix Plate (Fig. 1). The morphology and segmentation characteristics have important implications for the nature of spreading process because the morphotectonic variability may be controlled by a combination of plate separation rates, asthenospheric flow patterns and temperatures, and magma supply. We consider the bathymetric data over the extinct spreading center and examine the topographic feature with respect to various proposed morphological model.

BATHYMETRY DATA

The Bathymetric data, using SeaBeam 2000, were collected during a Korea Antarctic Research Program (KARP) conducted in austral summer of 1999/2000 onboard Korean vessel R/V Onnuri. The mapping covered an area between latitude 60° 10' and 61° 40' S, out of a maximum distance of approximately 70 km to either side of the Phoenix Ridge, P3. Fig. 1 shows Seabeam tracks, which are oriented almost perpendicular to the spreading axis. The track lines were spaced with 7 km, covered over the intersection between Phoenix Ridge and Hero Fracture Zone (HFZ) and half of the segment, P3, except for some local topographic highs.

ON-AXIS AND OFF-AXIS MORPHOLOGY

The morphology of P3 shows both of the slow- and intermediate-spreading characteristics. The segments between HFZ and Shackleton Fracture Zone show typical slow-moving discontinuities of the sharp boundary and depressions, whereas HFZ shows complex features which have a pronounced valley at the Phoenix Ridge and HFZ intersection, and shows wider fault zone and ridges at the southern part of the fracture zone abutted on a trench. The near-axis spreading center morphology shows very high relief, and is anomalous when compared to either fast or slow spreading ridges elsewhere. Well-developed nodal basin occurs at the intersection, at depths of 4500 – 5500 m, and is the only area in which any significant accumulation of sediment has occurred. The ridge crest rises to a shallowest point near the segment center. In the segment center, a prominent seamount that rises to a shallow 750 m depth and has a mean diameter of about 30 km, is present. The southwestern region of the axial seamount is flanked by two great ridges which rise to an approximately 2500 m depth. The northwestern flank is broader and further away from the ridge axis than the southeastern flank. It suggests that both of flanks are rifted parts of a former axial topographic high, but the different width of the ridges may be caused by asymmetric lithospheric stretching during the last extension stage.

The trend of tectonic fabrics is mainly N45° E parallel to spreading axis and N135° E parallel to fracture zone (Fig 2). Rotated and oblique fabrics observed on the southern domain separated the

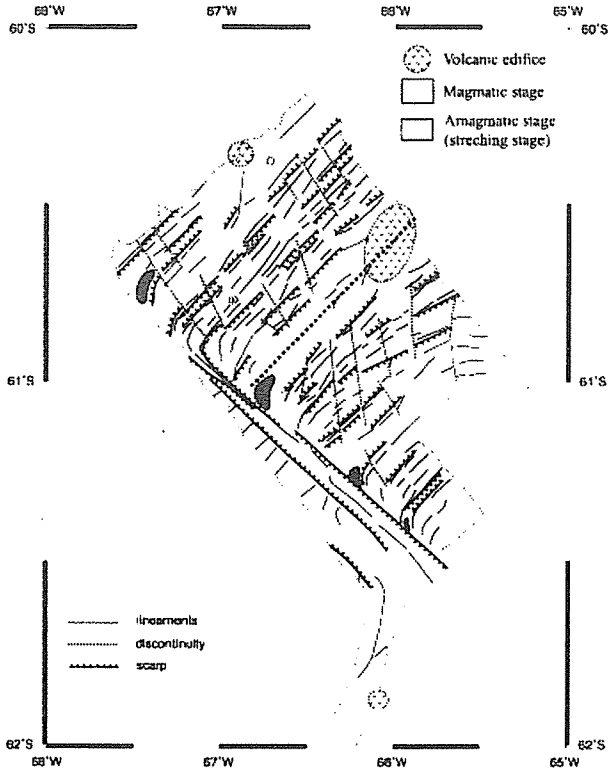

Figure 2. Line drawing interpretation and structural morphology.

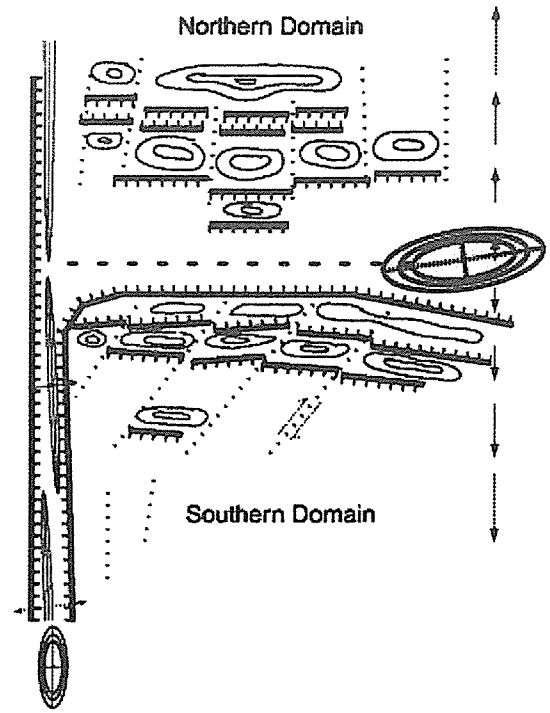

Figure 3. Schematic diagram of Phoenix Ridge outlining the relationship between the faulting patterns.

spreading axis as well as near transform and fracture zone. Rotated fabrics near transform and fracture zone are explained by transform shear, on the other hand, discontinuous and oblique fabrics on the southern domain may be caused by the variable or unstable spreading during the latest stage of spreading.

DISCUSSION AND CONCLUSION

The Phoenix Plate had evolved from an intermediate spreading ridge to a slow spreading ridge. At 9 Ma, the spreading rate of the Phoenix ridges decrease from 32 mm/yr. to 27 mm/yr or 16 mm/yr (Livermore, *et al.*, 2000). This reduction of spreading rates remains the topographic features on HFZ, which are the narrower fracture zone and the sharp boundaries at 50 km from the spreading axis, whereas they show the prominent ridges and the broaden fracture zone at above 50 km far away the axis which is typical intermediate-spreading fractures. The averaged depth of the seafloor of P3 is deeper than the calculated depth by using the predicted global depth relation with age. Moreover the relief of flanks is anomalous high. These are the predicted features by the numerical modelling, which are formed by the failure of crust with a decrease of spreading rate.

The study area can be divided into the northern block and the southern block by the spreading

axis. The lineaments of the northern domain are dominant parallel to the spreading axis, but in the southern domain, are some oblique to the spreading axis. Also, the direction of the discontinuities is parallel to spreading direction in northern domain, but changes an oblique angle in southern domain (Fig. 3). These features may be caused by the extensional stress across transform fault zone. The decrease of spreading rate may affect the relative increase of extensional stress, and at the last of spreading, the brittle oceanic crust would be deformed and fragmented.

Axial highs are observed at some extinct, slow-spreading ridges elsewhere, e.g., Powell basin (King, *et al.*, 1997) and Wharton basin (Hebert, *et al.*, 1999), but are by no means common. The abrupt reduction of spreading rate may result in increasing the temporary magma supply. Mantle melting beneath ocean ridges is caused by decompression as mantle adiabatically upwells, and that mantle upwelling results from plate separation. This fact means that the extent of mantle melting increase with increasing spreading rate. As spreading rate reduces, the extent of mantle melting will exceed normal melting extent with a reduced spreading rate, and may be erupted and form the anomalous highs. In addition, the depression with lithosphere cooling and the focused volcanism would increase the topographic relief.

REFERENCES

Hebert, H., Villemant, B., Deplus, C. and Diament, M., 1999, Contrasting geophysical and geochemical signatures of a volcano at the axis of the Wharton fossil ridge (N-E Indian Ocean), *Geophys. Res. Lett.*, 26, 1053-1056.

King, E. C., Leitchenkov, G., Galindo-Zaldivar, J., Maldonado, A. and Lodolo, E., 1997, Crustal structure and sedimentation in Powell basin, *in* Barker, P. F. and Cooper, A. K., (eds.), *Geology and Seismic stratigraphy of the Antarctic Margin, Part2*, American Geophysical Union, Washington D.C., 75-93.

Livermore, R., Balanya, J. C., Maldonado, et al., C., 2000, Autopsy on a dead spreading center: The Phoenix Ridge, Drake Passage, Antarctica, *Geology*, 28, 607-610.

Niu, Y., Bideau, D., Hekinian, R. and Batiza, R., 2001, Mantle compositional control on the extent of mantle melting, crust production, gravity anomaly, ridge morphology, and ridge segmentation: a case study at the Mid-Atlantic Ridge 33-35°N, *Earth Planet. Sci. Lett.*, 186, 383-399.

The 10th Seoul International Symposium on Polar Sciences
October 21-22, 2003, Incheon, Korea

VISUAL OBSERVATION EXPERIMENTS TO INVESTIGATE THE FORMATION PROCESSES OF GLOBULAR GAS HYDRATE

H. Shoji

New Energy Resources Research Center, Kitami Institute of Technology
165 Koen-cho, Kitami 090-8507, Japan [shojihts@mail.kitami-it.ac.jp]

ABSTRACT: Echograms obtained at the continental margin of North-East Sakhalin, Okhotsk Sea show many flare images, which may result from the gas bubble emissions from the seafloor. Gas hydrate obtained at Hydrate Ridge, Cascadia Margin show characteristic globular hydrate structure formed from rising gas bubbles. Laboratory experiments were conducted for the detailed formation processes, and a special apparatus to record tiny gas bubbles was constructed and successfully tested at Lake Baikal for the future observation at the continental margin of North-East Sakhalin.

INTRODUCTION

Submarine gas hydrate investigations have been conducted extensively in the Sea of Okhotsk by the joint Russian-German project, KOMEX[1]. Echograms obtained at the continental margin of North-East Sakhalin show hydroacoustic anomalies which are hypothetically coupled with gas seepages. Gas hydrate specimens from near-surface sediments of Hydrate Ridge, Cascadia Margin show a peculiar structure with pores (globular gas hydrate) that result from rising gas bubbles[2]. A similar structure could be observed at the North-East Sakhalin, if gas hydrate forms near the sea floor from gas bubbles seeping from a depth in the sedimant.

The purpose of this study is to form globular gas hydrate artificially in a laboratory to understand the formation processes.

LABORATORY EXPERIMENTS

A pressure cell was designed and constructed in the New Energy Resources Research Center, Kitami Institute of Technology to form gas hydrates from gas bubbles in water under a high hydrostatic pressure. Optical window in the cell allows to observe the detailed formation processes during experiments (Fig.1).

CO_2 gas bubbles were supplied through a nozzle of 0.5 mm inner diameter at the cell bottom.

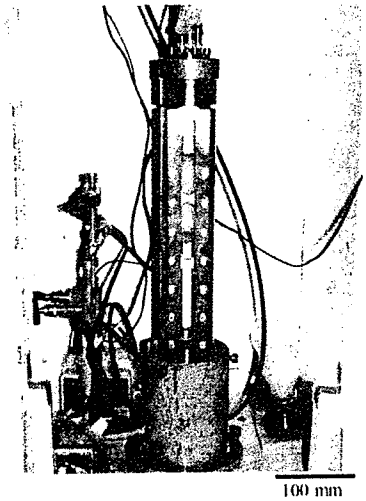

Figure 1. Pressure cell

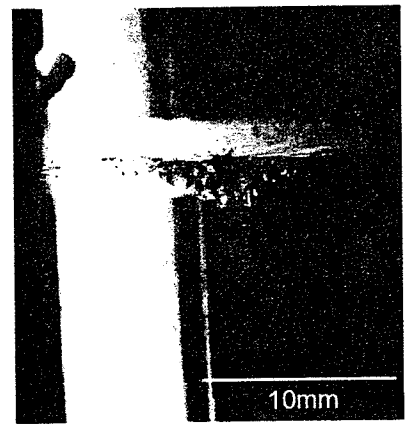

Figure 2. Globular gas hydrate

CO_2 gas bubbles were slowly but continuously supplied into the water to increase the hydrostatic pressure from the ambient pressure to 2.3 MPa. With the hydrostatic pressure (P) lower than about 1.4 MPa, gas bubbles simply ruptured at the water surface. Around P is close to 1.4 MPa, small pieces of gas hydrate appeared at the water surface when gas bubbles ruptured, and then grew to a thin film covering the entire water surface. Then gas bubbles rising from the cell bottom were trapped by the gas hydrate film and piled up depthward with bubble surface transforming into globular gas hydrate. Figure 2 shows globular gas hydrates formed at 274 K and around 2.3 MPa.

FIELD OBSERVATIONS AT LAKE BAIKAL AND AT THE OKHOTSK SEA

KOMEX project could not observe gas bubble emission from the seafloor at the continental margin of North-East Sakhalin, so far. This might be due to a smaller dimension of gas bubbles. A special video apparatus was designed and constructed in the New Energy Resources Research Center, Kitami Institute of Technology to observe gas bubbles of 0.1 mm size under water (Fig. 3a and b). The apparatus constructed was tested at Lake Baikal, and successfully recorded near-bottom particles of 0.1 mm size at a water depth of 1400 m. This apparatus will be used to detect tiny gas bubble emissions at the continental margin of North-East Sakhalin during the field operation of CHAOS project (hydro-Carbon Hydrate Accumulations in the Okhotsk Sea; an international collaboration effort among Russian, Japanese, Korean, German and Belgium researchers) in 2003.

REFERENCES

1) N. Biebow, T. Ludmann, B. Karp, and R. Kulinich, 2000. Cruise Reports: KOMEX V and VI: RV Professor Gagarinsky cruise 26, MV Marshal Gelovany cruise 1. GEOMAR Report, 88, 296 pp.

2) G. Bohrman, E. Suess, J. Greinert, B. Teichert, T. Naehr, 2002. Gas hydrate carbonates from Hydrate Ridge, Cascade convergent margin: Indicators of near-seafloor clathrate deposits., 102-107.

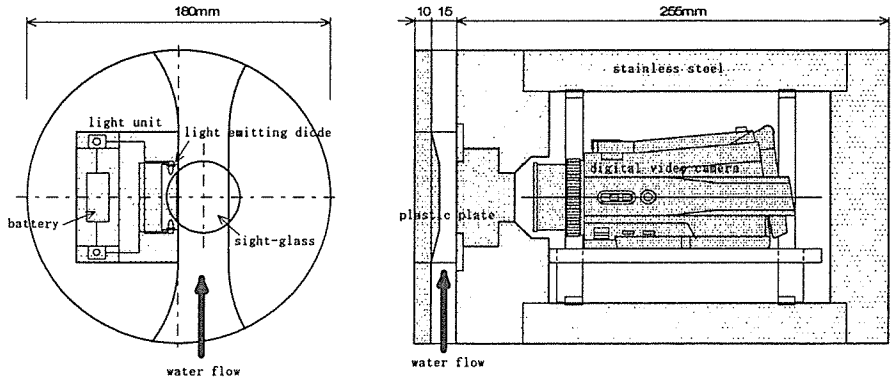

Figure 3a. Underwater video appararus

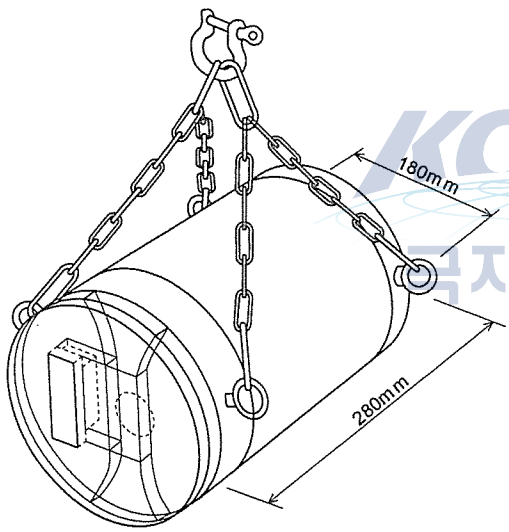

Figure 3b. Operation of video apparatus

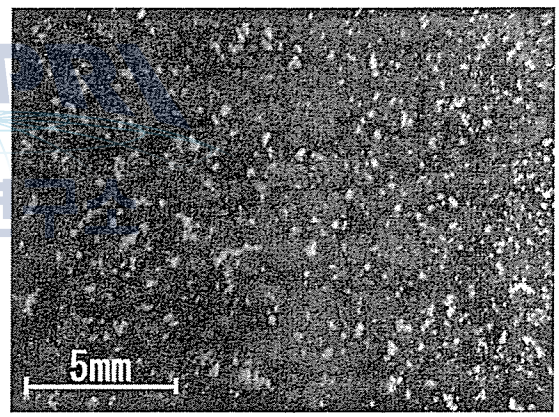

Figure 4. Tiny particles recorded at Lake Baikal

The 10th Seoul International Symposium on Polar Sciences
October 21-22, 2003, Incheon, Korea

GAS HYDRATE BSR-DERIVED HEAT FLOW VARIATION ON THE SOUTH SHETLAND CONTINENTAL MARGIN, ANTARCTIC PENINSULA

Young Keun Jin, Sang Heon Nam, Yeadong Kim, Kyu Jung Kim and Joo Han Lee

Korea Polar Research Institute, KORDI, Ansan P.O. Box 29, Seoul 425-600, Korea [ykjin@kordi.re.kr]

ABSTRACT: Bottom simulating reflector (BSR), representing the base of gas hydrate stability field, is widespread on the South Shetland margin (SSM), Antarctic Peninsula. With phase diagram for gas hydrate stability field, heat flow can be derived from BSR depth beneath the seafloor determined on multichannel seismic profiles. The heat flow values in the study area range from 50 mW/m2 to 85 mW/m2 with an average value of 65 mW/m2. The landward heat flow decrease from the South Shetland Trench would be attributed to the landward thickening of the accretionary prism and the upward advection of heat associated with fluid expulsion. The continental slope 1500 m to 3000 m deep, where BSRs are most distinct in the SSM, shows high variation of heat flow possibly due to complex tectonic activities in the study area. The heat flow high is observed near the NW-SE trending large-scale fault.

INTRODUCTION

Gas hydrates are ice-like crystalline solids composed of water molecules, with gas, commonly methane, encaged in a crystalline lattice. Gas hydrates form under low temperature and high pressure conditions when water is saturated with gas (Sloan 1998). They are stable in permafrost regions and at pressure-temperature conditions for seafloor below approximately 300-500 m water depth (Kvenvolden 1993).

Natural gas hydrates have increasingly attracted the attention of the scientific community mainly because of the vast amounts of methane that may be stored in gas hydrates, their potential role in climate change, and their possible interaction with seafloor stability.

Bottom simulating reflector (BSR), representing the base of gas hydrate stability field, is widespread on the South Shetland margin (SSM), Antarctic Peninsula (Figs. 1 and 2). In this study, we calculate heat flow using gas hydrate BSRs observed on multichannel seismic reflection profiles to examine heat flow variation on the South Shetland continental margin, Antarctic Peninsula. The results from this study could be provide better understanding into gas hydrate

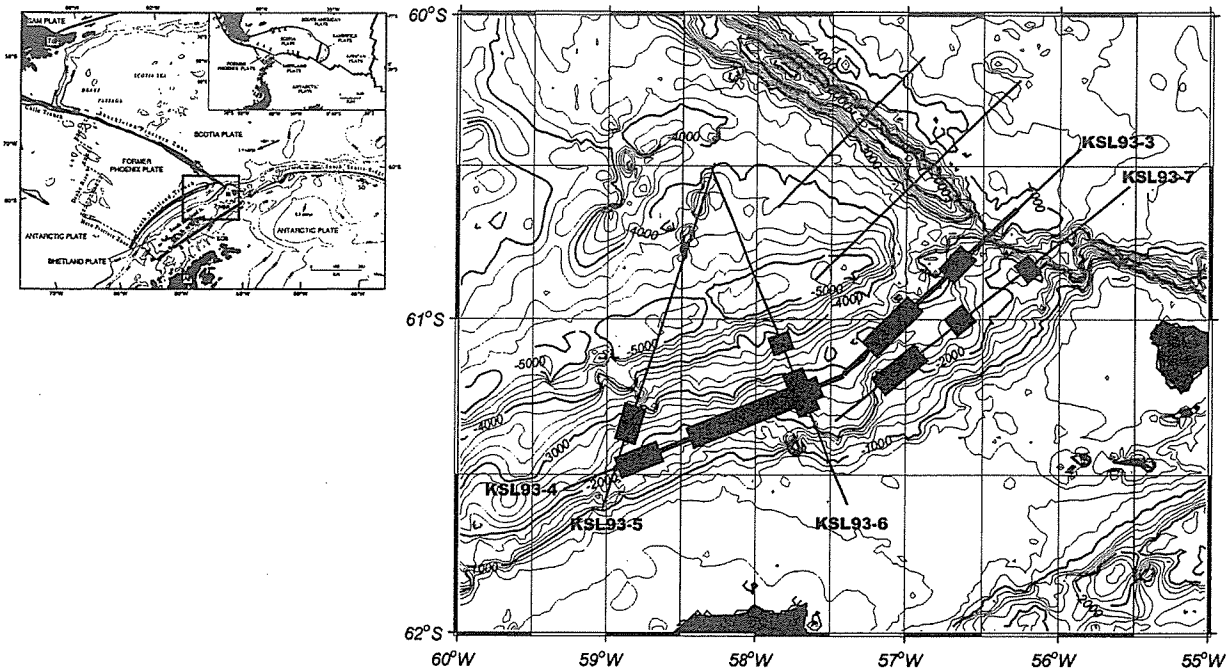

Figure 1. Location of multichannel seismic lines overlaid on bathymetric contour map. Distribution of BSRs observed on the profiles is marked with gray rectangles. Inset shows tectonic setting around the northern Antarctic Peninsula, in which the box indicates the study area. AP-Antarctic Peninsula, EI-Elephant Island, KGI-King George Island and SA-South America.

stability condition and thermal structures of the trench-margin system in the Antarctic Peninsula.

DATA AND METHODOLOGY

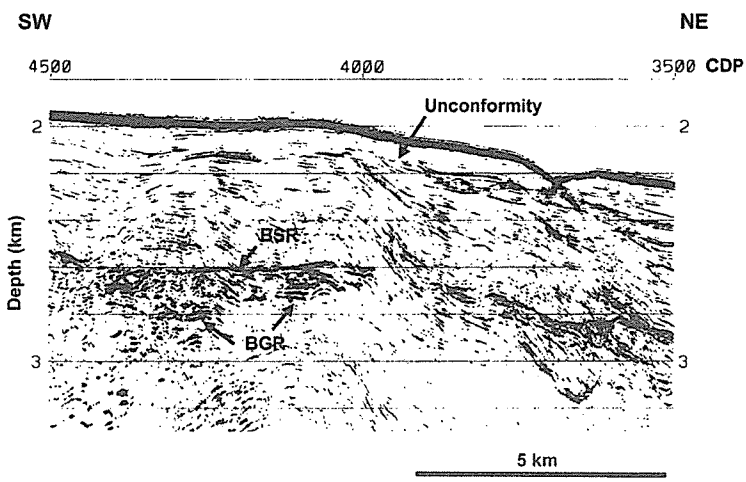

Figure 2. A depth-converted seismic section of profile KSL93-4 showing well-developed BSRs, base of gas reflector (BGR), and an unconformity just beneath the seafloor.

1. Seismic data

The Korean Ocean Research and Development Institute (KORDI) on RV *Onnuri* cruise in the 1993 austral summer. The locations of MCS profiles used for this study are shown in Fig. 2. Data were acquired with a 2400-m long, 96-channel hydrophone streamer and a 16-airgun source with a total volume of 22.6 l. Shots were fired at a spacing of

50 m, giving 24-fold coverage. The data sampling rate was 4 ms.

2. Heat flow calculation

1) Deth of BSR determined by conversion from seismic travel times using interval velocities from multichannel seismic (MCS) reflection data on the South Shetland continental margin

2) Lithostatic pressure (P) from depth-pressure relationship

$P = Pw + Ps = (\rho_w \cdot W + \rho_s \cdot z_{bsr}) \cdot g$

where, ρ_w:the density of sea water (1.05 g/cm3)

ρ_s:the density of sediments above BSR (1.9 g/cm3),

W:waer depth, z_{bsr}:depth below seafloor, g:the acceleration of gravity

3) Pressure-Temperature stability condition (Dickens and Quinby-Hunt, 1994)

$1 / T_{bsr} = 3.79 \text{ X } 10\text{-}3 - 2.83 \text{ X } 10\text{-}4 \log (P)$

where T_{bsr}: the temperature at the BSR depth in K, P : Pressure in MPa .

4) Thermal conductivity (Davis et al., 1990)

$k = 1.07 + 5.86 \times 10^{-4} \times z - 3.24 \times 10^{-7} \times z^2$

where k : the thermal conductivity in W/m °C, z : the depth below the seafloor in m

5) Heat flow (H) calculation

Assuming a linear temperature gradient and using the simple conductive heat transport relation. The seafloor temperature is °C at 2000 m and -0.3°C at 3000 m (Nowlin and Zenk 1988).

$H = k \times (T_{bsr} - T_{sea} / z_{bsr})$

RESULTS AND CONCLUSION

1. Regional Trend

The heat flow values in the study area range from 50 mW/m^2 to 85 mW/m^2 with an average value of 65 mW/m^2 (Fig. 3). A small deviation of heat flow values from the average one suggests that heat flow regime in the study is relatively stable. The landward heat flow decrease from the South Shetland Trench would be attributed to the landward thickening of the accretionary prism and the upward advection of heat associated with fluid expulsion.

2. Local variation

The continental slope 1500 m to 3000 m deep, where BSRs are most distinct in the SSM, shows

high variation of heat flow possibly due to complex tectonic activities in the study area (Fig. 4). The heat flow high is observed near the NW-SE trending South Shetland Fault (SSF). The SSF would be related to a fracture zone in the Phoenix plate or a transfer fault across the Bransfield Basin.

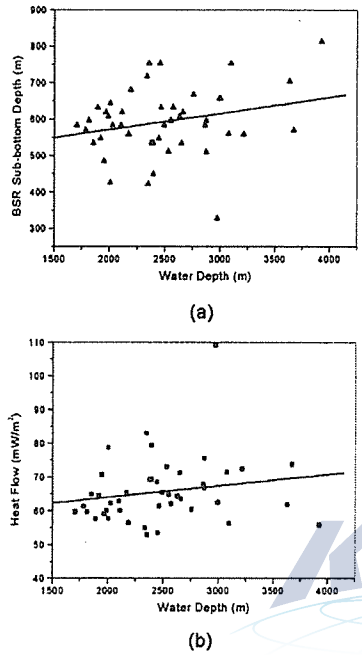

Figure 3. Graphs showing the regional distributions of (a) BSR sub-bottom depths and (b) heat flows with respect to water depth on all seismic profiles. Solid straight lines in the graphs indicate general trends of the distibution.

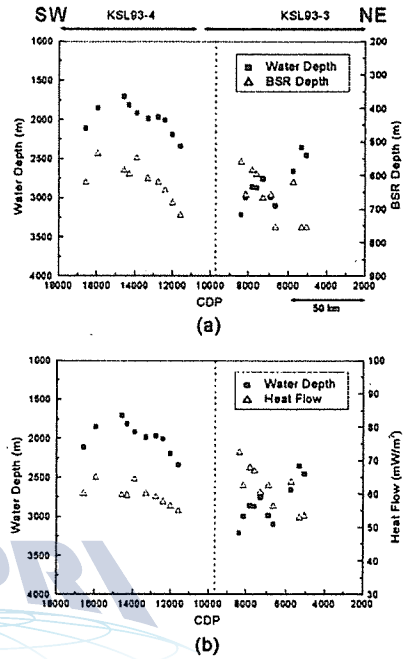

Figure 4. Graphs showing the distributions of (a) water depths and BSR depths and (b) water depths and heat flow values along profiles KSL93-3 and KSL93-4. The dashed line indicates the location of the South Shetland Fault.

INTRODUCTION TO ICE CORE DRILLING PROGRAM ON AMERY ICE SHELF IN THE 2002/2003 ANTARCTIC SUMMER SEASON

Yuansheng Li, Dejun Tan, Zengdi Pan, Zhaoqian Dong, Bo Sun and Jiahong Wen

Polar Research Institute of China, 451, Jinqiao Road, Shanghai, 200129, China [yshli@sh163e.sta.net.cn]

The Chinese Amery Ice Shelf Oceanographic Research program officially commenced in August of 2002. The main objectives of the program are to quantify the interaction between the ocean and the Amery Ice Shelf; to determine the implications of the this interaction for the discharge of grounded ice and to the formation of bottom water; and to derive a long term record (from ice cores and some other information) of the time variability of the interaction. It is intended to build on previous glaciological investigations of the Lambert Glacier drainage basin and of the Pryds Bay oceanography. Before this program, the Australian scientists already have carried out the hot water drilling program at several sites on the Amery Ice shelf from 1999-2002. And they will be continuously to conduct the program on the Amery Ice Shelf in 2003/2004 Antarctic summer season.

To achieve these aims the operational requirement is to produce a series of field investigations of the Amery Ice Shelf at selected locations in order to sample a range of in situ parameters and ice cores (both for continental ice core and marine ice core). The field working includes the surface ice radar determinations, ice core drilling program, hot water drilling program, mass balance measurements, high resolution GPS observations and oceanographic observations around the edge of Amery Ice Shelf and the Prydz Bay. The program is from 2002 to 2005. The 2002-2003 Antarctic summer season was to carry out an ice core drilling at the chosen site and investigations of surface ice radar, GPS, mass balance and oceanography at several selected locations both in the Amery Ice Shelf and at the edge of Amery Ice Shelf in the ocean.

7 selected sites were carried out the investigations of surface ice radar, GPS and mass balance, and one site for ice core drilling on the Amery Ice Shelf, and 12 sites were carried out for oceanographic measurements (XCTD, ADCP and LADCP) in the edge of the Amery Ice Shelf in 2002/2003 Antarctic summer season.

296ms ice core was obtained at the site of A2. The Japanese National Institute of Polar Research supported a 500ms ice core drill system for us. There are three parts of ice for this ice core: 33 meters firn, 242 meters continental ice and 20 meters marine ice. The most of the continental ice is the broken ice. The interface between the continental ice and the marine ice is 275 meters in depth

at the drill site. The temperature profile and the ice density profile were obtained from the borehole. The depth of the borehole is 302ms. The data and ice core samples of this field investigation are processing now.

The 10th Seoul International Symposium on Polar Sciences
October 21-22, 2003, Incheon, Korea

724 M DEEP ICE CORE FROM AKADEMII NAUK ICE CAP SEVERNAYA ZEMLYA (RUSSIAN ARCTIC) - ELECTRICAL CONDUCTIVITY MEASUREMENTS AND ISOTOPIC RECORD

D. Fritzsche[1], R. Schütt[1], H. Meyer[1], H. Miller[2] and F. Wilhelms[2]

[1] Alfred Wegener Institute for Polar and Marine Research, P.O.Box 600149, 14473 Potsdam, Germany [dfritsch@awi-potsdam.de]
[2] Alfred Wegener Institute for Polar and Marine Research, P.O.Box 120161, 27515 Bremerhaven, Germany

In the Eurasian Arctic, the archipelago of Severnaya Zemlya is the most eastern one which is covered by a considerable ice cap, giving the opportunity to study regional climate signals from the Holocene period.

The Academii Nauk ice cap (Komsomolets Island) was chosen for drilling a deep ice core because it is the thickest and coldest ice cap on Severnaya Zemlya. A suitable drilling site was found at 80°31'N 94°49'E by the help of airborne radio-echo sounding data and SAR interferometry. The ice thickness was 724 m at this location. Drilling was carried out between 1999 and 2001 reaching bedrock. It was a joint project of the Alfred Wegener Institute (Germany), the Arctic and Antarctic Research Institute, and the Mining Institute (Russia, St. Petersburg both). An electromechanical ice core drill (KEMS-112M) was used, the same type as at Vostok Station, Antarctica.

The paper presents the results of electrical conductivity measurements (DEP) of the whole ice core. Several zones with high conductivity were assumed to be caused by major volcanic eruptions. By help of catalogues of historical volcanic events we used these signals for core dating of the upper 245 meters. The time scale developed this way is in good agreement with horizons of enriched radioactivity caused by nuclear weapon tests in the early 1960's and by the Chernobyl accident.

The $\delta^{18}O$ record fits almost perfectly to values published earlier by Klementev et al. for Akademii Nauk, however, we have no evidence for the age model used in this Russian paper. We found annual accumulation rates in the isotope record and in the electrical data indicating none-steady state conditions of this glacier in the past. Hence, the core ages are overestimated by flow models. There seems to be an age discordance in the deepest part of the core.

For Akademii Nauk ice cap the isotope data indicate a climate warming since app. 1860 which is much higher than found at central Greenland (GRIP/GISP2), Devon Island or Hans

Tausen ice cap.

REFERENCE

Klementev, O.L.; Potapenko, V. Yu.; Savatyugin, L.M. & Nikolaev, V.I.: Studies of the internal structure and thermal-hydrodynamic state of Vavilov Glacier, Archipelago Severnaya Zemlya. IAHS Publ. 208, 1991, p.49-59

The 10th Seoul International Symposium on Polar Sciences
October 21-22, 2003, Incheon, Korea

INTRODUCTION OF THE CHINESE POLAR CRYOSPHERIC DATABASE SYSTEM (CPCDS)

Xiang Qin[1], Dahe Qin[2] and Yongjian Ding[2]

[1] Laboratory of Remote Sensing Information Sciences, Institute of Remote Sensing Applications, Chinese Academy of Sciences (CAS), P.O.Box9718, Beijing 100101, China [qinxiang@lab.irsa.ac.cn]
[2] Cold and Arid Regions Environmental and Engineering Research Institute, CAS, No.260 West Donggang Road, Lanzhou 730000, China [dhqin@cma.gov.cn and dyj@ns.lzb.ac.cn]

The Chinese Polar Cryospheric Database System(CPCDS) have been built. CPCDS can be divided into three levels. The bottom level is composed of Polar Fundamental Geo-spatial Database (PFGD) and data input, editing, management, communication, analysis and output, which offers on-line info-service and query. The top level, Geo-spatial Data Warehouse (GDW) is based on PFGD by integrating cryospheric data, GIS and other methods. GDW offers query, on-line analysis and output by data maintenance and exchange.

Based on Microsoft Windows2000 Server operating system, the CPCDS was established by database management system–SQL Server7.0. It is made up of six sub-databases: glacier physics, glacier chemistry, sea ice, meteorology, remote sensing and GIS map. All those basic information and observational data of ice sheets, glaciers, frozen earth, snow, sea ice, topography are stored in 150 tables. The former four sub-databases mainly include: glacier movement, radar survey, glacier temperature, snow/ice crystal, density, rigidity, mass balance; pH value, conductivity rate, main ions, isotopes, organic substances, gas of surface snow, snow pit and ice core; sea ice extent and areas, sea ice thickness and salinity; all kinds of weather elements on the ground and upper air. The last two sub-databases mainly include: remote sensing images for the Polar Regions, topographic data.

The homepage and web pages of CPCDS by Sybase PowerDynamo, Internet Information Server5.0 and FrontPage2000 with two protocols in data translation in CPCDS: HTTP and FTP was established for internet users, while for intranet users, a CPCDS data management software by PowerBuilder7.0 was manufactured independently. Users admitted by CPCDS can query, download, manage, and export all information they concerned.

The 10th Seoul International Symposium on Polar Sciences
October 21-22, 2003, Incheon, Korea

NATURAL VARIATIONS IN LEAD, CADMIUM, COPPER AND ZINC CONCENTRATIONS AND THEIR SOURCES IN VOSTOK ANTARCTIC ICE FROM 65,000 TO 240,000 YEARS BP

Sungmin Hong[1,*], Kang Hyun Lee[1], Claude F. Boutron[2,3], Christophe P. Ferrari[2,4], Jean Robert Petit[2], Carlo Barbante[5,6], Kevin Rosman[7], Vladimir Y. Lipenkov[8]

[1] Polar Research Institute of Korea Ocean Research and Development Institute, Ansan, PO Box 29, Seoul 425-600, Korea [smhong@kordi.re.kr]
[2] Laboratoire de Glaciologie et Géophysique de l'Environnement, CNRS, B.P. 96, 38402, Saint Martin d'Hères Cedex, France
[3] Observatoire des Sciences de l'Univers et Unité de Formation et de Recherche de Physique, Université Joseph Fourier de Grenoble (Institut Universitaire de France), B.P. 68, 38041 Grenoble, France
[4] Polytech Grenoble, Université Joseph Fourier de Grenoble, 28 avenue Benoît Frachon, B.P. 53, 38041 Grenoble, France
[5] Department of Environmental Sciences, University of Venice, Ca' Foscari, 30123 Venice, Italy
[6] Centre for Studies on Environmental Chemistry and Technology-CNR, University of Venice, Ca' Foscari, 30123 Venice, Italy
[7] Department of Applied Physics, Curtin University of Technology, GPO Box U 1987, Perth, WA 6845, Australia
[8] Arctic and Antarctic Research Institute, Beringa Street 38, 199397, St Petersburg, Russia

We present new data on the changing occurrence of Pb, Cd, Cu, and Zn in ancient Antarctic ice back to the penultimate glacial period and the preceding interglacial period (237,200 years). They are the first data ever obtained on changes in these heavy metals in Antarctic ice during the last two climatic cycles.

The data were obtained by analysing sections of the 3,623-m Vostok deep ice cores, which were drilled in a fluid filled hole at the Russian Vostok Station in East Antarctica (78°28′S, 106°48′E, elevation 3,488 m, mean temperature -55°C) [*Petit et al.*, 1999]. Twenty sections (lengths of 35-45 cm, diameter of 10 cm) were selected, representing different climatic conditions as shown in Fig. 1. A newly derived glaciological timescale (GT4) gives an age of 238 ky BP at a depth of 2,755 m [*Petit et al.*, 1999]. The poor quality of the core above ~900 m prevented the analysis of sections above that depth.

All the samples were decontaminated by mechanically chiselling successive veneers of ice from the outside toward the centre inside a class 100 laminar flow clean bench in a -12°C cold room, as described in detail elsewhere [*Candelone et al.*, 1994]. We then determined the Pb, Cd, Cu, Zn, and Al concentrations by Graphite Furnace Atomic Absorption Spectrometry (GFAAS)

using a Perkin Elmer 4110ZL instrument equipped with a Zeeman background corrector [*Hong et al.*, 2000]. Pb, Cd, and Cu levels were determined by GFAAS after preconcentration (by a factor of up to 55) by non-boiling evaporation, as described in detail by Görlach and Boutron [1990]. Zn and Al were measured by direct GFAAS using multiple injections (up to 5 × 50 μl). The precision is estimated to be better than 5% for the highest concentrations and to decrease to about 20% for the lowest [*Hong et al.*, 2000].

The full profile of the concentration from the outside toward the centre of each core section was determined to check the efficiency of the decontamination procedures, thereby validating the reliability of the measured concentrations. Good plateaus of the Pb, Cd, Cu, and Zn concentrations were observed for all the core sections analysed, indicating that the concentrations measured in the inner cores represented original concentrations in the ice.

Changes in Pb, Cd, Cu, and Zn concentrations as a function of the age of the ice are illustrated in Fig. 1., together with the deuterium profile of Petit et al. [1999]. The concentration ranges in the Vostok ice are 0.45 to 21.3 pg/g for Pb, 0.03 to 0.62 pg/g for Cd, 1.6 to 45.9 pg/g for Cu, and 3.48 to 126 pg/g for Zn. As shown in Fig. 1, the Pb, Cd, Cu, and Zn concentrations have varied remarkably over the last two glacial-interglacial cycles, and are much higher during cold glacial periods than during interglacials. In particular, the concentrations peak during very cold climate stages, such as stages 4.2 and 6.2. The estimated contributions from rock and soil dust and volcanoes are also shown as open squares and triangles, respectively, in Fig. 1. Our new Vostok data indicate that the rock and soil dust contribution explains most of the measured concentrations of Pb, Zn, and Cu during glacial periods, while this contribution is minor for Cd over the complete glacial-interglacial period.

REFERENCES

Candelone, J.-P., S. Hong and C.F. Boutron, An improved method for decontaminating polar snow and ice cores for heavy metal analysis, *Anal. Chim. Acta 299*, 9-16, 1994.

Görlach, U and C.F. Boutron, Preconcentration of lead, cadmium, copper and zinc in water at the pg g^{-1} level by non-boiling evaporation, *Anal. Chim. Acta 236*, 391-398, 1990.

Hong, S., A. Lluberas and F. Rodriguez, A clean protocol for determining ultralow heavy metal concentrations: its application to the analysis of Pb, Cd, Cu, Zn and Mn in Antarctic snow, *Korean J. Pol. Res.*, *11*, 35-47, 2000.

Petit, J.R., J. Jouzel, D. Raynaud, N.I. Barkov, J.M. Barnola, I. Basile, M. Bender, J. Chappellaz, M. Davis, G. Delaygue, M. Delmotte, V.M. Kotlyakov, M. Legrand, V.Y. Lipenkov, C. Lorius, L. Pépin, C. Ritz, E. Saltzman, M. Stievenard, Climate and atmospheric history of the past 420,000 years from the Vostok ice core, Antarctica, *Nature 399*, 429-436, 1999.

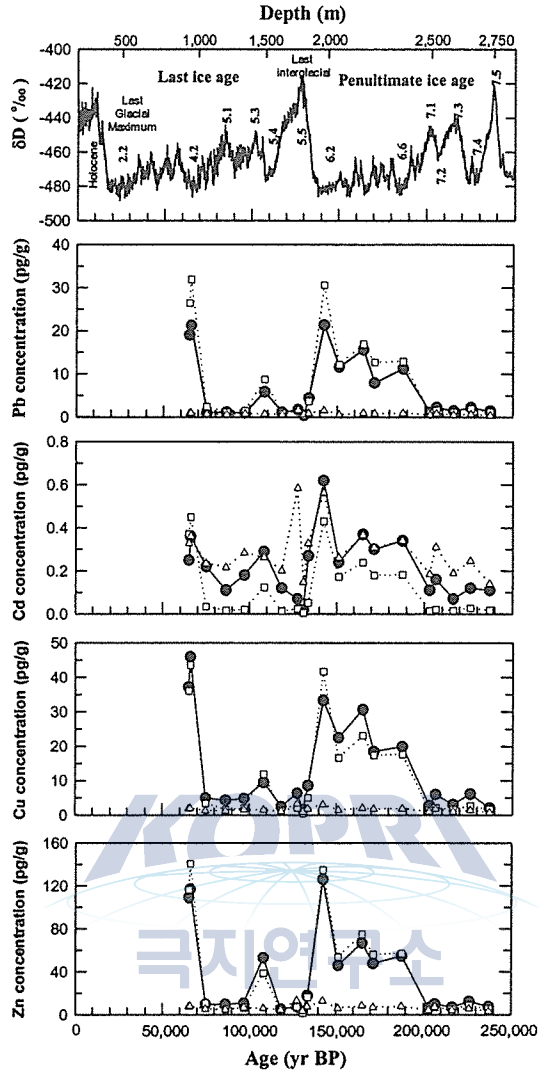

Figure 1. Variations with depth of the deuterium content of the Vostok ice (top) from [*Petit et al.*, 1999] and the Pb, Cd, Cu, and Zn concentrations over the past two climatic cycles (240,000 years). Also shown are estimated contributions from rock and soil dust (open squares) and volcanoes (open triangles).

FLUCTUATION OF ICE SHEET ELEVATION IN EAST ANTARCTICA SINCE THE LATE PLIOCENE

Xiaohan Liu, Ping Kong, Feixin Huang, Xiaoli Li and Aimin Fang

Institute of Geology and Geophysics, Chinese Academy of Sciences

The Cenozoic history of the East Antarctic Ice Sheet elevation has been the subject of much debate. We have carried out in the Grove Mountains, as first time, a synthetic land-based investigation. The preliminary results of direct geological and topographic measurements, coupled with desert soil, plant fossils from sedimentary pebbles, and in-situ cosmogenic nuclide (^{10}Be and ^{26}Al) exposure ages suggest that the ice surface elevation was never higher than ~ 120m above present ice surface since at least 2.6 My in the Grove Mountains, inland of the East Antarctic Ice Sheet. The fluctuation history around Last Glacial Maximum and Penultimate demonstrated only some light ascend and descend of ice surface altitude.

The 10th Seoul International Symposium on Polar Sciences
October 21-22, 2003, Incheon, Korea

VARIATIONS OF TOTAL OZONE AMOUNT AND ERYTHEMAL ULTRAVIOLET RADIATION AT KING SEJONG STATION IN WEST ANTARCTICA

Bang Yong Lee[1], Hi-Ku Cho[2], Yun-Gon Lee[2] and Young-In Won[1]

[1] Korea Polar Research Institute, KORDI, Ansan P.O. Box 29, Seoul 425-600, Korea [bylee@kordi.re.kr]
[2] Global Environment Laboratory, Yonsei University, Seoul 120-749, Korea

ABSTRACT: Temporal characteristics of total ozone amount and solar radiations are investigated using the updated data from satellite and ground-based measurements at King Sejong station in West Antarctica during the period from 1995 to 2001. Solar radiations are composed of horizontal global solar irradiance(285～3000 nm; GL), surface UV irradiance(290～385 nm; UV), erythemal UV-B irradiance(280～315 nm; EUV-B) and TOMS-EUV irradiance(280～400 nm). Total ozone amount was measured from the satellites NOAA/SBUV and Earth Probe/TOMS and Brewer ozone spectrophotometer at King Sejong station. Horizontal global solar irradiance, surface UV irradiance and erythemal UV-B irradiance are directly measured by using Eppley Pyranometer, Eppley Photometer and Robertson-Berger UV-Biometer at King Sejong station. TOMS-EUV irradiance around King Sejong station was obtained from Nimbus-7/EP TOMS data erythemally weighted since 1979. Annual mean value of total ozone was 276 DU with maximum of 303 DU in December and minimum 237 DU in September. Annual mean values of GL, UV, EUV-B and TOMS-EUV were 7.16 $MJm^{-2}day^{-1}$, 0.48 $MJm^{-2}day^{-1}$, 1.13 $kJm^{-2}day^{-1}$ and 2.07 $kJm^{-2}day^{-1}$, respectively. The regression analyses indicate significant trends of decrease 15.3 %/decade for total ozone while for TOMS-EUV, increase 25.2 %/decade during September and October which is a season occurring strong ozone loss in the lower stratosphere over Antarctica. Radiative amplification factor for EUV-B irradiance was 1.15, 1.59 and 1.58 at solar zenith angles of 60°, 70° and 80°, respectively.

INTRODUCTION

The Antarctic region has become an important research site for ozone depletion (Stolarski, 1988; Center for Atmospheric Science, 1998) and its impact on UV-B radiation (Lubin et al., 1989; Madronich, 1993; WMO, 1995; UK, 1997; Wardle et al., 1997; Cho et al., 1998; WMO, 2002). Decrease in total amount of ozone increases harmful Ultraviolet-B (UV-B) (wavelength; 280～315 nm) radiation that reaches the Earth's surface. UV-B radiation is very sensitive to

stratospheric ozone amount, and if stratospheric ozone is depleted, much more UV-B radiation reaches the Earth's surface, and its measured values during the ozone depletion period can easily exceed those of summer (Roy et al., 1994).

King Sejong station (62.2°S, 58.8°W) established in 1988 is located on King George Island situated at the boundary of the Antarctic ozone hole in most of the time. The location is also within the area covered by annual Antarctic vortices that are commonly developed over the Weddell Sea in Antarctica (Turner et al., 1993) and a borderline with one of climatically significant surface regions of the circumpolar low pressure zone situated between 60° S and the coast of the Antarctic Continent on the average (Dolgin, 1987). UV-B radiation is extremely important for marine ecosystem in this region (Kang et al., 1997). However, in comparison with other Antarctic locations, no active research has been performed in connection with ozone depletion and UV-B radiative variation in the region of King George Island, West Antarctica.

For this reason, we concentrated more on the measurement of erythemal UV-B radiation to study the characteristic relationship between the Antarctic ozone amount and erythemal UV-B radiation and its variation at King Sejong station from January 1995 to December 2001. In addition, the effect of total ozone variation on erythemal UV-B radiation was examined at King Sejong station located on the ozone holes boundary for the same period by using recent data.

MEASUREMENTS AND DATA ACQUISITION

(1) Total Ozone

To understand temporal variation of daily total ozone in Dobson Units (DU) and the interrelation between decrease in ozone and increase in erythemal UV-B radiation at King Sejong station, we analysed total ozone data. Those data were obtained from NOAA-SBUV/2 (Solar Backscattered Ultraviolet Radiometer/Version 2) (1995. 1～1996. 12) and Earth Probe/TOMS (1996. 8～2001. 12) over the station, and also measured by Brewer Ozone Spectrophotometer (SCI-TEC #122, Canada) during the period of 1998. 1～2001. 12 at the station. In order to know the difference between the two kinds of data, we compared data from Earth Probe/TOMS with those from the Brewer of for the period from January 1998 to December 2001.

(2) Horizontal global solar irradiance and surface UV irradiance

Horizontal global solar irradiance (GL) data are measured by Eppley pyranometer, and surface UV irradiance (UV) data by Eppley UV photometer from January 1995 to December 2001 with every 10 minutes interval at the station.

3) Erythemal UV-B irradiance

Eerythemal UV-B irradiance (EUV-B) data were measured by Robertson-Berger type UV-Biometer (Solar Light Co., Model 501) with every 5 minutes at the station. Data used in this study covered the period from January 1995 to December 2001.

RESULTS AND DISCUSSION

To ascertain the data quality of total ozone, we compared data measured by the Brewer at the station with those obtained from Earth Probe/TOMS during the period from January 1998 to December 2001. There are high relationship(correlation coefficient 0.9) between those data. Figure 1 shows long term annual trends of total ozone and TOMS erythemal UV radiation at the station. In this figure, we could find that TOMS erythemal UV radiation was negatively correlated to total ozone over King Sejong station. Total ozone has decreased with a rate of about 6.5 % per decade over King Sejong station during the period from January 1979 to December 2001. During that period, the annual average total ozone was 293.6 DU, and the maximum trend occurred in spring with its rate of -15.3 % per decade over the station. To investigate the variation of erythemal UV-B irradiance depending on total ozone at the station, Figure 2 shows power law regression for Radiation Amplification Factors (RAF) between erythemal UV-B irradiance at 60°, 70°, and 80° of solar zenith angles (SZA) and TOMS total ozone at the station. As a result, at solar zenith angles of 60°, 70°, and 80°, each RAF shows 1.15, 1.59, and 1.58, respectively. In a usual interpretation of RAF, a value of 2 indicates that a 1 % decrease in ozone will result in a 2 % increase in irradiance. During winter season, radiation drops nearly to zero and increases slowly as the day gradually lengthen; by summer, radiation can be measured up to 20 hours per day at King Sejong station. The large values through the selected period in this figure represent close to cloud-free or

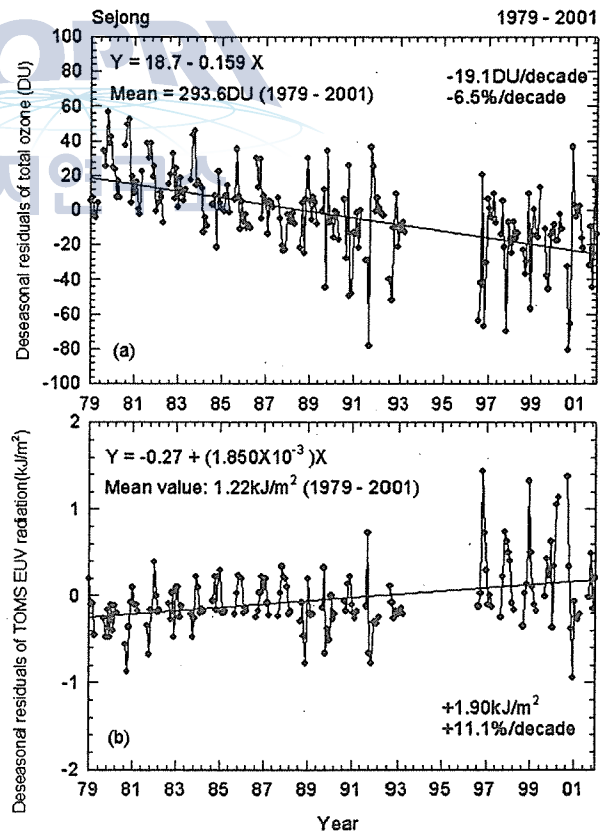

Figure 1. Long term annual trends of total ozone and TOMS erythemal UV (280-400nm) for annual mean.

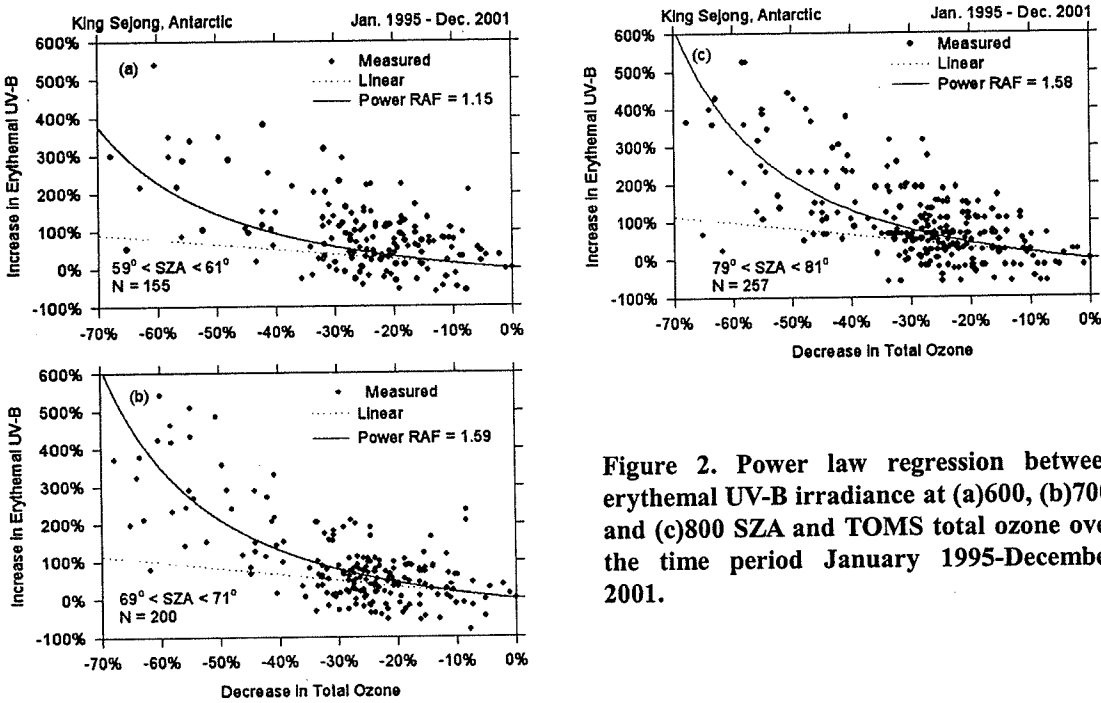

Figure 2. Power law regression between erythemal UV-B irradiance at (a)600, (b)700, and (c)800 SZA and TOMS total ozone over the time period January 1995-December 2001.

small cloud cover conditions. Higher values of erythemal UV-B radiation were recorded around noon time in December as a value of 83.4mWm^{-2}. We show time series of daily representative total ozone and measured erythemal UV-B irradiance as daily averaged values at King Sejong station during the 7 years from January 1995 to December 2001.

REFERENCES

Center for Atmospheric Science, 1998: The ozone hole tour. <http://www.atm.ch.cam.ac. uk>

Cho, H.-K., H.-J. Kwon and C.-Y. Choi, 1998: Increase of the surface erythemal ultraviolet-B radiation by the ozone layer depletion. J. Kor. Meteoro. Soc., 34(2), 272-281.

Dolgin, I. M., 1987: Climate of Antarctica. Printsman Press, Faridabad.

Kang, S.-H., J.-S. Kang, K.-H. Chung, M.-Y. Lee, B. Y. Lee, H. Chung, Y. Kim and D.-Y. Kim, 1997: Seasonal variation of nearshore Antarctic microalgae and environmental factors in Marian Cove, King George Island, 1996. Kor. J. Polar Res., 8(1, 2), 9-27.

Lubin, D., J. E. Frederick, C. R. Booth, T. Lucas and D. Neuschuler, 1989: Measurements of enhanced springtime ultraviolet radiation at Palmer station, Antarctica. Geophys. Res. Lett., 16, 783-785.

Madronich, S., 1993: UV radiation in the natural and perturbed atmosphere. In UV-B Radiation and Ozone Depletion (Edited by Tevini M.), 17-69, Lewis Publishers, Ann Arbor.

Roy, C. R., H. P. Gies and D. W. Tomlinson, 1994: Effects of ozone depletion on the ultraviolet radiation environment at the Australian stations in Antarctica. In Ultraviolet radiation in Antarctica: Measurements and Biological effects. (Edited by Weiler C. S. and Penhale P. A.), Antarct. Res. Ser. , 62, 1-15, Amer. Geophys. Union, Washington, D.C.

Stolarski, R. S., 1988: The Antarctic ozone hole. Scientific American, 258(1), 30-36.

Turner J., T. A. Lachlan-Cope, D. E. Warren and C. N. Duncan, 1993: A mesoscale vortex over Halley station, Antarctica. Mon. Wea. Rev., 121, 1317-1336.

UK Stratospheric Ozone Review Group, 1997: Stratospheric Ozone 1996. Dept. of the Environment, United Kingdom.

Wardle, D. J., J. B. Kerr, C. T. McElroy and D. R. Francis(eds), 1997: Ozone Science: A Canadian Perspective on the Changing Ozone Layer. Environment Canada, Toronto.

WMO, 1995: Scientific Assessment of Ozone Depletion: 1994. Executive Summary, NOAA/NASA/UNEP/WMO, WMO Global Ozone Research and Monitoring Project-Report No. 37, 36pp.

WMO, 2002, Executive Summary, Scientific Assesment of Ozone Depletion: 2002, Reeleased by WMO/UNEP on 23 August 2002.

The 10th Seoul International Symposium on Polar Sciences
October 21-22, 2003, Incheon, Korea

VARIABILITY OF REGIONAL ATMOSPHERIC CIRCULATION RELATED WITH RECENT WARMING IN THE ANTARCTIC PENINSULA

Jeong-Soon Lee[1], Tae-Yong Kwon[1], Bang-Yong Lee[2], Ho Il Yoon[2] and Jeong-Woo Kim[3]

[1] Department of Atmospheric and Environmental Sciences, Kangnung National University, Kangnung 210-702, Korea [jslee98@knusun.kangnung.ac.kr]
[2] Korea Polar Research Institute, KORDI, Ansan P.O. Box 29, Seoul 425-600, Korea
[3] Department of Earth Sciences, Sejong University, Seoul 143-747, Korea

This study examines the relationship among temperature, wind, and sea level pressure to understand recent warming in the vicinity of the Antarctic Peninsula. To do this, the surface air temperature, NCEP/NCAR reanalysis wind data and sea level pressure data for the period of 40 years are analyzed. The 40-year surface air temperature data in the Antarctic Peninsula reveals relatively the larger warming trends for autumn and winter than other seasons (IPCC, King, Lee). The variability of surface air temperature in this region is compared with that of the regional atmospheric circulation. The surface air temperature is positively correlated with frequency of northwesterlies and negatively correlated with frequency of southeasterlies (Fig. 1). This relation is more evident in the northern tip of the Peninsula for autumn and winter. The trend analysis of wind frequency in the study area shows that there has been increasing and decreasing trends in the frequency of northwesterlies and southeasterlies, respectively, in the northwestern part of the Weddell sea for autumn and winter. And also it is found that these winds are closely related with decreasing of sea level pressure in the southeastward region of Antarctic Peninsula (Fig. 2). Furthermore from the seasonal variation of sea level pressure in this area, it may be presumed that decreasing of sea level pressure in the southeastward region of Peninsula is related with warming in the vicinity of Peninsula for autumn and winter. Therefore it can be explained that recent

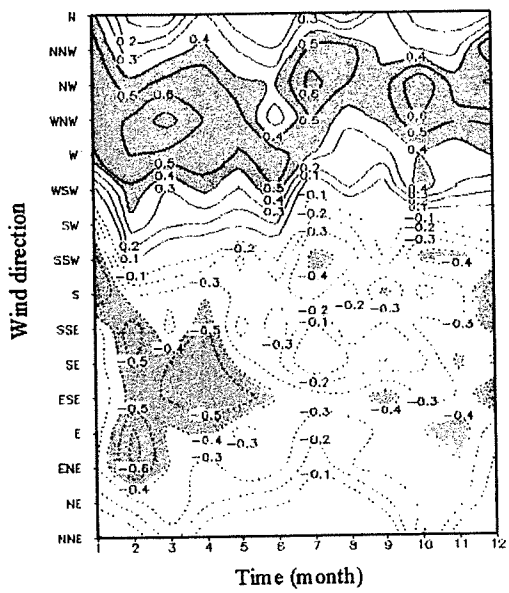

Figure 1. Correlation coefficient between surface air temperature (°C) and frequency of wind direction (%) at Esperanza for the period of 1961-2001.

warming in the vicinity of Antarctic Peninsula is caused by positive feedback mechanism, that is, the process that warming in the vicinity of Antarctic Peninsula can lead to the decrease of sea level pressure in the southeastward region of Peninsula and these pressure decrease in turn lead to the variation of wind direction in northwestern part of Weddell sea, again the variation of wind direction enhances the warming in the Antarctic Peninsula (Fig. 3).

REFERENCES

IPCC. 2001. Climate Change 2001: The Scientific Bases [Houghton, J.T., Y. Ding, D.J. Griggs, M. Noguer, P.J. van der Linden, X. Dai, K. Maskell, and C.A. Johnson (eds.)]. Cambridge University Press, Cambridge, UK, 881 pp.

King, J.C. 1994. Recent climate variability in the vicinity of the Antarctic Peninsular. Int. J. Climatol. 14, 357-369.

Lee, B.-Y., T.-Y. Kwon, J.-S. Lee and Y.-I. Won. 2002. Surface air temperature variations around the Antarctic peninsula: Comparison of the west and east sides of the peninsula. Ocean and Polar Res., 24(3). 267-278.

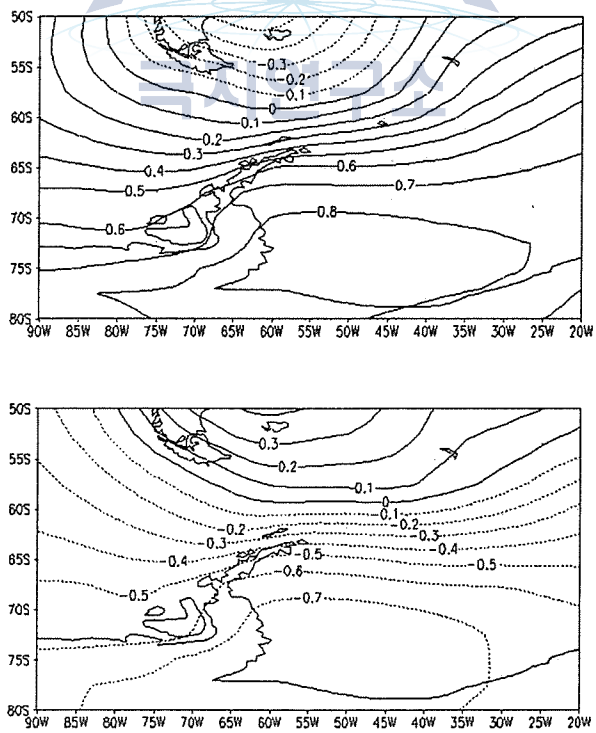

Figure 2. Correlation coefficient between mean sea level pressure and (a) mean frequency rate of SE in 62.5-67.5°S, 55-40°W and (b) mean frequency rate of NW in 62.5-67.5°S, 55-40°W for winter.

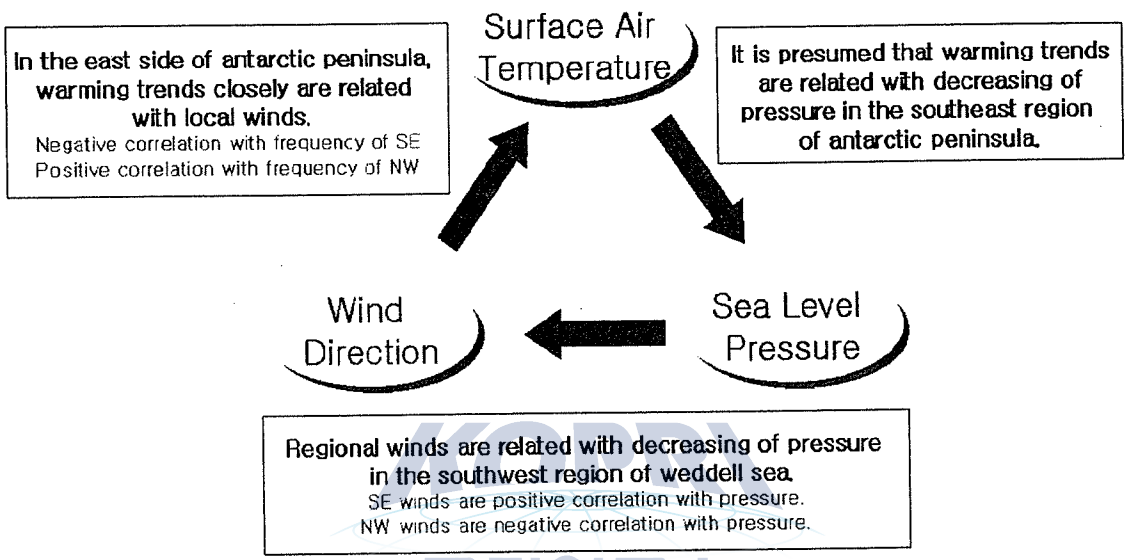

Figure 3. A possible mechanism for recent warming in Antarctic Peninsula: Temperature-Pressure-Wind Feedback.

The 10th Seoul International Symposium on Polar Sciences
October 21-22, 2003, Incheon, Korea

THE SURFACE UV-A AND ERYTHEMAL UV-B RADIATION CHANGES AT KING SEJONG STATION OF WEST ANTARCTICA

Kyu-Tae Lee[1], Joon-Bum Jee[1], Won-Hak Lee[1], Youn-Joung Kim[1], Bang Yong Lee[2] and Young-In Won[2]

1 Department of Atmospheric and Environmental Sciences, Kangnung National University
[ktlee@kangnung.ac.kr]
2 Korea Polar Research Institute, KORDI

The solar radiation model was used to investigate the UV radiation at the surface of King Sejong Station(62.3°S, 58.7°W) in West Antarctica, and the results calculated by this model were compared with the values measured by UV-Biometer and UV-Ameter during 1999-2000.

In this study, the parameterization of solar radiative transfer process was by Chou and Lee (1996). The total ozone amounts measured by Brewer Ozone Spectrophotometer and the aerosol data of McMurdo station(77.8°S, 163.2°E) by Nakajima *et al.* (1996) was used as the input data of the solar radiative transfer model. The surface albedo is assumed to be 0.20, 0.85 each in summer and winter of West Antarctica.

The sensitivity test of solar radiative transfer model was investigated with the variation of total ozone, aerosol amount, and surface albedo. When the cosine of solar zenith angle is 0.3, Erythemal UV-B radiation at surface decreased 73% with the 200% increase of total ozone from 100 DU to 300 DU, but the decrease of UV-A radiation was about 1%. For the same solar zenith angle, UV-A radiation was decreased 31.0% with the variation of aerosol optical thickness from 0.0 to 0.3 and Erythemal UV-B radiation was decreased only 6.1%. The variation of surface's Erythemal UV-B radiation with the increase of surface albedo was about twice of UV-A.

The surface Erythemal UV-B and UV-A radiation at King Sejong Station calculated by solar radiative transfer model were compared with the measured values (Fig. 1). In this Figure the model calculated Erythemal UV-B radiation at the surface coincided well with the measured values except for cloudy day. But the difference between the model calculated and measured UV-A radiation at the surface was larger than the difference of Erythemal UV-B radiation because of scattering effect by thin cloud.

REFERENCE

Chou, M.-D. and K. T. Lee. 1996. Parameterization for the absorption of solar radiation by water vapor and ozone. J. Atmos. Sci., 53, 1203-1208.

Nakajima, T, G. Tonna, R. Rao, P. Boi, Y. J. Kaufman and B. N. Holben. 1996. Use of sky brightness measurements from ground for remote sensing of particulate polydispersions. Appl. Opt., 35, 2672-2686.

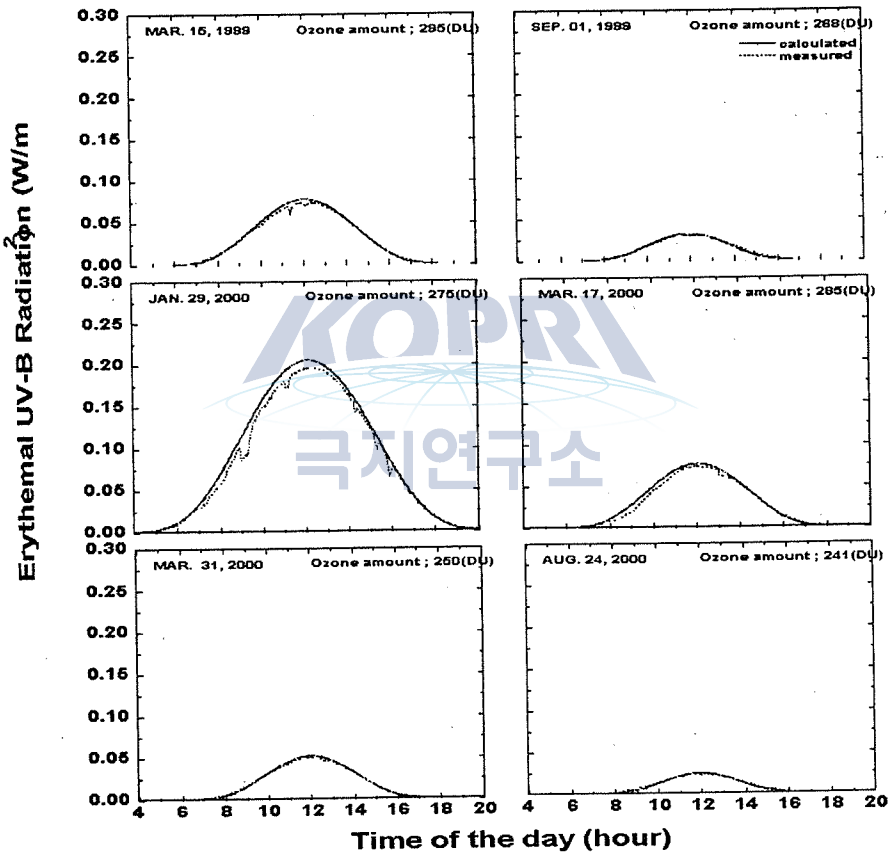

Figure 1. The measured and calculated Erythemal UV-B radiation at King Sejong station of West Antarctica.

The 10th Seoul International Symposium on Polar Sciences
October 21-22, 2003, Incheon, Korea

CLIMATOLOGICAL CHARACTERISTICS OF THE POLAR IONOSPHERE BASED ON THE SONDRESTROM AND CHATANIKA INCOHERENT SCATTER RADAR MEASUREMENTS

Young-Sil Kwak[1] and Byung-Ho Ahn[2]

[1] Department of Astronomy and Atmospheric Sciences, Kyungpook National University, Daegu, 702-701 Korea [ys-kwak@hanmail.net]
[2] Department of Earth Science, Kyungpook National University, Daegu, 702-701 Korea [bhahn@knu.ac.kr]

INTRODUCTION

Since they came into operation in 1960s, incoherent scatter radars have contributed significantly in advancing our understanding of the polar ionosphere, as well as the solar wind-magnetosphere-ionosphere coupling [e.g., *Brekke et al.*, 1974; *Kamide and Brekke*, 1975; *Araki et al.*, 1989; *Ahn et al.*, 1999]. We examine the climatological characteristics of the polar ionosphere in terms of the ionospheric conductance and electric field estimated from measurements by the Sondrestrom and Chatanika IS radars, which cover approximately the polar cap and auroral regions. By combining these two quantities, it is further possible to deduce the overhead ionospheric current distributions. The ionospheric current density, thus obtained, is compared with the corresponding ground magnetic disturbance. Also estimated is the global field-aligned current affecting the ground magnetic disturbance, particularly on the D component.

DATABASE

The ionospheric conductivity and the electric field measurements utilized in this study were obtained from the Sondrestrom radar (geographic latitude, longitude: 66.90°N, 50.90°W; geomagnetic latitude, longitude: 74.36°N, 42.40°W) for 109 days between 1983 and 1999 and the Chatanika radar (geographic latitude, longitude: 65.10°N, 147.45°W; geomagnetic latitude, longitude: 64.75°N, 105.00°W) for a total of 43 days between 1977 and 1983. The mean *Kp* indices for both the 109 and 43 days were 2_+~3-. The magnetic field was estimated based on the IGRF-1995 model [*Barton*, 1997]. The MSIS-90 model [*Hedin*, 1991] was used in taking the neutral densities and temperatures used to drive ion-neutral and electron-neutral collision

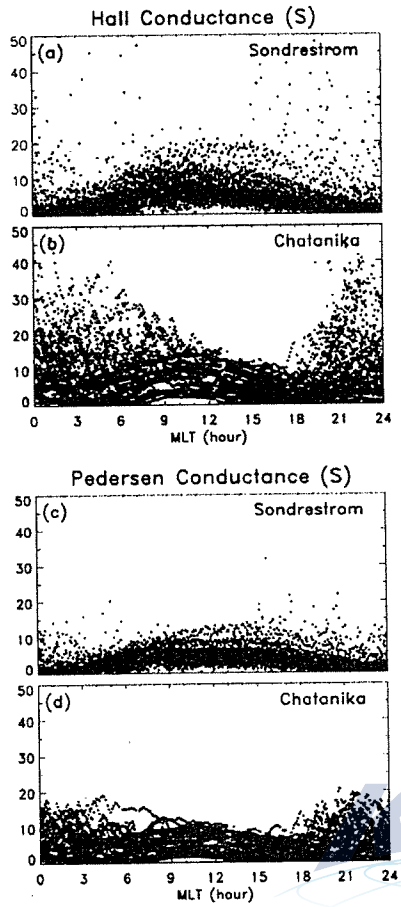

Figure 1. Magnetic local time variations (MLT) of the ionospheric conductance.

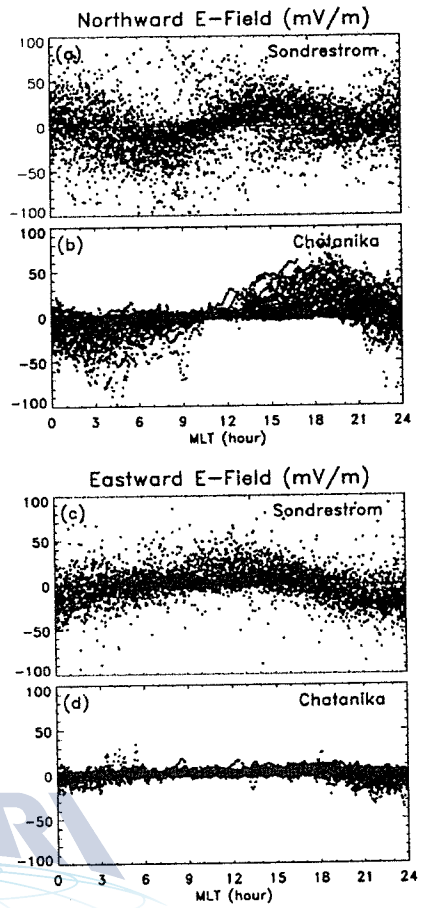

Figure 2. Same as Figure 1, but for the electric fields.

frequencies in estimating the conductivity.

RESULTS AND DISCUSSION

Figure 1 shows the magnetic local time (MLT) variations of the ionospheric conductance over the Sondrestrom and Chatanika radars constructed by superposing the entire 109-day and 43-day measurements, respectively, where the conductance is calculated by integrating the conductivities over the height range from 90 to 200 km. One can easily see that the sun determines largely the conductance over Sondrestrom, which varies smoothly and maximizes near the local noon sector, although there is sporadic conductance enhancement associated with auroral particle precipitation before 0600 MLT and after 1500 MLT. On the other hand, one can notice that the ionospheric conductance in the dayside over the Chatanika radar is dominated by solar EUV radiation, while the nighttime conductance distribution is significantly affected by auroral precipitation.

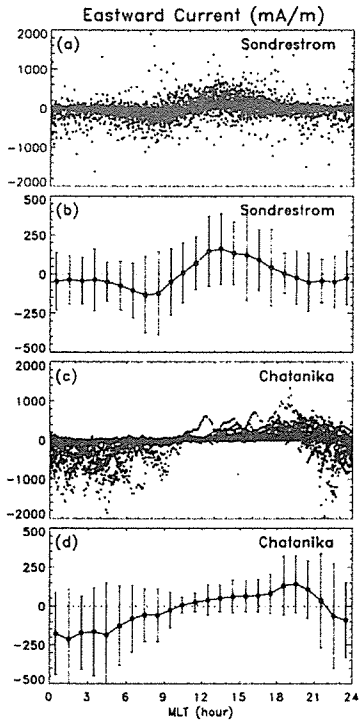

Figure 3. MLT variations (a,c) and hourly mean values (b.d) of the eastward currents.

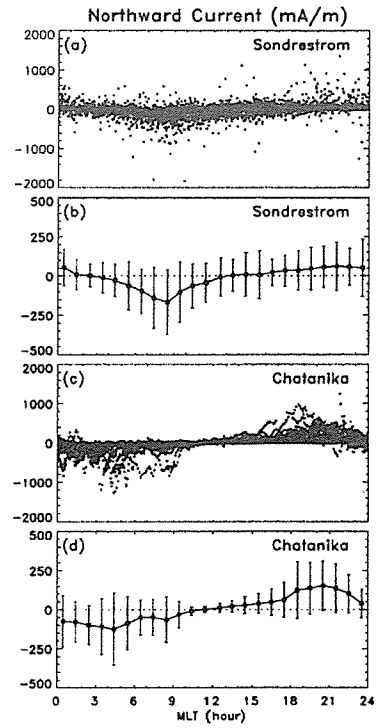

Figure 4. Same as Figure 3, but for the northward currents.

The magnetic field local time variations of the electric fields over the Sondrestrom and Chatanika radars are examined in the same way as the conductance and shown in Figure 2. The regions of the maximum north-south electric fields over the Chatanika radar are located approximately at the dawn and dusk, around 0400-0500 MLT and around 1900-2000 MLT, respectively, while they tend to shift towards dayside over Sondrestrom, around 0800-0900 MLT and 1300-1400 MLT. The east-west component over Sondrestrom is slightly strong by a factor of about 4 than Chatanika. However, the east-west component over Chatanika is generally weak, except for the premidnight sector, around 2200-2300 MLT.

The ionospheric horizontal current densities over Sondrestrom and Chatanika are estimated by combining the conductance and the electric field obtained from Figure 1 and 2, and the result is shown in Figures 3 and 4. From Figure 3, one can see that the maximum eastward and westward currents over Sondrestrom are found around 1300-1400 MLT and around 0800-0900 MLT, respectively. It is interesting to note that the E-W current over Sondrestrom flows more shifted toward sunlit hemisphere, 0600-1200-1800 MLT than over Chatanika. On the other hands, the maximum eastward and westward currents over Chatanika are found around 1800 MLT and around midnight, respectively. Thus east-west ionospheric current over Chatanika flows dominantly in the night hemisphere, 1800-0000-0600 MLT. From Figure 4 showing the north-south ionospheric current, one can see that a strong southward current flows over

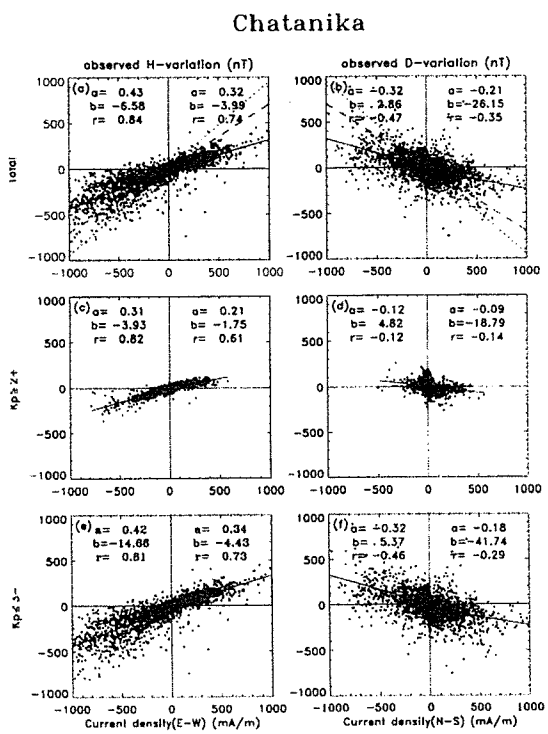

Figure 5. Relationship between the ionospheric current estimated from the Chatanika radar and the corresponding ground magnetic disturbance.

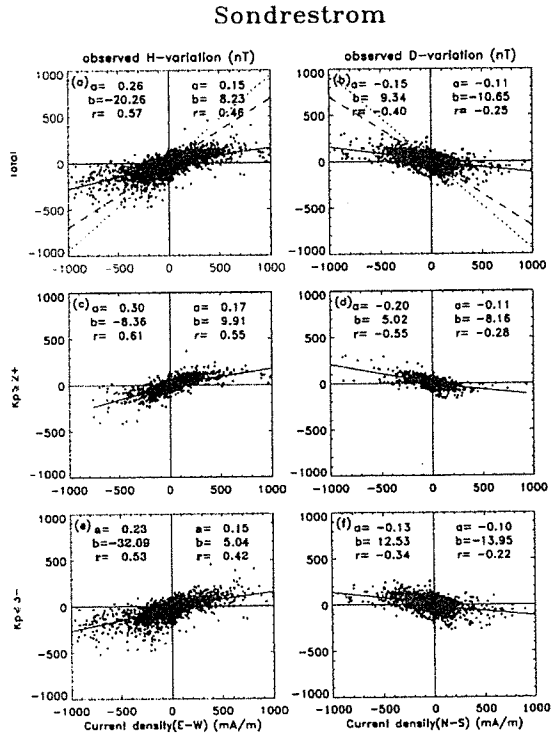

Figure 6. Same as Figure 5, but for Sonderestrom.

Sondrestrom in the prenoon sector, while the north-south current over Chatanika flows prominently in the dawn and dusk sectors.

Figures 5 and 6 show the relationship between the height-integrated ionospheric current (J_E, J_N) estimated from the radar and the corresponding ground magnetic disturbance (ΔH_{obs}, ΔD_{obs}). Here we represent the relation between the two physical quantities as the correlation coefficient, r, and the coefficients, a, b, of a linear fit, $J_E = a\,\Delta H_{obs} + b$ and $J_N = a\,\Delta D_{obs} + b$, where is given as the solid line. For comparison, the linear relations based on the infinite overhead current approximation for f=2/3 [*Kamide and Brekke*, 1975] and 9/10 [*Tanskanen et al.*, 2001] are also given as the dotted and dashed lines, respectively. The assumption of infinite sheet current approximation is far from realistic, underestimating the current density by a factor of 2 or more. It is particularly serious for higher latitude region and during quiet period with auroral electrojet being retreated poleward. Thus one should be cautious in inferring ionospheric current distribution from ground magnetic disturbance data. The correlation between ΔH and J_E is higher than the one between ΔD and J_N, indicating that field-aligned current affects significantly ΔD. During quiet period, neutral wind seems to play an important role particularly on north-south ionospheric current.

The global field-aligned currents in the evening and morning sides over Chatanika and Sondrestrom are estimated and shown in Table 1. The total upward or downward FAC are quite

comparable and they are approximately 5.9×10^5 A and 2.2×10^5 A over Chatanika and Sondrestrom, respectively. With enhancement of magnetic activity, FAC increases drastically over Chatanika by a factor of 4 or 5 but the increment is insignificant over Sondrestrom.

REFERENCES

Ahn, B.-H., B. A. Emery, H. W. Kroehl, and Y. Kamide, *J. Geophys. Res., 104*, 10031-10040, 1999.

Araki, T., K. Schlegel, and H. Luhr, *J. Geophys. Res. ,94*, 17185-17199, 1989.

Barton, C. E., *J. Geomag. Geoelectr., 49*, 123-148, 1997.

Brekke, A., J. R. Doupnik, and P. M. Banks, *J. Geophys. Res., 79*, 3773-3790, 1974.

Hedin, A. E., *J. Geophys. Res., 82*, 2851-2853, 1991.

Kamide, Y., and A. Brekke, *J. Geophys. Res., 80*, 587-594, 1975.

Tanskanen, E. I., A. Viljanen, T. I. Pulkkinen, R. Pirjola, L. Häkkinen, A. Pulkkinen, and O. Amm, *J. Geophys. Res., 106*, 13119-13134, 2001.

Table 1. Global field-aligned current

	Chatanika		Sondrestrom	
	Evening side (upward FAC)	Morning side (downward FAC)	Evening side (upward FAC)	Morning side (downward FAC)
Total	6.3×10^5 A	5.5×10^5 A	2.0×10^5 A	2.4×10^5 A
Kp≤2+	2.2×10^5 A	1.3×10^5 A	2.9×10^5 A	2.0×10^5 A
Kp≥3-	8.2×10^5 A	1.1×10^6 A	1.3×10^5 A	3.4×10^5 A

The 10th Seoul International Symposium on Polar Sciences
October 21-22, 2003, Incheon, Korea

CLOUDY BAND AND AIR INCLUSIONS OBSERVED IN DEEP ICE CORE SAMPLES FROM GRIP, GREENLAND

Kimiko Shimohara[1], Hitoshi Shoji[1] and Sepp Kipfstuhl[2]

[1] New Energy Resources Research Center, Kitami Institute of Technology, 165 Koen-cho, Kitami 090-8507, Japan [dse00002@std.kitami-it.ac.jp]
[2] Alfred Wegener Institute for Polar and Marine Research, Columbusstrasse D-27515 Bremerhaven, Germany

ABSTRACT: Cloudy band is milky-colored layers in deep ice cores observed in depth zones of colder periods in Wisconsin age ice. Microscopic observations were conducted on air inclusions, looking for light scattering sources causing the cloudiness. Number density of air inclusions within cloudy bands were measured in the GRIP, Greenland ice core specimen and revealed that number density of micro-bubbles smaller than 30 μm in equivalent diameter is approximately 100 /mm^3, and is a major source for the light scattering.

INTRODUCTION

Polar ice sheets contain paleo-climate information in the physical and chemical stratigraphy. Several investigations were made to measure core properties in the field just after core recovery. Deep ice cores from Greenland and Antarctica are observed to be transparent below the depth of air bubble-hydrate transition. However, some milky-colored layers are found in fresh ice cores from much deeper places, called cloudy bands. Gow and Williamson (1976) observed a series of cloudy bands in the Byrd Station, Antarctica deep ice core, which is of volcanic origin and should be discussed separately. Hammer et al. (1978) observed that micro-particle peak concentrations occur in visible cloudy bands in the Wisconsin age ice of the Camp Century ice core. These micro-particles are interpreted as continental dust. Hammer et al. (1985) observed a strong anti-correlation between stable isotope ratio and continental dust concentration on the Dye 3, Greenland deep ice core. Detailed electric conductivity measurements (ECM) revealed that ECM signal decreases in cloudy ice due to the alkalinity (Hammer, 1989). Outcome of GRIP core analysis, combined with its sister program, GISP 2 is published in a special issue of Journal of Geophysical Research, Vol. 102, No. C12 in 1997. Meese et al. (1997) determined a depth-age scale on the GISP 2, Greenland ice core by considering cloudy band features and others. They also discuss about the core continuity below a depth of 2800 m based on the

observation of disturbed cloudy band layers.

Cloudy band observation is a non-destructive and fast technique to obtain preliminary information on ice cores. However, characterization of cloudy band is needed to utilize as a potential core signal and to compare with other core signals. Cloudy band appears where light is scattered by tiny air inclusions. However, no direct measurement was made for the number density considerations. This paper reports about the results of such microscopic observations.

EXPERIMENTS

A thin section specimen (66 x 30 x 3.2 mm) was prepared from a depth of 2207.51 m of the GRIP, Greenland ice core drilled during the GRIP field operation in 1990-92 (Pauer et al., 1999). This sample includes cloudy band layers of which a photographic picture was taken under a side-illumination condition and compared with a photograph taken immediately after core recovery to investigate any change taken place during 8 years interval of volume relaxation process.

A photograph of the specimen was scanned along a vertical line with different widths to examine an appropriate gray value curve representing the cloudy band structure. Air inclusions were observed under an optical microscope and photographic recording was made to measure size distribution and number density of air bubble, air hydrate and plate like inclusion. Image analysis was made for an observation depth interval from 2207.51 to 2207.57 m with a horizontal width of 1.93 mm. Higher magnification was adopted to observe much smaller air bubbles in which a horizontal width was 0.79 mm. These smaller air bubbles were observed to move towards higher temperature side in the ice specimen under a microscope, when a heating rod was applied to an edge of the specimen. This confirms that these microscopic images are of high pressure air bubbles, not solid particles. Vertical variation in number density of each type of air inclusion obtained was compared with gray value curve to examine a major source for light scattering that forms cloudy band layers.

All experiments were carried out in a cold room laboratory at –20 ℃.

RESULTS AND DISCUSSIONS

No change in major features of cloudy band such as each layer thickness and shape are found by a comparison of two images with 8 years interval. This suggests that cloudy band feature is a potential ice core signal, and preserves the stratigraphic information even after several years storage in a cold room laboratory.

Three gray value curves with scanning line widths of 0.08, 0.79 and 1.93 mm respectively were compared with photographic image, showing that line width should be larger than about 1

mm for gray value curves to eliminate high frequency noise and represent cloudy band structure.

Microscopic observations were made on air bubbles smaller than 10 μm for a depth interval from 2207.518 to 2207.533 m with an observation area width of 0.79 mm. Size distribution of air bubble splits into two zones with an almost vacant range between 30 and 50 μm. Number density of micro-bubbles (smaller than 30 μm) is about 100 /mm^3, and is two to three order of magnitude higher than the other air inclusions. Regular air bubbles larger than 50 μm could be formed by dissociation of air hydrate after core recovery, since the core contained no air bubble at a depth of 2208 m. However, cloudy bands were visible even immediately after core recovery.

A number density curve of micro-bubbles (smaller than 10 μm) has a good fit with gray value curve as expected. Another good fit was obtained between plate like inclusions and gray value curve. A continuous, microscopic observation with time after core recovery shows a transformation of micro-bubbles to plate like inclusions in GRIP ice core samples (J. Kipfstuhl, unpublished), which confirms that cloudy bands in fresh ice cores observed in the field is caused by light scattering mainly from micro-bubbles.

Micro-bubble position distribution in a thin section specimen is measured for the size smaller than 10 μm. The position map obtained shows some horizontal arrays of micro-bubbles in general, suggesting that micro-bubbles are preferentially existing in a curved plane such as sub-boundaries or triple junction of sub-boundaries. These findings further suggest that micro-bubbles could be formed and grow after core recovery by diffusion of intra-lattice air molecules nucleated at sites of some impurities or crystal lattice defects.

REFERENCES

Gow, A. J., Williamson, T. (1976): Rheological implications of the internal structure and crystal fabrics of the West Antarctic ice sheet as revealed by deep core drilling at Byrd Station. CRREL Report 76-35, 25p.

Hammer, C. U., Clausen, H. B., Dansgaard, W., Gundestrup, N., Johnsen, S. J., Reeh, N. (1978): Dating of Greenland ice cores by flow models, isotopes, volcanic debris, and continental dust. J. Glaciol., 20, 82, 3-26.

Hammer, C. U., Clausen, H. B., Dansgaard, W., Neftel, A., Kristinsdottir, P., Johnson, E. (1985): Continuous impurity analysis along the Dye 3 deep core. Greenland Ice Core: Geophysics, Geochemistry, and the Environment, ed. by Langway, C. C., Jr., Oeschger, H., Dansgaard, W. , American Geophys. Union, Washington, DC, 90-94 (Geophys. Mono. 33)

Hammer, C. U. (1989): Dating by physical and chemical seasonal variations and reference horizons. The Environmental Record in Glaciers and Ice Sheets, ed. by Oeschger, H. and Langway, C. C., Jr., John Wiley and Sons Limited, Chichester, 99-121.

Meese, D. A. Gow, A. J., Alley, R. B., Zielinski, G. A., Grootes, P. M., Ram, M., Taylor, K. C., Mayewski, P. A., Bolzan, J. F. (1997): The Greenland Ice Sheet Project 2 depth-age scale: Methods and Results. J. Geophys. Res., 102, C12, 26411-26423.

Pauer, F., Kipfstuhl, F., Kuhs, W. F., Shoji, H. (1999): Air clathrate crystals fom the GRIP deep ice core, Greenland: a number-, size- and shape distribution study. J. Glaciol., 45, 149, 22-30.

The 10th Seoul International Symposium on Polar Sciences
October 21-22, 2003, Incheon, Korea

GEOCHEMICAL TRENDS AND MILANKOVITCH CYCLES WITHIN SEDIMENT FROM THE NORTH ATLANTIC OCEAN

Sangmin Hyun[1], Naokazu Ahagon[2] and Ho Il Yoon[3]

[1] South Sea Institute of Korea Ocean Research and Development Institute [smhyun@kordi.re.kr]
[2] Mutsu Institute for Oceanography, Japan Marine Science and Technology Center (JAMSTEC)
[3] Korea Polar Research Institute, Korea Ocean Research and Development Institute

ABSTRACT: A geochemical study of sediment samples taken from North Atlantic Ocean Drilling Program (ODP) site 980 was undertaken to evaluate possible Milankovitch cycles and their inter-relationships with climatically determined geochemical variations. Wide variations were found in both total organic carbon (TOC) and carbonate carbon throughout the column; TOC varied from about 0.1 to 0.6 %, and the carbonate content from about 8 to 83 %. Possible causes of such extreme fluctuations include time-dependent changes, either in Milankovitch cycles of biogenic oceanic productivity or in the dissolution patterns of carbonate. To evaluate the underlying reasons for these large fluctuations we analyzed the spectral patterns of both organic carbon and carbonate, but with all TOC and $CaCO_3$ data interpolated at every 2.5 kyr and detrended prior to analysis of the spectra. The resulting spectra were evaluated in the upper (2.5-472.5 ka) and lower (475-945 ka) sections of the column, and in the sequence as a whole (2.5-945 ka). The results show a strong 100-ky Milankovitch cycle that is particularly apparent within the upper section (2.5-472 ka). However, the tilt and precession cycles are not always clear; a potential source of error is the lack of age control in the high-frequency range, where there was insufficient sampling. On the other hand, it is possible that variations in % $CaCO_3$ fail to reflect tilt and precession cycles because of some local environmental condition, and further study is necessary to ascertain the precise cause of the 100-ka cycle and its application in paleoceanographic interpretation.

INTRODUCTION

The results of the North Atlantic Ocean Drilling Program (ODP) Leg 162 (Fig. 1) established that high amplitude oscillations exist in the carbonate and total organic carbon (TOC) records of the last 2.8 myr. (Jansen et al., 1996; 1988). Earlier, Henrich (1989) recognized long-term cyclic variations in glacial and interglacial sedimentology and paleoceanography patterns associated

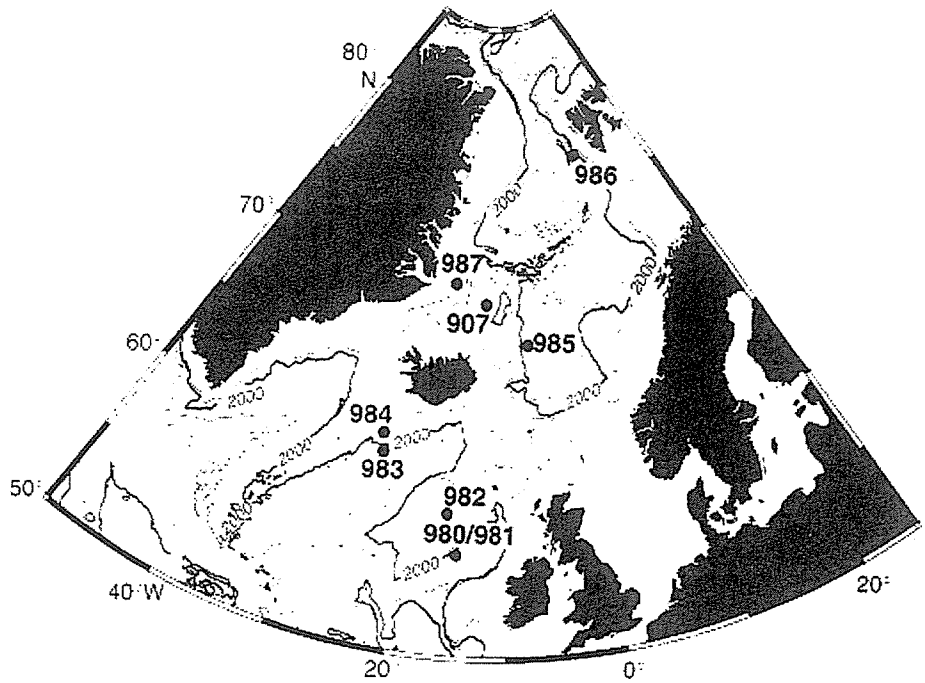

Figure 1. Map view of sites drilled during Leg 162 and studied site 980.

with Northern Hemisphere climatic changes that extended from the late Pliocene into the Quaternary. Oritz et al. (1999) demonstrated that significant sub-Milankovich variability, with periods centered about 7.6-8.4 and 4.8-6.1 kyr, exist not only during the periods of major Northern Hemisphere glaciation following 2.5 myr, but also before the late Pliocene intensification of Northern Hemisphere glaciation. All of these results imply that Milankovitch variability is, at the very least, implicated in climatic and paleoceanographic changes in the North Atlantic Ocean.

Possible causes of carbonate and TOC oscillation include time-dependent changes in oceanic productivity, carbonate dissolution, and carbonate and TOC dilution by terrigenous materials. In the present study, analytical values of TOC and biogenic carbonate were subjected to spectral analysis to evaluate whether the TOC and/or the carbonate variations can be related to fluctuations in Milankovitch cycles.

METHODS AND MATERIALS

A total of 160 samples from ODP Site 980 were analyzed for their TOC and biogenic carbonate contents. The total carbon (TC) content of unacidified, powdered samples was measured using a CHNS analyzer (EA 1112). The TOC content of the samples was then determined, following treatment with 1-N hydrochloric acid. The amount of biogenic carbonate was derived from the difference between the TC and TOC measurements:

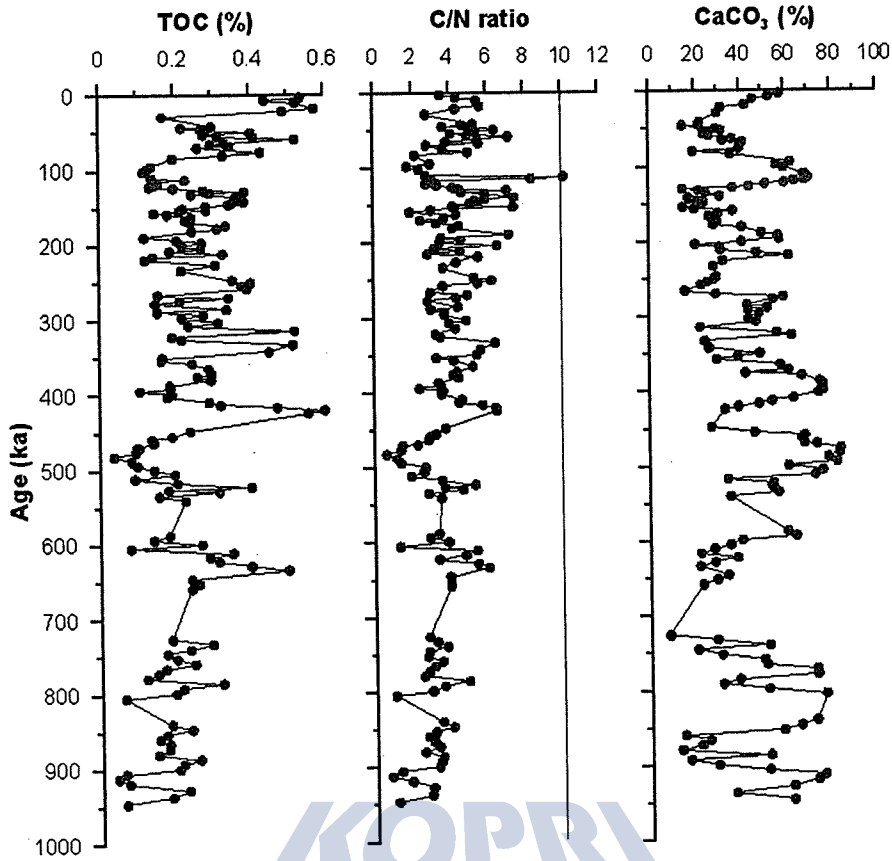

Figure 2. Vertical profiles of TOC, C/N ratio of organic matter and carbonate content. An extreme fluctuations of both TOC and carbonate is shown throughout the core column.

$CaCO_3$ (wt%) = (TC wt% -TOC wt%)* (100/12).

The age control point used in this study is that cited by Channel and Lehman (1999) and the biostratigraphy is that deduced by Jansen et al., (1996).

RESULTS AND DISCUSSION

The TOC and carbonate contents show wide variation throughout the core column. There is a six-fold variation in TOC, from 0.1 to 0.6%, and a ten-fold variation in carbonate, from 8 to 83% (Fig. 2). The C/N ratio of TOC was below 10, except in one sample, indicating that most of the organic matter was produced biogenically in situ (cf. Muller, 1977; Stein, 1990).

The striking ten-fold variation in the carbonate content of the column results from time-dependent changes in oceanic productivity, carbonate dissolution, or carbonate dilution by terrigenous materials. Previous comparative studies of glacial and interglacial sediments and paleoceanography have shown high variation in the carbonate record, especially among sediments younger than 0.6 Ma (Henrich, 1989; McManus et al., 1999; Oritz et al., 1999). Similarly, Hyun et al. (1999) found that sediments from the North Atlantic ODP Site 983 have

cyclic Ti/Al variations, which they interpreted as reflecting variations in potential surface productivity and, to a lesser extent, dilution from input of terrigenous material.

Overall, the excursions of TOC show high amplitude. They exhibit a repeated cyclic variation at 100-kyr intervals over the last 600 kyr. The excursions in biogenic carbonate show a similar pattern of cyclic variation, also with a 100-kyr interval. The results of the spectral analysis show typical 100-kyr cyclic variations in both the TOC and carbonate records (Fig. 3 and 4). However, this 100-kyr Milankovitch frequency pattern is not dominant throughout the core; it occurs only in the upper, 0 to 472.5-kyr section. This approximate 100-kyr cycle is similar to that found in a previous study by Henrich (1989) in the North Atlantic Ocean. The reason for the absence of a 100-kyr cycle in the lower part of the column, and the nature of the tilt and precession cycles require further study if the relationship between Milankovitch cycles and paleoceanographic variations is to be ascertained.

REFERENCES

Channell, J.E.T., Lehman, B., 1999. Magnetic stratigraphy of North Atlantic Sites 980-984. Proc. ODP scientific Res., 162, 113-130.

Henrich, R., 1989. Glacial/interglacial cycles in the Norwegial Sea: sedimentology, paleoceanography, and evolution of Late Pliocene to Quaternary Northern Hemisphere climate. Proc. ODP scientific Res., 104, 189-215.

Hyun, S., Joseph D. Oritz, M.E. Raymo and Asahiko Taira, 1999. Low-frequency oscillations in site 983 sediments: Relationship between carbonate and productivity proxies. Proc. ODP scientific Res., 162, 197-207.

Jansen, E., Bleil, U., Henrich, R., Kringstad, L and Slettemark, B., 1988. Paleoenvironmental changes in the Norwegian Sea and the Northeast Atlantic during the last 2.8 m.y.: Deep Sea Drinning Project/Ocean Drilling Program Sites 610, 642, 643 and 644. Paleoceanography, 3, 563-581.

Jansen, E., Raymo, M.E., Blum, P., et al., 1996. Proc. ODP, Initial Reports, 162: College Station, TX (ocean Drilling Program), 1182 pp.

McManus, J.F., Oppo, D.W. and Cullen, J.L., 1999. A 0.5 million year record of millennial-scale climate variability in the North Atlantic. Science, 283, 971-975.

Muller, P.J., 1977. C/N ratio in Pacific deep-sea sediments: effect of inorganic ammonium and organic nitrogen compound sorbed by clays. Geochim. Cosmochim. Acta, 41, 765-776.

Oritz, J. D., Mix, A.C., Harrism S.E. and O'Connell, S.B., 1999. Diffuse spectral reflectance as a proxy for percent carbonate content in North Atlantic sediments.

Paleoceanography, 14, 171-186.

Stein, R., 1990. Organic carbon content/sedimentation rate relationship and its paleoenvironmental significance for marine sediments. Geo-Mar. Lett., 10, 37-44.

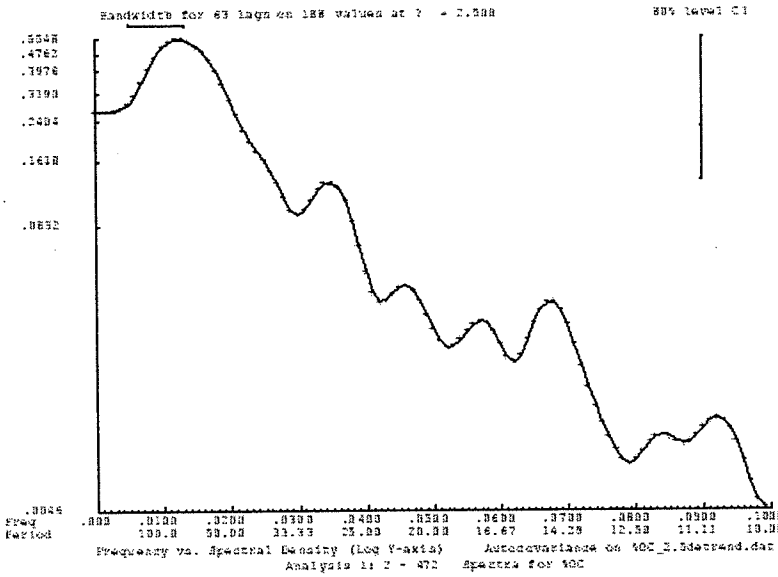

Figure 3. Result of the spectral analysis of TOC. A strong Earth's orbital factor (100-ka Milankovitch cycle) is shown, but tilt and precession cycle are not clear.

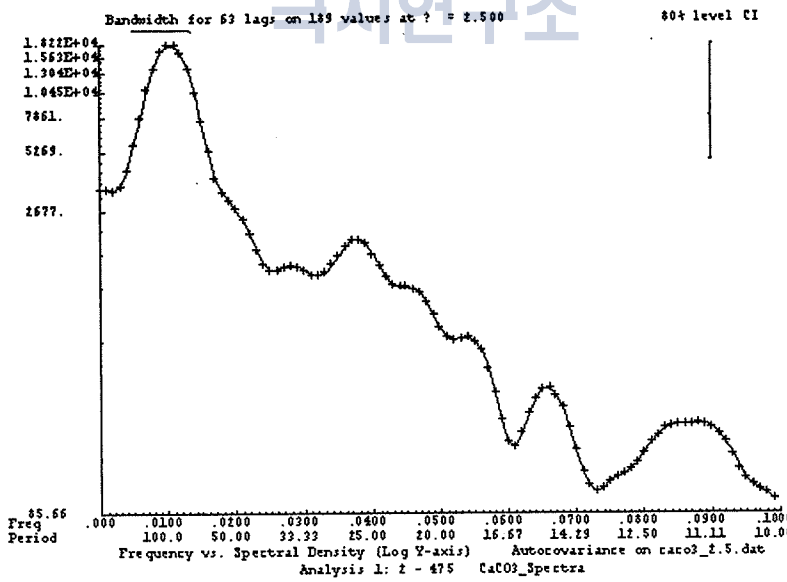

Figure 4. Result of the spectral analysis in carbonate content. A strong Earth's orbital factor is shown in upper section (2.5-472.5 ka).

The 10th Seoul International Symposium on Polar Sciences
October 21-22, 2003, Incheon, Korea

OCEANOGRAPHIC MECHANISM OF REGIONAL WARMING IN THE ANTARCTIC PENINSULA

Kyu-Cheul Yoo[1], Ho Il Yoon[1], Jae-Kyung Oh[2], Tae-Yong Kwon[3] and Cheon Yun Kang[1]

[1] Korea Polar Research Institute, Korea Ocean Research & Development Institute, South Korea
[kcyoo@kordi.re.kr]
[2] Dept. of Oceanography, Inha Univ. of Incheon
[3] Dept. of Atmospheric and Environmental Sciences, Kangrung Natl. Univ.

Due to rapid warming of the Antarctic Peninsula (AP) over last several decades, ice shelves have retreated over the peninsula, and sea-ice extent has decreased over the Bellingshausen Sea. On the contrary, the interior of the Antarctic continent has exhibited weak cooling, and sea-ice concentration has increased and the length of the sea-ice season has increased over much of eastern Antarctica and the Ross Sea. The atmospheric mechanism about these phenomena has a little known, but the configuration of the oceanographic mechanism has not yet constrained. Antarctic Circumpolar Current (ACC) is the important key to approach the close examination because it is a powerful influence on the climate of much of earth. We suggest the oceanographic mechanism from oceanographic data (1996-2002) in Marian Cove (King George Island of the northern AP) adjacent to the southern boundary of ACC and NCEP/NCAR (62.5°S, 57.5°W) reanalysis of wind data (1961-2001). Due to topographical situation between south America and AP, stronger westerly wind forcing in summer since 1970s (first mode) is accompanied by frequent intrusion of warm surface water (>1.0℃) (corresponding to surface water of southern Polar Front) as well as a southerly migration of the January 0.0℃, resulting in regional warming unlike to other places (eastern Antarctica and the Ross Sea). Recent abrupt glacier retreat and collapse of ice-shelves in this area are likely to be related to increasing ocean swell and storminess (second mode) due to the sustaining wind forcing (north-west sector) in fall after 1994. Therefore, the oceanographic mechanism of rapid warming in AP will be the combination between first- and second mode and the regional warming can be closely related with the fluctuation of atmospheric- and oceanographic circulation.

The 10th Seoul International Symposium on Polar Sciences
October 21-22, 2003, Incheon, Korea

EAST ASIAN MONSOON VARIATION DURING THE LATE PLEISTOCENE TO HOLOCENE: PALEOCLIMATE CHANGES INDICATED BY PROXY RECORDS FROM JEJU ISLAND, KOREA

Seung Hyoun Lee[1], Yong Il Lee[1], Ho Il Yoon[2] and Cheon Yun Kang[2]

[1] School of Earth and Environmental Sciences, Seoul National University, Seoul 151-747, Korea [lshkingdom@hanmail.net]
[2] Korea Polar Research Institute, Korea Ocean Research and Development Institute, Ansan P.O. Box 29, Korea

INTRODUCTION

The pattern of climate in eastern Asia is dominated by the summer and winter monsoons (Gao, 1962). Summer monsoon is a warm, moist and maritime air onto the continent and winter monsoom, a cold and dry air out of the north-central Asia. The alternation of paleosols and loess units in the Loess Plateau of central China has been used as a proxy record of variations in the strength of the East Asian summer and winter monsoons over the past 2.5Ma (An *et al.*, 1990, 1991a; Ding *et al.*, 1995). The study of Lake Biwa in Japan shows that about 10 ㎛-size quartz grains were originated from aeolian dust and that quartz grains larger than 20 ㎛ were originated from fluvial sediments (Xiao *et al.*, 1997). Eolian quartz flux to Lake Biwa shows a similar pattern to the quartz median diameter record of the Chinese Loess (Xiao *et al.*, 1995) and the SPECMAP $\delta^{18}O$ record (Martinson *et al.*, 1987). However, Xiao *et al* (1997) reported that the eolian quartz flux record apparently lags ca. 5000 yr behind the loess and $\delta^{18}O$ records during MIS 6/5 and 2/1 transitions. The Korean Peninsula is located in the midway of jet stream from China to Japan. Thus, the comparison of the Korean Peninsula data with climate change records of Chinese Loess Plateau and Lake Biwa can be used to check the synchrony of climate events in East Asia. In this study, we reconstruct paleo-monsoonal climate change as well as environmental change of Jeju Island using paleo-lake sediments during the last 27,000 yr.

STUDY AREA AND MATERIAL

A 5 m long sediment core BH-4B was obtained from the paleo-lake, which is located at about 1 km north of Oedolgoe, southern part of Jeju Island. It is an ellipsoidally shaped basin with 800 m across in NW-SE direction and 500 m across in NE-SW direction. The basement

rock in the study area consists of Quaternary trachyte. It is believed that the study area was a caldera lake formed by parasitic volcanism. It is a closed basin without inlet and outlet and sediment input filled up the lake. A 5-m long sediment core, BH-4B, obtained from the study area consists of dark gray to black peaty mud (0-2 m depth interval) and dark brown mud (below 2 m depth) with thin layers of thickness of 1 to 5 mm. Core BH-4B consists of 50～60 % clay, 30～40 % silt and 1～10 % sand. In general, the core is poorly sorted (1.0～2.0 ϕ) with some very poorly sorted (2.0～4.0 ϕ) sand-rich intervals.

CHRONOLOGY

Matsuoka *et al* (1995) reported AMS ^{14}C data and core description from a 9.5-m long core sediment obtained from the same paleo-lake. Their AMS ^{14}C data at depths of 100 cm, 300 cm and 500 cm from the core top were 8,730±70, 13,630±160 and 26,700±150 yr BP. In this study volcanic glasses collected at depth of 444 cm from core BH-4B are used to determine chronology. The collected volcanic glasses represent Aira-Tn (AT) tephra, characterized by glass shard of bubble walled type. The age of the AT tephra is known to be around 24 to 25 ka (Arai *et al.*, 1981; Machida, 1999). Based on the Matsuoka *et al.*'s AMS ^{14}C data and AT tephra of this study, the core sediment dates back to age of 27,000 yr BP.

RESULTS AND DISCUSSION

The core BH-4B has much variable total organic carbon (TOC) concentration and magnetic susceptibility (MS) values, ranging from 2.4 to 17% and from 250×10^{-6} to 25×10^{-6} CGS, respectively. Around at depth of 330 cm, ca 18 ka, the TOC concentration is the lowest and MS value the highest, representing Last Glacial Maximum (LGM), indicating that the East Asian winter monsoon was strong. Also, TOC concentration and MS values suggest that abrupt climate phase shifting from cold and arid, associated with strong winter monsoon, to warm and humid climate condition, strong summer monsoon, occurred during 12-10 ka, representing the Pleistocene - Holocene boundary (Fig. 1). In contrast to MS data in Chinese Loess Plateau, high MS values are due to high input of unweathered magnetic minerals from the basalt with high contents of magnetic minerals such as magnetite and maghemite, indicating winter monsoon intensity. This is supported by the variation of major elements contents. The high alkaline and alkaline earth elements contents in sediments deposited during 27,000 to 12,000 cal yr BP indicate high input of unweathered detritus due to decrease of weathering intensity by cold climate and weak vegetation cover. The latter is supported by low TOC contents (<5%). After the Pleistocene - Holocene boundary, the dramatic decline in the contents for alkaline and alkaline earth elements reflects the reduction of mineral inwash, caused by decrease of soil

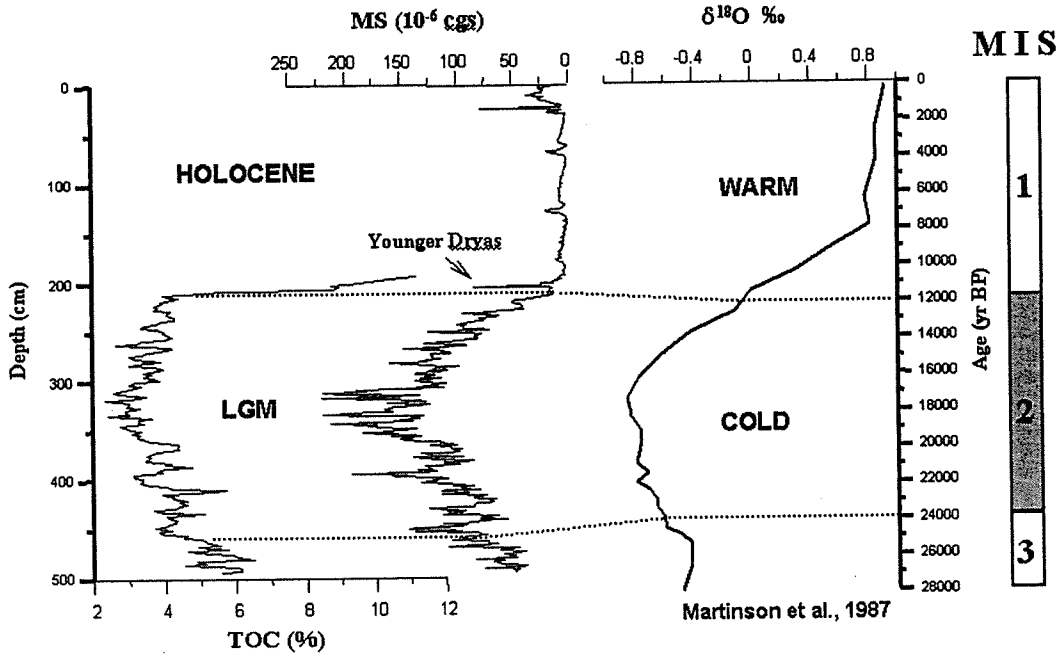

Figure 1. Time series of the last 27,000 yr BP comparing the total organic carbon contents and magnetic susceptibility of the paleo-lake sediments in Jeju Island, Korea and SPECMAP $\delta^{18}O$ record (Martinson et al., 1987).

erosive activity, expanded vegetation cover and the abrupt climatic amelioration at the beginning of the Holocene. This change is marked by a sharp upturn in the organic carbon content. Such a change is supported by the increase of the Chemical Index of Alteration (CIA; Nesbitt and Young, 1982) and the decrease of the Index of Compositional Variability (ICV; Cox *et al.*, 1995) upsequence. In the North Atlantic region and Greenland ice cores the Younger Dryas is marked by abruptly cold climate change event during 11-10 ka (Mangerud *et al.*, 1974 and Dansgaard *et al.*, 1989). The TOC and MS data of studied Jeju core sediments show a short-lived Younger Dryas event during 11,200 to 10,800 cal yr BP, but the intensity of Younger Dryas event did not reach that of LGM.

The studied paleo-lake core sediment has two restricted source materials with distinctively different chemical signatures: (1) eolian dust blown from continental Asia and (2) basement rock composed of trachyte. Thus, REE distribution patterns and Eu anomalies of sediments suggest mixing of basement detritus and eolian dust with varying proportions, indicative of varying intensity of winter monsoon. The chondrite-normalized ratio of Eu/Eu* (where $Eu/Eu^* = Eu/[(Sm)(Gd)^{1/2}]$) for core sediments ranges from 0.77 to 0.97 and profile of Eu/Eu* shows gradual decrease of negative Eu anomaly upsequence, indicating gradually decrease of eolian dust input to paleo-lake because of weakness of winter monsoon. However, the Eu/Eu* record shows that eolian dust input reached its maximum just prior to the LGM compared to the results of MS, TOC and major elements. Thus, TOC and MS data show a time lag behind the eolian

dust flux record during the MIS 2. Xiao *et al* (1997) reported that the eolian quartz flux record apparently lags ca. 5000 yr behind Chinese loess during MIS 2/1 transition. The results of this study show that MS, TOC and major elements record is identical with eolian quartz flux record of Lake Biwa and SPECMAP $\delta^{18}O$ record of deep-sea sediments, but eolian dust input record for Eu/Eu* is identical with quartz median diameter record of Chinese loess (Xiao *et al.*, 1995). The disparity in these two data sets can be accounted for by the fact that the climate in China and Jeju Island had different timing of its change.

REFERENCES

An, Z.S., Liu, T.S., Lu, Y.C., Porter, S.C., Kukla, G.J., Wu, X.H. and Hua, Y.M., 1990, The long-term paleomonsoon variation recoreded by the loess-paleosol sequence in central China. Quaternary International, 718, 91-95.

An, Z.S., Kukla, G.J., Porter, S.C., and Xiao, J.L., 1991a, Magnetic susceptibility evidence of monsoon variation on the Loess Plateau of central China during the last 130,000 years. Quaternary Research, 36, 29-36.

Arai, F., Oba, T., Kitazato, H., Horibe, Y. and Machida, H., 1981, Late Quaternary tephrochronology and palaeo-oceanography of the sediments of the Japan Sea. The Quaternary Research of Japan, 20, 209-230.

Cox, R., Lowe, D.R., Cullers, R.L., 1995, The influence of sediment recycling and basement composition on evolution of mudrock chemistry in the southwestern United States. Geochim. Cosmochim. Acta 59, 2919-2940.

Dansgaard, W., White, J.W.C. and Johnsen, S.J., 1989, The abrupt termination of the Younger Dryas climatic event. Nature, 33, 532-534.

Ding, Z.L., Liu, T.S., Rutter, N.W., Yu, Z.W., Guo, Z.T. and Zhu, R.X., 1995, Ice-volume forcing of East Asian winter monsoon variations in the past 800,000 years. Quaternary Research, 44, 149-159.

Gao, Y.X., 1962, On some problems of Asian monsoon. In: Y.X. Gao, Some questions about the east asian monsoon. Beijing Science Press, p.1-49

Geological Society of Korea, 1999, Geology of Korea. Sigma press, p.474-477.

Machida, H., 1999, The stratigraphy, chronology and distribution of distal marker-tephras in and around Japan. Global and Planetary Change, 21, 71-94.

Mangerud, J., Andersen, S.T., Berglund, B.E. and Donner, J.J., 1974, Quaternary stratigraphy of Norden: a proposal for terminology and classification. Boreas, 3, 109-127.

Martinson, D.G., Pisias, N.G., Hays, J.D., Imbrie, J., Moore, T.C., Jr. and Shackleton, N.J., 1987, Age dating and the orbital theory of the ice ages: Development of a high-resolution 0 to 300,000 year chronostratigraphy. Quaternary Research, 27, 1-29.

Matsuoka, K., Kim, M.H., Takemura, K., Nagaoka, S. and Lee, J.B., 1995, Geologic age and facies of the boring core sediments from Cheju Island, Korea. Natural Science, 35, 135-145.

Nesbitt, H.W., Young, G.M., 1982, Early Proterozoic climates and plate motions inferred from major element chemistry of lutites. Nature, 299, 715-717.

Xiao, J., Inouchi, Y., Kumai, H., Yoshikawa, S., Kondo, Y., Liu, T.S. and An, Z.S., 1997, Eolian quartz flux to Lake Biwa, central Japan, over the past 145,000 years. Quaternary Research, 48, 48-57.

Xiao, J.L., Porter, S.C., An, Z.S., Kumai, H. and Yoshikawa, S., 1995, Grain size of quartz as an indicator of winter monsoon strength on the Loess Plateau of central China during the last 130,000 yr. Quaternary Research, 43, 22-29.

The 10th Seoul International Symposium on Polar Sciences
October 21-22, 2003, Incheon, Korea

OCCURRENCE OF VIVIANITE IN LATE PLEISTOCENE LACUSTRINE SEDIMENTS AT SOGWIPO, JEJU ISLAND, KOREA

Seung Hyoun Lee[1], Yong Il Lee[1], Ho Il Yoon[2], Cheon Yun Kang[2] and Yaedong Kim[2]

[1] School of Earth and Environmental Sciences, Seoul National University, Seoul 151-747, Korea [lshkingdom@hanmail.net]
[2] Korea Polar Research Institute, Korea Ocean Research and Development Institute, Ansan P.O. Box 29, Korea

INTRODUCTION

In generally, phosphate minerals of sedimentary origin are formed in highly productive areas of the oceans where upwelling of nutrient-rich water occurs (Piper *et al.*, 1995), but iron-rich phosphate minerals are reported in restricted environment with no upwelling such as lacustrine environments (De las Heras *et al.*, 1989). In the lacustrine system, main source of phosphorus is organic matter such as zooplankton, faecal pellets, fish teeth and bones, and bird debris (Porter and Robbins, 1981; Haberyan, 1984; Tiercelin, 1991). Vivianite is an iron phosphate mineral forming during early diagenesis in lacusrine systems which receive large inputs of detrital terrigenous organic matter, and with low availability of calcium, rich iron, limited sulfate, neutral to low acidic pH, and mildly oxidizing to reducing conditions (Berner, 1980; Nriagu, 1972; De las Heras *et al.*, 1989; Stamatakis and Koukouzas, 2001), and it is authigenic iron mineral that forms during the early diagenesis in lacustrine environments with limited sulfate provision (Berner, 1980). We report the occurrence of vivianite in Korean Pleistocene lacustrine sediments and examine the importance of vivianite as indicator of paleolacustrine environments.

STUDY AREA AND MATERIALS

A 8.19 m long sediment core BH-4A was obtained from the paleo-lake, which is located at about 1 km north of Oedolgoe, southern part of Jeju Island. It is an ellipsoidally shaped basin with 800 m across in NW-SE direction and 500 m across in NE-SW direction. The basement rock in the study area consists of trachyte erupted during the Quaternary. It is believed that the study area was a caldera lake formed by a parasitic volcanism. Continuous sediment input filled up the lake and it is a closed basin without inlet and outlet. The obtained core sediments are analyzed by X-radiograph, magnetic susceptibility (MS), total organic carbon (TOC), EPMA,

zoom microscope and SEM.

RESULTS

Vivianites occur at three horizons at depths 493 cm, 509 cm, and 526 cm from the core top. Fig. 1 shows detailed sedimentary facies between 440 and 550 cm in core BH-4A. The lower part of the studied core interval is severely deformed and shows burrow-fill structure. The middle part consists of the alternation of thin layers and massive mud. The upper part is characterized by a massive to slightly bioturbated thick mud unit and indistinct layers. Vivianites occur in the slightly bioturbated mud (Fig. 1), which is above the well preserved thin layers or burrow-fill structure. The content of CaCO3 between 440 and 550 cm ranges from 0.2 to 0.66 wt% and is much smaller than total carbon. This means that there was no significant terrigenous carbonate input and little living organism such as ostracod. The content of TOC ranges from 3 to 6 wt%. Downcore variations of magnetic susceptibility from the studied interval are high ranging from 40×10^{-6}CGS to 300×10^{-6}CGS (Fig. 1).

DISCUSSION

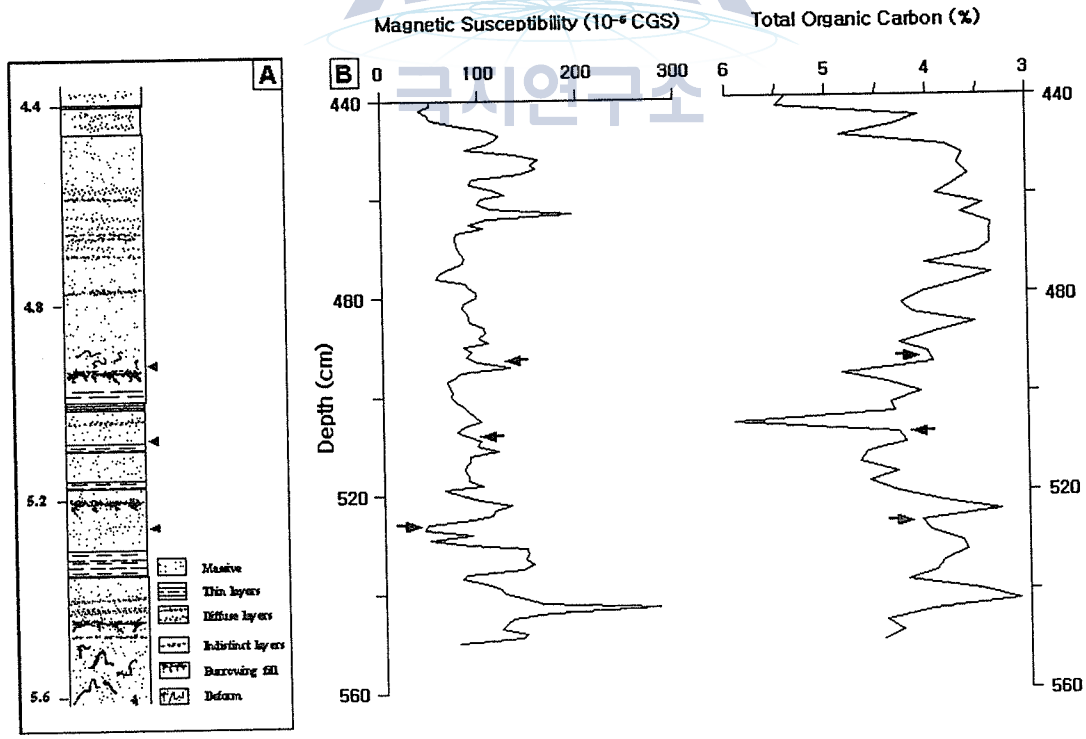

Figure 1. (A) Detailed columnar section from depth 440cm to 550cm. Arrow heads represent horizons at which vivianites occur. (B) Vertical profiles of Magnetic Susceptibility (MS) and Total Organic Carbon (TOC) in core BH-4A. MS pattern shows inverse correlation with TOC pattern.

1. Sedimentary Facies

Based on the absence of traction current structures, silt layers were deposited by fall-out of silt size particles from interflows which flew along or near the thermocline, when incoming sediment-laden water is denser than water in the epilimnion but less dense than the cold water of the hypolimnion (Einsele, 1991). The studied lake is a closed lake without distinct channels draining from the surrounding hills. Thus, most sediments coming into the lake were supplied from surrounding hills during rainfall or storms. On the X-radiographs of the core BH-4A, thin silt layers seem to have been deposited by interflows and massive mud by settling from suspension during warm and humid climate. The burrow-fill structures are formed by mass flow during heavy storms. These sediments contain much oxygen, because they were supplied directly from surrounding hills into lake bottom, allowing bioturbation. X-radigraph shows that mud unit alternates with silt layer and that vivianite occurred in the mud unit above the silt layer. The mud unit which has high organic matter content, seems to have supplied phosphorus to form vivianite. The silt layer supplied from surrounding volcanic rock, seems to have supplied Fe ion to form vivianite. Therefore, after the iron-rich sediments were supplied into the lake during the period of high rainfall or of heavy rainstorm, muddy sediments with high organic contents were further accumulated under warm and calm conditions, which led to vivianite formation.

2. Formation of vivianite, intermediate TOC

Detrital terrigenous organic matter takes an important portion of organic matter received in lakes and play an important role supplying phosphorus to form phosphate minerals (De las Heras *et al.*, 1989). Rich organic matter originated from detrital terrigenous input and diatom blooming, indicates that climate was warm and humid at that time. Also, bottom water might have been weakly oxic or anoxic to preserve organic matter, preventing organic matter from decomposition by bacteria. Vivianite occurred with intermediate TOC of about 4 wt%. This suggests that vivianite formed under mildly oxidizing/reducing conditions. The reason why vivianite did not occur in the high TOC zone seems that decomposition of organic matter generate SO_4^{2-}. In the marine environment, the authigenic iron mineral that form during early diagenesis of organic rich, anoxic sediments is normally pyrite (FeS_2), because of sufficient dissolved SO_4^{2-} in seawater. However, in lacustrine sediments, because of low initial SO_4^{2-} and restricted supply of S by sulfur reduced bacteria, iron authigenic minerals that forms during early diagenesis are vivianite and siderite. In organic matter-rich freshwater sediments such as coal swamp, organic matter itself can furnish sufficient sulfur and this allows conversion of most reactive detrital iron to pyrite not vivianite (Berner, 1980).

High MS values indicate that sediments have iron-bearing minerals such as magnetite and maghemite (Schwertmann and Taylor, 1977). MS and TOC pattern of Core BH-4A shows inverse correlation. This suggests that organic matter caused dilution effect of MS. Sediments which have weakly magnetic components, such as organic matter, quartz and clay minerals, may also display apparent depletion of magnetic property, through dilution effects (Maher, 1998).

CONCLUSIONS

The vivianite occurs in the core sediments which were obtained from Jeju Island, Korea. X-radiograph shows that vivianite occurs among alternating mud and silt layers. Mud unit has high organic matter content and seems to be a source of phosphorus. Silt layer alternated with mud shows high MS value and seems to have supplied Fe ion for vivianite. After the iron-rich sediments were supplied into the lake during the period of high rainfall or of heavy rainstorm, muddy sediments with high organic contents were further accumulated under warm and calm conditions, which led to vivianite formation. Result of TOC analysis shows that vivianite occurs in the intermediate TOC zone. This is because the sulfur generated by the decomposition of organic matter precipitates pyrite and prevents the formation of vivianite. This indicates that vivianite is formed under mildly oxidizing/reducing conditions to preserve the proper organic matter. This study shows that vivianite is a useful indicator mineral of paleolacustrine environmental condition such as high organic matter, mildly oxidizing to reducing conditions of lake water and warm and humid climates.

REFERENCES

Berner, R.A., 1980. Early diagenesis A theoretical approach. Princeton University Press, p.210-211.

De las Heras, X., Grimalt, J.O., Albaiges, J., Julia, R. and Anadon, P., 1989, Origin and diagenesis of the organic matter in Miocene freshwater lacustrine phosphates (Cerdanya Basin, Eastern Pyrenees). Organic Geochemistry, 14, 667-677.

Einsele, G., 1991. Sedimentary basins: Evolution, facies, and sediment budget. Springer, p.75-93.

Geological Society of Korea, 1999. Geology of Korea. Sigma press, p.474-477.

Haberyan, K.A., 1984. Copepod fecal pellets and microfossil deposition in Lake Tanganyika. Thesis. University of Georgia, Athens, USA, p.151.

Maher, B.A., 1998. Magnetic properties of modern soils and Quaternary loessic paleosols: paleoclimatic implications. Palaeogeography, Palaeoclimatology, Palaeoecology, 137, 25-54.

Nriagu, J.O., 1972. Stability of vivianite and iron-pair formation in the system Fe3(PO4)2-H3PO4-H2O. Geochim. Cosmochim. Acta, 36, 459-470.

Piper, D.Z., Isaacs, C.M. and Medrano, M.D., 1995. Occurrence of Fe-Ca, and Ca-phosphate minerals in

concretions within the Monterey Formation: a record of uplift of the Santa Maria Basin, California. US geol. Surv. Bull. 1995-C, C1-C15

Porter, K.G. and Robbins, E.J., 1981. Zooplankton fecal pellets link fossil fuel and phosphate deposits. Science, 212, 931-933.

Schwertmann, U. and Taylor, R.M., 1977. Iron oxides. In: Dixon, J.B., Weed, S.B.(Eds.), Minerals in Soil Environments. Soil Sci. Soc. Am., Madison, 145-180.

Stamatakis, M.G. and Koukouzas, N.K., 2001. The occurrence of phosphate minerals in lacustrine clayey diatomite deposits, Thessaly, Central Greece. Sedimentary Geology, 139, 33-47.

Tiercelin, J.J, 1991. Natural resources in the lacustrine faces of the Cenozoic rift basins of East Africa. Spec. Publ. Int. Ass. Sediment, 13, 3-37.

The 10th Seoul International Symposium on Polar Sciences
October 21-22, 2003, Incheon, Korea

MICROFABRIC ANALYSIS OF LAMINATED DIATOM OOZE IN THE HOLOCENE SEDIMENTS FROM THE EASTERN BRANSFIELD STRAIT, ANTARCTIC PENINSULA

Jang Jun Bahk[1], Ho Il Yoon[2], Yeadong Kim[2], Cheon Yun Kang[2] and Sung Ho Bae[2]

[1] Global Environment Research Laboratory, Korea Ocean Research and Development Institute, Ansan, P.O. Box 29, Seoul 425-600, Korea [jjbahk@kordi.re.kr]
[2] Korea Polar Research Institute, Korea Ocean Research and Development Institute, Ansan, P.O. Box 29, Seoul 425-600, Korea

Selected intervals of Holocene laminated sediments from the eastern Bransfield Strait (cores EB-2 and GC00-13; Fig. 1), Antarctic Peninsula were analyzed using high-resolution section images of impregnated samples to reveal potential annual-to-seasonal scale signatures of the lamination. The analyzed intervals consist of alternating diatom ooze (DO) and terrigenous laminae. Microfabric analysis of the DO laminae reveals three types of monospecific laminae (types I-CRS, I-RS, and I-CT) and two types of multispecific laminae (types IIa and IIb) (Figs 2 & 3). The monospecific DO laminae are characterized by predominance of single diatom species of *Chatoceros* resting spores (Type I-CRS), *Corethorn*, (Type I-CT) or *Rhizosolenia* (Type I-RS), whereas the multispecific DO laminae comprise mixed assemblages of diatoms which sometimes show an upward change in species abundance (Type IIb) (Figs 2 & 3). The

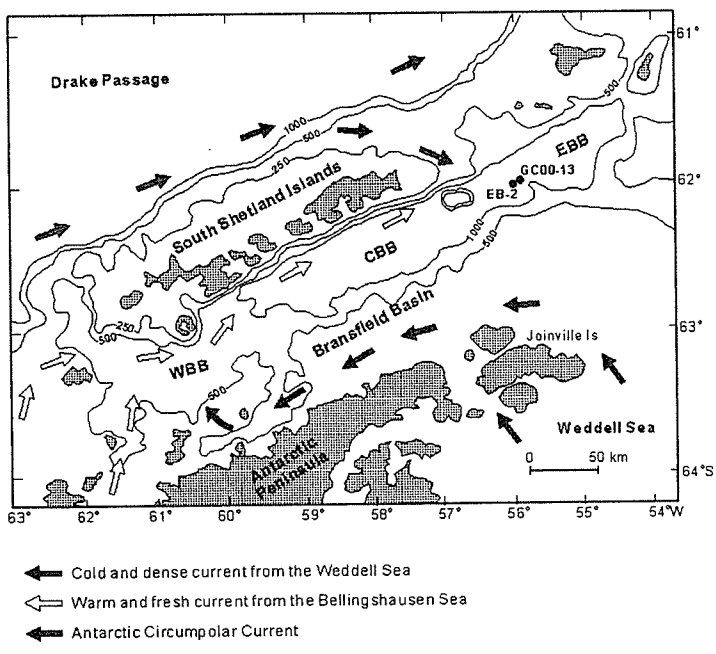

Figure 1. Core locations and general surface circulations in the Bransfield Strait. WBB, CBB and EBB denote the Western, Central, and Eastern Bransfield basins, respectively. Contours are in meters.

upward changes in diatom species abundance within individual laminae suggest a probable sequence of diatom flux events which mainly reflects rapid settling of *Chatoceros* resting spores during spring blooms in a stratified surface ocean, followed by mass sedimentation of *Corethron* or *Rhizosolenia* with onset of autumn/winter mixing (Fig. 4). The couplets of monospecific DO and terrigenous laminae often repeat itself (Fig. 3), most likely representing successive spring or autumn diatom fluxes intervened by terrigenous fluxes during the rest of year.

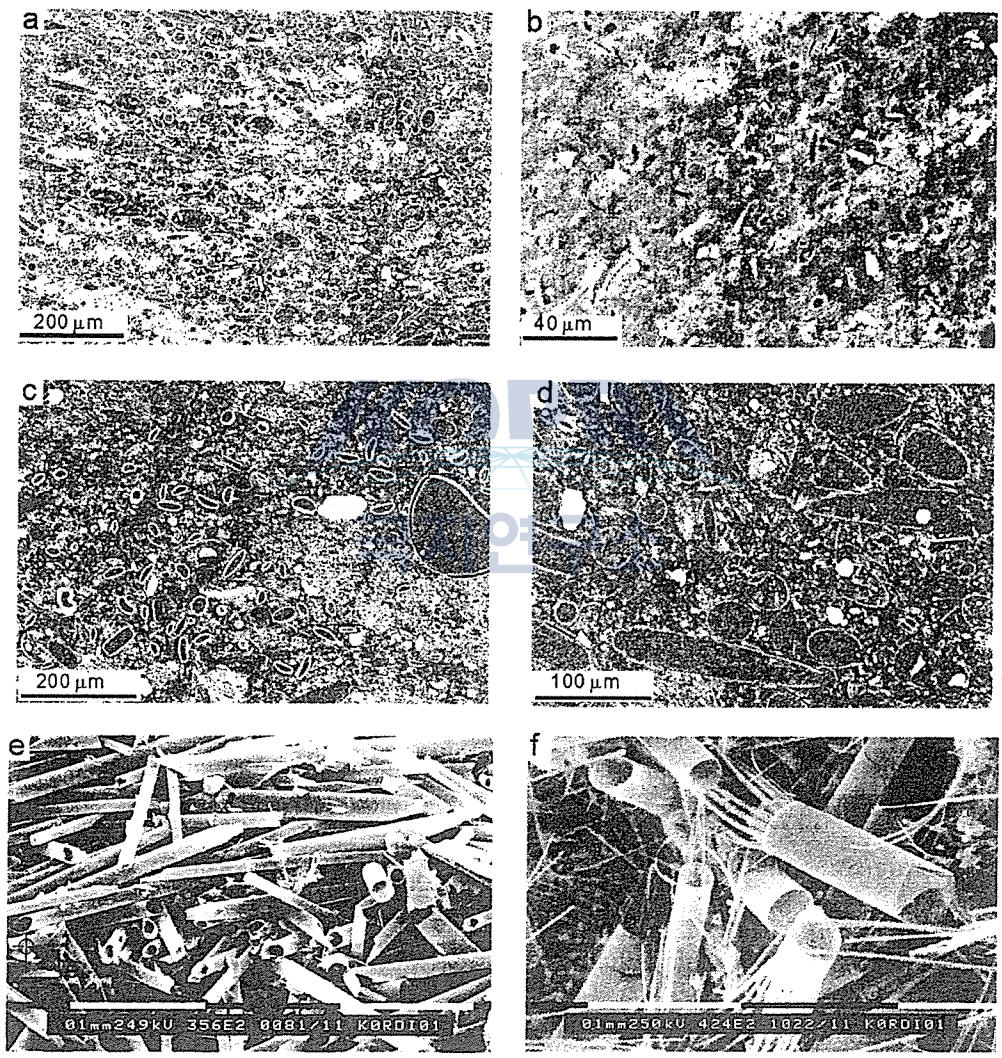

Figure 2. Backscattered electron images (a-d) and topographic secondary electron images (e, f) of monospecific diatom ooze laminae; image locations are shown in Fig. 3 (a) *Rhizosolenia*-dominant lamina, (b) *Chaetoceros* (resting spore)-dominant lamina; upward to the upper left corner, (c) abundant *Thalassiosira* antarctica resting spores within clayey matrix, (d) *Corethoron*-dominant lamina, (e) *Rhizosolenia*-dominant lamina, (f) *Corethron*-dominant lamina. Note near intactness of the frustules in (e) and f).

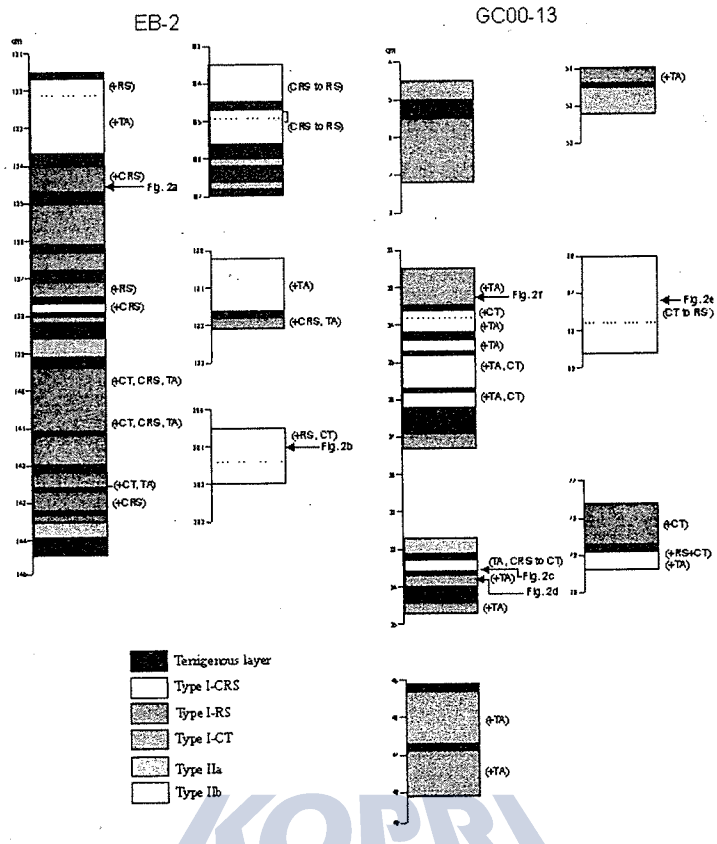

Figure 3. Schematic logging of laminated diatom ooze intervals showing types of each lamina (see text for the definitions). Symbols in the brackets indicate subordinate species composition (with plus signs) or upward changes in species abundance in diatom ooze laminae. CRS=*Chaetoceros* resting spore, CT=*Corethron* spp., RS=*Rhizosolenia* spp. (including *Proboscia* spp.), and TA=*Thalassiosira antarctica*. Dotted lines indicate an abrupt change in species abundance within single diatom ooze lamina. Locations of figure 2 are indicated with arrows.

Rhizosolenia spp.	Autumn mass sedimentation of diatoms which have grown during the period of summer stratification.
Corethron spp.	
Chaetoceros resting spore	Spring blooms of *Chaetoceros*, terminated with rapid aggregation and sinking of resting spore.
(*Thalassiosira antarctica*)	Surface water intrusion from the Weddell Sea during the early spring (?)

Fig. 4. Model sequence of diatom species abundance within single diatom ooze lamina and its interpretation.

The 10th Seoul International Symposium on Polar Sciences
October 21-22, 2003, Incheon, Korea

LATE QUATERNARY PALEOENVIRONMENT OF THE SAINT ANNA TROUGH, ARCTIC RUSSIA

Jae Il Lee, Yaedong Kim and Ho Il Yoon

Korea Polar Research Institute, KORDI, P.O.Box 29, Ansan 425-600, Korea [leeji@kordi.re.kr]

Three gravity core samples have been obtained from the Saint Anna Trough, Russian Arctic, in September 2001 (Fig. 1). Water content, magnetic susceptibility, organic matter content, total nitrogen and sulfur content, and grain size of the samples have been analyzed for the reconstruction of the paleoenvironment during the Late Quaternary time. For the identification of mineral composition, bulk sample and clay-size fraction were analyzed by X-ray diffraction method. To understand controls of the sedimentary composition and changes in provenance, trace and rare earth element concentrations were analyzed and correlated with other results.

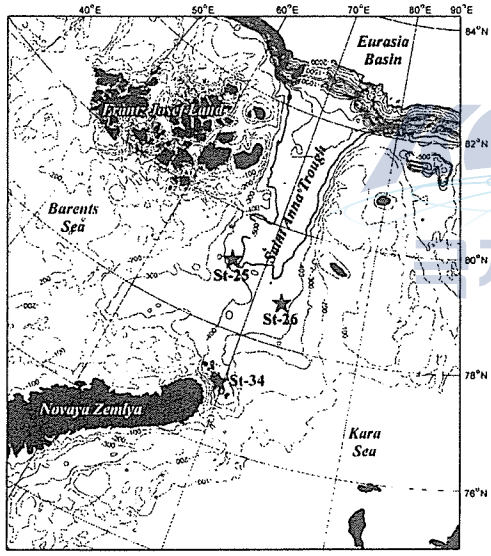

Figure 1. Sampling site of cores St-25, -26 and -34 from the Saint Anna Trough. Areas below 300m water depth is shaded to delineate the shape of the trough.

Dark gray massive diamicton facies have been observed in the lower part of the cores St-25 and –34. In the bottom of the St-25 core, a mudrock clast of about 10cm in length were found in the diamicton facies. Sets of subparallel striations are developed on more than one surface of the clast, which is characteristic surface texture of the clast deposited in glacial environment. This facies was interpreted to be glaciogenic diamicton deposited during the Last Glacial Maximum in the Saint Anna Trough.

Mineral composition and trace and REE concentrations of the core St-25 and -34 suggest major change in sedimentary provenance between glacial and interglacial periods. Type of organic matter of the cores St-25 and -34, identified based on C/N ratio, also changed during this time from dominantly terrestrial organic matter in glacial period to marine organic matter in interglacial period. Sediment composition of the diamicton facies of the St-25 and –34 is slightly different from each other, implying different sediment sources.

The 10th Seoul International Symposium on Polar Sciences
October 21-22, 2003, Incheon, Korea

FORMATION AND DISSOCIATION PROCESSES OF GAS HYDRATES COMPOSED OF METHANE AND CARBON DIOXIDE BELOW THE ICE POINT

A. Hachikubo, K. Yamada, T. Miura, K. Hyakutake, K. Abe and H. Shoji

New Energy Resources Research Center, Kitami Institute of Technology
[hachi@snow2.civil.kitami-it.ac.jp]

INTRODUCTION

Gas hydrates are crystalline clathrate compounds composed of water and gases, and are stable at low temperature and high pressure conditions. Huge amounts of natural gases are stored in hydrate crystals in deep-sea sediments and permafrost.

Gas hydrates in permafrost area exist in the condition of temperature below the ice point. The pressure condition, which critically affects the stability of hydrate, is complicated since the hydrate crystals are fixed in ice or frozen soil. Although many studies have been made on kinetics of hydrate formation and dissociation, little is known how the gas hydrates form or dissociate at the temperature below the ice point. In addition, natural gas hydrates are composed of mixed gases and their each component may affect the kinetics and their maintenance processes.

To understand the formation and dissociation behavior of gas hydrate and investigate the controlling factors for the phase transition of gas hydrate, experiments of its formation and dissociation were conducted by monitoring pressure and temperature variations.

EXPERIMENTAL METHODS

Samples of gas hydrate were formed from powder ice (mean grain size: less than 0.05mm) and guest gases (methane, carbon dioxide and their mixture: 25, 50, 75mol%CH4) in a pressure cell. Temperature and pressure in the cell were measured by a platinum thermometer and a pressure gauge, respectively. The cell was immersed in a temperature-controlled liquid-bath and the temperature was kept below the ice point.

Ice powder (35g) was added into the cell and the guest gas was charged over the anticipated equilibrium pressure at the controlled temperature (range: 260.7-272.6K). The pressure started to decrease by a formation of hydrate and close to the equilibrium value. The period that the

internal pressure decreases and reaches to the equilibrium value is defined as "formation time", and the difference between the maximum and the equilibrium pressures is also defined as "delta P" (range: 0.18-1.8MPa), which corresponds to the degree of supercooling for hydrate formation.

Besides, the gas was discharged or recharged from the equilibrium condition and the hydrate started to dissociate or form to maintain the equilibrium pressure, respectively. The periods that the phase transition proceeds and the pressure difference between the present and the equilibrium values reaches to less than 0.01MPa are defined as "formation/dissociation times". A value of discharged/recharged pressure is also defined as "delta P".

RESULTS AND DISCUSSION

1. Formation of hydrate from powder ice and gas

A relation between formation time and delta P is shown in Fig.1. The data were almost in the range of 1-10 hours and seemed to have no dependence on both delta P and mixing ratio of gases. It indicates that a formation speed of hydrate from ice and gas is not determined only by a degree of supercooling.

Fig.2 shows a time variation of the internal pressure. When the delta P was more than 1MPa and the formation time was less than five hours, the internal pressure rapidly decreased at the last stage of formation process and reached to an equilibrium condition. This tendency was often observed in case of carbon dioxide. The formation time of carbon dioxide hydrate was small and it reached to less than 20 minutes when the temperature was more than 272.2K, whereas more than hundred hours were needed to form methane hydrate and reach to an equilibrium condition, as shown in Fig.1. From these results it is possible that a liquid film on the ice surface effects to the formation process of gas hydrate.

2. Formation and dissociation of hydrate from equilibrium condition

Fig.3 shows a relation between formation/dissociation time and delta P. The internal pressure of the cell was changed about 0.05-0.6MPa by charge or removal of gas. When the delta P was less than 0.1MPa, which corresponds to about 1.5K for methane and about 3K for carbon dioxide as a degree of supercooling, formation/dissociation time was small. On the other hand, the formation/dissociation time increased as delta P and its dispersion also increased largely. In case of dissociation for carbon dioxide hydrate, it is often observed that the dissociation speed rapidly increased and reached to an equilibrium condition at the last stage of the dissociation. It indicates that a self-preservation effect may affect and limit the speed of hydrate dissociation.

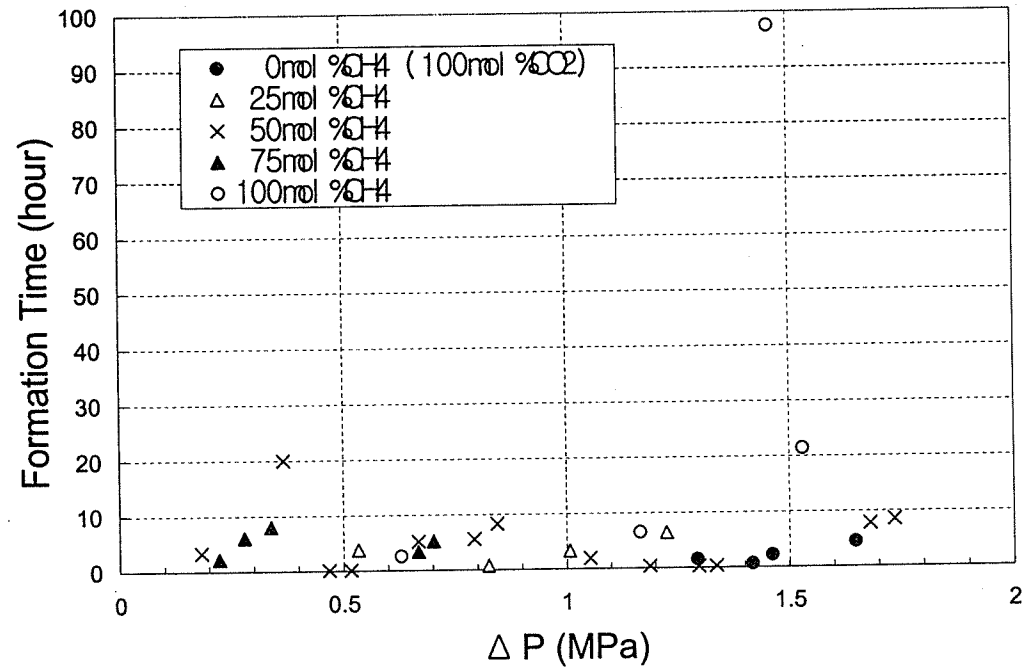

Figure 1. A relation between formation time and delta P.

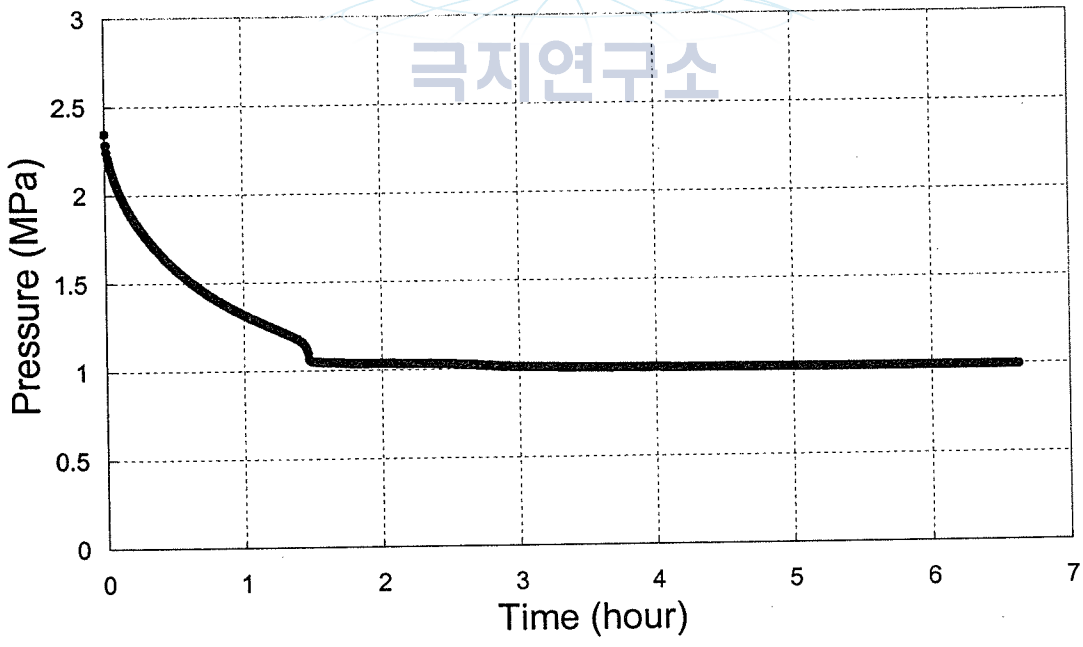

Figure 2. A time variation of the internal pressure at the formation of carbon dioxide hydrates.

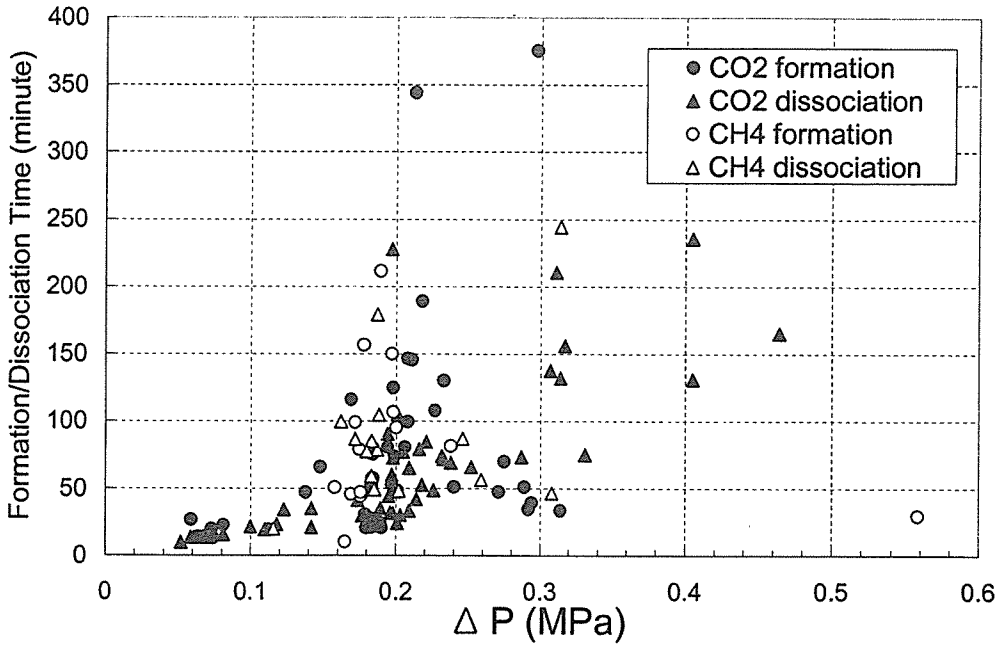

Figure 3. The data of formation/dissociation time plotted against delta P.

The 10th Seoul International Symposium on Polar Sciences
October 21-22, 2003, Incheon, Korea

VISUAL OBSERVATIONS OF TUBULAR GAS HYDRATE FORMATION IN A PRESSURE CELL WITH WATER AND SEAFLOOR SEDIMENT

K. Hyakutake[1], O. Kitamura[1], S. Kataoka[1], A. Hachikubo[1], H. Shoji[1] and L. Mazurenko[2]

[1] Kitami Institute of Technology, 165 Koen-cho, Kitami 090-8507, Japan [hyakutak@mail.kitami-it.ac.jp]
[2] All-Russia Research Institute for Geology and Mineral Resources of the Ocean, 1 Angliyskiy Street, St.Petersburg 190121, Russia

ABSTRACT: Echograms obtained at the continental margin of North-East Sakhalin, Okhotsk Sea show many flare images, which may result from the gas bubble emissions from the seafloor. Laboratory experiments were conducted for the detailed formation processes of tubular gas hydrate under gas bubble emission conditions for the future observation at the continental margin of North-East Sakhalin.

INTRODUCTION

Submarine gas hydrate investigations have been conducted extensively in the Sea of Okhotsk by the joint Russian-German project, KOMEX[1)]. Echograms obtained at the continental margin of North-East Sakhalin show hydroacoustic anomalies which are hypothetically coupled with gas seepages. Gas bubble emissions from the seafloor could be resulted in formations of tubular gas hydrate, such as pipe-shaped gas hydrate formed in the sediment layers and/or chimney structures above the seafloor. The purpose of this study is to form tubular gas hydrate artificially in a laboratory to understand the formation processes in details.

CHIMNEY STRUCTURE

A pressure cell was designed and constructed in the New Energy Resources Research Center, Kitami Institute of Technology to form gas hydrates from gas bubbles in water under a high hydrostatic pressure. Optical window in the cell allows to observe the detailed formation processes during experiments (Fig.1).

CO_2 gas bubbles were supplied from the cell bottom through a nozzle of 1.0 mm inner diameter. CO_2 gas bubbles were continuously supplied into the water to increase the hydrostatic pressure from the ambient pressure to the experimental pressure, 3.0 MPa. The water

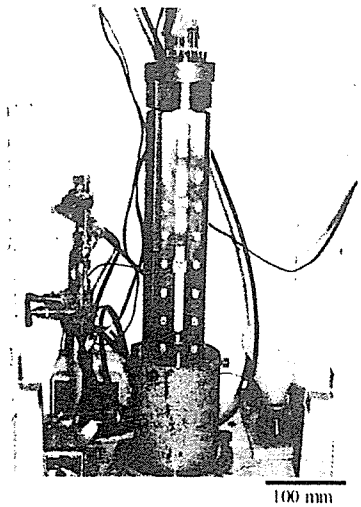

Figure 1. Pressure cell.

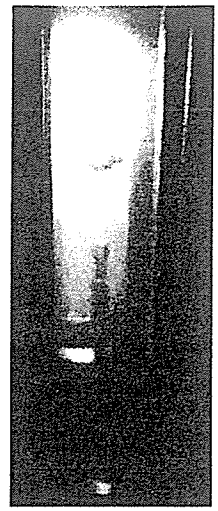

Figure 2. Chimney structure in water; C

temperature was kept to be close to the freezing point. A gas hydrate chimney started to form from the top edge of the nozzle and grew upward with releasing gas bubbles sometimes. Figure 2 shows such chimney gas hydrate formed. A continuous video-recording revealed that the growth rate is not constant, but is closely related with gas bubble conditions at the top of the chimney.

PIPE-SHAPED STRUCTURE IN THE SEAFLOOR SEDIMENT

Figure 3. Pipe-shaped gas hydrate in the sea floor sediment; P

Tubular gas hydrate was formed in a pressure cell by using CH_4 gas and seafloor sediment from the Black Sea (silty clay). No tubular gas hydrate was formed when water content is lower than 50 wt% due to the difficulty in gas bubble flow. Figure 3 shows pipe-shaped structure of gas hydrate formed in the seafloor sediment. Hydrostatic pressure, temperature and water content are 4.2 MPa, 274 K and 70 wt% respectively. Experimental data obtained with various conditions of gas bubble release rate revealed that an appropriate range of the release rate values exists for pipe-shaped gas hydrate formation in the sediment. These findings will be utilized to detect tubular gas hydrate at the continental margin of North-East Sakhalin during the field operation of CHAOS project (hydro-Carbon Hydrate Accumulations in the Okhotsk Sea; an international collaboration effort among Russian, Japanese, Korean, German and Belgium researchers) in 2003.

REFERENCES

1) N. Biebow, T. Ludmann, B. Karp, and R. Kulinich, 2000. Cruise Reports: KOMEX V and VI: RV Professor Gagarinsky cruise 26, MV Marshal Gelovany cruise 1. GEOMAR Report, 88, 296 pp

The 10th Seoul International Symposium on Polar Sciences
October 21-22, 2003, Incheon, Korea

FORMATION PROCESSES OF MASSIVE GAS HYDRATE IN A PRESSURE CELL WITH WATER-SATURATED SEDIMENT CONDITIONS

O. Kitamura, S. Kataoka, K. Hyakutake, A. Hachikubo and H. Shoji

Kitami Institute of Technology, 165 Koen-cho, Kitami 090-8507, Japan [mcv02005@std.kitami-it.ac.jp]

ABSTRACT: Echograms obtained at the continental margin of North-East Sakhalin, Okhotsk Sea show many flare images, which may result from the gas bubble emissions from the seafloor. Natural samples obtained near the seafloor show a feature of massive layer of dense gas hydrate. Laboratory experiments were conducted for the detailed formation processes of massive gas hydrate with various conditions by changing size of sediment particles, with one or two sediment layers, and with or without gas bubble emissions for the future observation at the continental margin of North-East Sakhalin. Experimental results show that massive gas hydrate is formed when the nucleation is limited and water flow with dissolved gas takes place easily in the sediment.

INTRODUCTION

Submarine gas hydrate investigations have been conducted extensively in the Sea of Okhotsk by the joint Russian-German project, KOMEX[1]. Echograms obtained at the continental margin of North-East Sakhalin show hydroacoustic anomalies which are hypothetically coupled with gas seepages. Gas hydrate samples obtained are of massive layer of dense hydrate. This suggests that massive gas hydrate forms under gas bubble emissions at the continental margin of North-East Sakhalin. The purpose of this study is to form massive gas hydrate artificially in a laboratory to understand the formation processes in details.

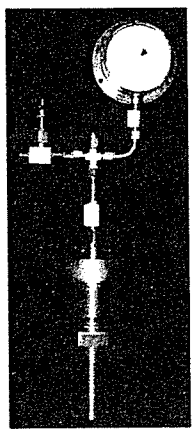

Figure 1. Pressure cell, A

SINGLE LAYER EXPERIMENTS

Land soil was sieved into three types; coarse sand, fine sand and silty clay. Each of them was put into a pressure cell, type A (Fig.1) and water saturated. The water used was saturated with CO_2 gas at 274 K and ambient pressure beforehand. Then CO_2 gas was supplied into the cell

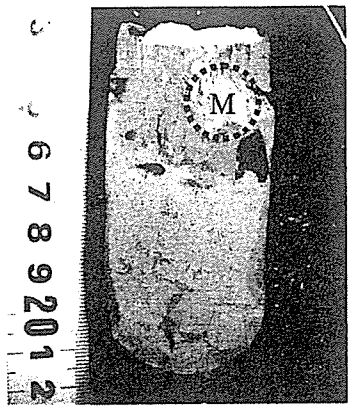

Figure 2. Massive hydrate; M

to increase the pressure up to 4.0 MPa, higher than liquid CO_2 pressure for easy dissolution into water. Then the cell is kept at 274 K for 24 hours for the formation of gas hydrate. The cell is moved to a cold room at 258 K to freeze the water. After residual water is frozen, the sample is taken out from the cell and examined for the size of gas hydrate in a cold room. The largest size (a few centimeter) of hydrate mass was observed in silty clay (Fig.2), which is quite resembled to an ice lens formation in frozen ground.

TWO LAYERS EXPERIMENTS WITH GAS BUBBLE EMISSIONS

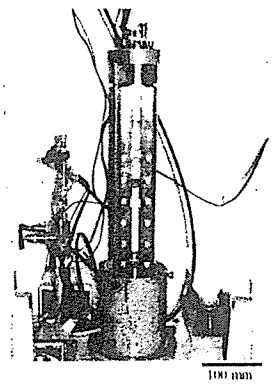

Figure 3. Pressure cell, B

Another pressure cell, type B designed and constructed in the New Energy Resources Research Center, Kitami Institute of Technology was used to form gas hydrates with two layers of soil/sediment particles from gas bubbles in water under a high hydrostatic pressure (Fig.3). Sand and silt were selected by sieving land soil. Clay was obtained from bottom sediment at Lake Baikal.

Soil/sediment layers were water saturated, but the water was not CO_2 saturated beforehand. CO_2 gas bubbles were supplied from the cell bottom through a nozzle of 1.0 mm inner diameter. CO_2 gas bubbles were continuously supplied into the water to increase the hydrostatic pressure from the ambient pressure to the experimental pressure close to 3.0 MPa. The water temperature was kept at 274 K. Figure 4 shows such massive gas hydrate formed in a lower layer. Rising velocity of gas bubbles increases when particle size increases. Therefore, rising velocity decreases when air bubbles penetrate from the lower layer to the upper layer under the situations shown in Fig. 4. The decrease in the rising velocity at the layer boundary may result in the accumulation of gas bubbles in the lower layer, leading to an enhancement of gas molecule dissolution into the water. This may cause the formation of massive gas hydrate only in the lower layer.

These findings may be helpful to understand massive gas hydrate formation processes at the continental margin of North-East Sakhalin. A field operation of CHAOS project (hydro-Carbon Hydrate Accumulations in the Okhotsk Sea; an international collaboration effort among Russian, Japanese, Korean, German and Belgium researchers) is planned in 2003.

REFERENCES

N. Biebow, T. Ludmann, B. Karp, and R. Kulinich, 2000. Cruise Reports: KOMEX V and VI: RV Professor Gagarinsky cruise 26, MV Marshal Gelovany cruise 1. GEOMAR Report, 88, 296 pp.

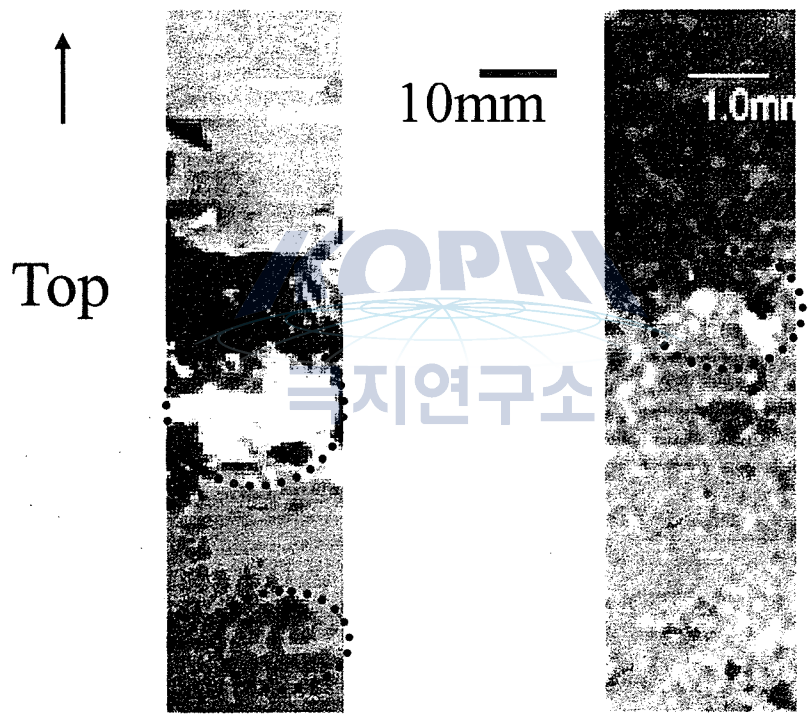

Figure 4. Massive hydrate; (a) left, Clay is upper and silt is lower. Gas hydrate is observed in a lower (silt) layer. (b) right, Silt is upper and sand is lower. Gas hydrate is observed in a lower (sand) layer.

The 10th Seoul International Symposium on Polar Sciences
October 21-22, 2003, Incheon, Korea

PHASE EQUILIBRIUM STUDIES ON MIXED GAS HYDRATES COMPOSED OF METHANE AND CARBON DIOXIDE BELOW THE ICE POINT

T. Miura, A. Hachikubo, K. Hyakutake, K. Abe and H. Shoji

Kitami Institute of Technology, 165 Koen-cho, Kitami 090-8507, Japan [mcv02028@std.kitami-it.ac.jp]

INTRODUCTION

Gas hydrates are crystalline compounds that are formed by cages constructed by water molecules and inclusions that are molecules of guest gases. High pressure and low temperature conditions are necessary for the stability of gas hydrates. Gas hydrates attract our attention as a new energy resource since large amount of gas hydrates of which inclusions are mainly methane and other hydrocarbons are distributed in permafrost areas and marine sediments in continental margins.

Hydrate phase equilibria for mixed gases and water system have been studied by many researchers, but no previous study has been conducted for mixed gases and ice system, which will be needed to discuss the stability of gas hydrate in permafrost areas. Beside this, it has been investigated recently that natural gas hydrate can be replaced with carbon dioxide hydrate, because it is useful not only for exploitation of natural gas hydrate but also a sequestration of carbon dioxide. The aim of this study is to obtain the phase equilibria for ice, mixed gases (methane and carbon dioxide) and their hydrate system below the ice point.

APPARATUS AND METHODS

Experiments of gas hydrate formation and dissociation were performed with a high-pressure cell made of stainless steel, of which internal volume capacity is 120 ml, and is durable to the pressure up to the maximum value of 20 MPa. Inner temperature and pressure were measured by a platinum-resistance thermometer and a pressure gauge (KEYENCE AP-14), respectively.

First, approximately 10g of powder ice made from pure water were put into the high-pressure cell and it was placed in the temperature-controlled bath, which maintains below the ice point. Next, a mixed gas composed of methane and carbon dioxide at a specified ratio (25, 50 and 75mol%CH_4) was supplied to the high-pressure cell to form gas hydrate. After that, phase boundary of gas hydrate was obtained by controlling pressure or temperature of the high-

pressure cell. Internal pressure can be changed by a piston in an extra chamber. When the pressure was increased or decreased by the piston, the hydrate started to form or dissociate and the pressure closed to an equilibrium value. In another method, we can obtain equilibrium data easily by changing the temperature of the pressure cell.

RESULTS

Phase equilibria of gas hydrate composed methane, carbon dioxide and their mixture are shown in Fig.1. The results obtained from a pressure-change method and a temperature-change method agreed fairly well each other. Phase boundary of the mixed gas hydrate composed of methane and carbon dioxide closely approached that of the simple carbon dioxide hydrate (Fig.1). This means that carbon dioxide is easier to be fixed in hydrate than methane. This tendency corresponds to the results above the ice point reported by literature.

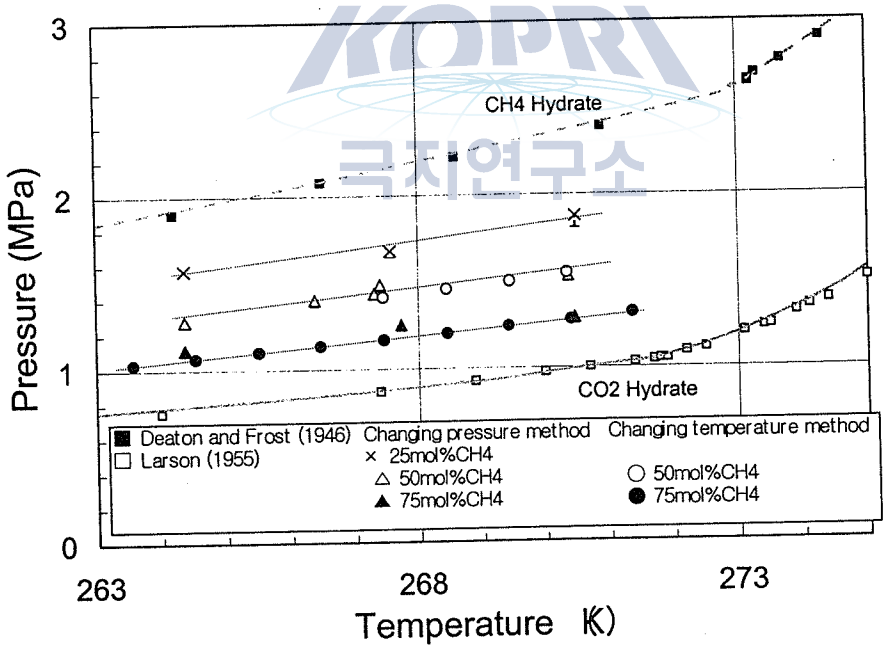

Figure 1. Hydrate-phase boundary of mixed gas (carbon dioxide and methane).

The 10th Seoul International Symposium on Polar Sciences
October 21-22, 2003, Incheon, Korea

CP-MAS ^{13}C-NMR STUDY ON THE CRYSTALLOGRAPHIC STRUCTURE OF NATURAL GAS HYDRATE IN THE BOTTOM OF THE OKHOTSK SEA AND LAKE BAIKAL

M. Kida[1], H. Sakagami[1], H. Minami[1], Y. Nunokawa[1], N. Takahashi[1], T. Matveeva[1], H. Shoji[1], S. Takeya[2], Y. Kamata[2], T. Ebinuma[2], H. Narita[2], V. Soloviev[3], K. Wallmann[4], N. Biebow[4], A. Obzhirov[5], A. Salomatin[5], J. Poort[6], O. Khlystov[7] and M. Grachev[7]

[1] Kitami Institute of Technology, 165 Koen-cho, Kitami 090-8507, Japan [dme03002@std.kitami-it.ac.jp]
[2] National Institute of Advanced Industrial Science and Technology, 2-17 Tukisamu Higashi Toyohira-ku, Sapporo 062-8517, Japan
[3] All-Russian Research Institute for Geology and Mineral Resources of the Ocean, 1, Angliyskiy Avenue, 190121 Saint-Petersburg, Russia
[4] GEOMAR, Research Center for Marine Geosciences, Wischhofstrasse, 1-3, D-24148, Kiel, Germany
[5] Pacific Oceanological Institute, Far East Branch of Russian Academy of Sciences, 43, Baltiyskaya Street, 690041, Vladivostok, Russia
[6] Renard Center of Marine Geology, University of Gent, Krijgslaan 281 S8, 9000 Ghent, Belgium
[7] Russian Academy of Sciences Siberian Branch Limnological Institute, 3 Ulan-Batorskaya, Irkutsk 664033, Russia

INTRODUCTION

A natural gas hydrate encaged several hydrocarbons exists in natures, such as seafloor and inside of permafrost layer, is expected as future natural gas resources.

A gas hydrate is an ice-like substance, which encaged gas molecules in the polyhedral cages consist of hydrogen-bonded water molecules. Three types of gas hydrate structures, structure I, structure II and structure H are known to exist in nature. Crystallographic structures are dependent on kind of encaged guest molecules. Structure I and structure II hydrates consist of two different size cages, and structure H consist of three different cages. The geometry of cages is shown in Table 1. In natures, gas hydrates are known to encage natural gas components of hydrocarbons or inorganic gases

Table 1. The Geometry of cages

Hydrate Structure	Cage		Number of Cages / Unit cell
I	Small	12-hedron	2
	Large	14-hedron	6
II	Small	12-hedron	16
	Large	16-hedron	8
H	Small	12-hedron	3
	Medium	12-hedron	2
	Large	20-hedron	1

(Davidson et al. 1986). In the mono-component gas, it is known that such small guest molecules as methane, ethane, carbon dioxide or hydrogen sulfide form structure I hydrate, such larger molecules as propane or iso-butane form structure II hydrates. In the case of a natural gas hydrate, it is necessary to discuss hydrate structures in multi-gas components. Recently, it was reported that CH_4 + C_2H_6 mixed gas form structure II hydrates depending on these gas components (Subramanian et al., 2000). It has revealed that hydrate structures of the multi-components differ from that of the mono-component, however details on hydrate structures are poorly understood. For natural gas hydrates, it is conceivable that the gas volume densities vary by a change of hydrate structure by the presence of multi-components. Therefore, determinations of crystallographic structure of multi-components gases are required for estimation of natural resources.

In this study, we carried out CP-MAS ^{13}C-NMR measurements to reveal relations between gas compositions and crystallographic structures of artificial multi-components hydrate samples; CH_4+C_2H_6, CH_4+C_3H_8 and CH_4+CO_2. For natural gas hydrate samples, we measured two samples obtain at the Okhotsk Sea and Lake Baikal.

EXPERIMENT

Artificial multi-components gas hydrates were prepared from ice particles (0.5–1.0 mm) and each gas component using a Milling-type high-pressure vessel (1×10^{-3} m^3). The feed gas pressures at sample preparations are shown in Table 1.

For natural gas hydrate samples of the Okhotsk Sea, the sample was obtained from the Okhotsk Sea Offing of northeast Sakhalin in KOMEX (***Kurili-Okhotsk Marine EXperiment***) Project 2002. The sampling point was at lat. 54°26.811' N, long. 144°04.870' E and 695m water depth.

Lake Baikal sample was obtained from south of Lake Baikal where the point at lat. 51°55.203' N, long. 105°38.080' E and 1393 m water depth. This sample was obtained in collaboration with New Energy Resources Research Center, Kitami Institute of Technology and Russian Academy of Sciences Siberian Branch Limnological Institute.

^{13}C-NMR measurements were done using a NMR apparatus (JEOL model JNM-AL400, 400 MHz). ^{13}C-NMR spectra were measured using the probe for solid samples at a frequency of 100 MHz. These measurements were done at 183 K or 193 K using cooling dry nitrogen gas the temperature of which was controlled by the variable temperature unit (~ 183 K) and the cooling vessel (JEOL). The measurement method is Cross-Polarization - Magic Angle Spinning (CP-MAS) method with zirconia sample tube for solid samples.

RESULTS AND DISCUSSION

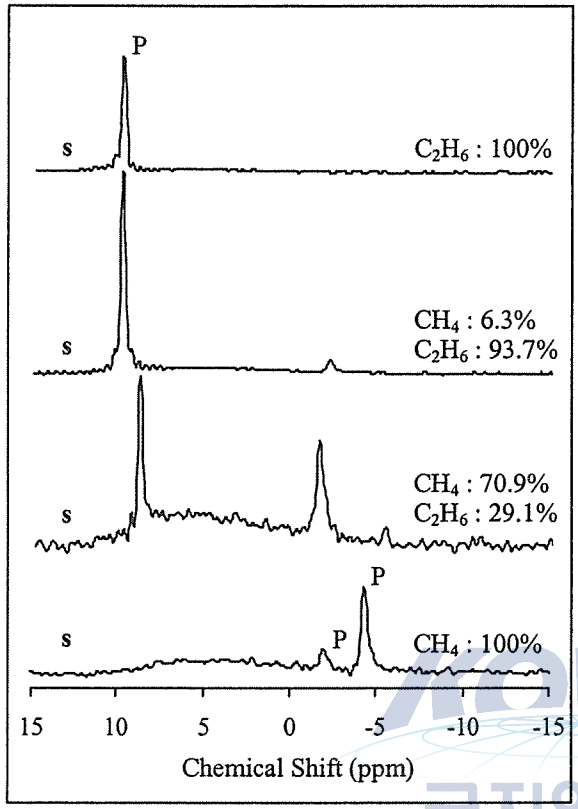

Figure 1. CP-MAS ^{13}C-NMR Spectra of CH_4+C_2H_6 Hydrates

shows a change of chemical shifts depending on the gas components. It expresses that CH_4+C_2H_6 hydrates with 20 – 40 % ethane are of structure II.

In case of CH_4+C_3H_8 and CH_4+CO_2 hydrate samples, structural change depending on the gas components were not measured. All CH_4+C_3H_8 samples were of structure II hydrates and all CH_4+CO_2 samples were of structure I hydrates.

A ^{13}C-NMR spectrum of natural gas hydrate in the Okhotsk Sea is shown in Figure 3. Only two peaks assigned methane were observed at –2.09 ppm and –4.52 ppm. From this spectrum, it has become clear that the sample in the Okhotsk Sea is of structure I hydrate which does not

Figure 1 shows ^{13}C-NMR spectra of artificial CH_4+C_2H_6 hydrates. Pure methane form structure I hydrate and shows peaks at –2.04 ppm (P1) and –4.42 ppm (P2) due to methane molecules in small cages; 12-hedron and large cages; 14-hedron respectively. Mixed gas hydrate samples with 70.9 % methane and 29.1 % ethane showed a large shift of P2 position and a large shift of P1 position were not observed.

Pure ethane hydrate is of structure I and shows only a peak at 9.81 ppm (P3) due to ethane molecules in large cages of 14-hedron. In the sample with 70.9 % methane and 29.1 % ethane, P3 position sifted to 8.36 ppm. These chemical shifts of large cage indicate a change of large cage from 14-hedral cage to 16-hedral cage, that is, a change of hydrate structure from structure I (sI) to structure II (sII). Figure 2

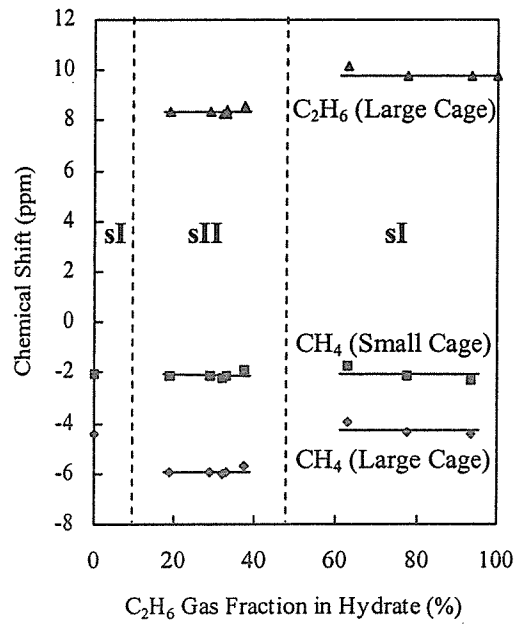

Figure 2. Changes of ^{13}C chemical shifts depending on the gas components.

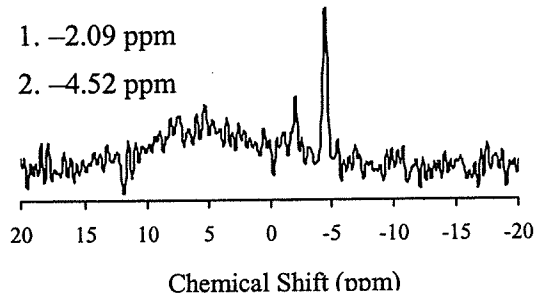

Figure 3. ^{13}C CP-MAS NMR Spectrum of Natural Gas Hydrate in the Okhotsk Sea.

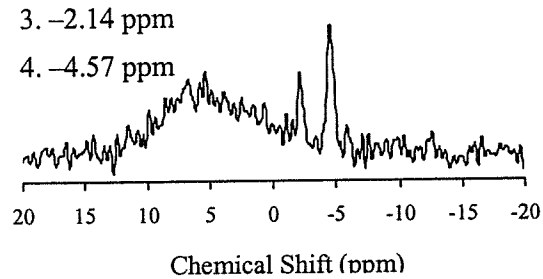

Figure 4. ^{13}C CP-MAS NMR Spectrum of Natural Gas Hydrate in Lake Baikal.

contain any hydrocarbons except methane.

For the natural sample in Lake Baikal, a ^{13}C-NMR spectrum is shown in Figure 4. Only two methane peaks were observed at –2.14 ppm and –4.57 ppm like the sample in Okhotsk Sea. This sample as well as the Okhotsk Sea sample is of structure I and the principal component is methane.

REFERENCES

D.W. Davidson, S.K.Garg, S.R.Gough, Y.P.Handa, C.I.Ratciffe, J.A. Ripmeester, J.S.Tse and W.F.Lawson: *Geochimica et Cosmochimica Acta*, **1986**, Vol.50, 619-623.

S.Subramanian, R.A.Kini, S.F.Dec, E.D.Sloan Jr.: *Chemical Engineering Science*, **2000**, 55, 1981-1999.

The 10th Seoul International Symposium on Polar Sciences
October 21-22, 2003, Incheon, Korea

SOME FEATURES OF GAS HYDRATES IN THE SEA OF OKHOTSK

T. Matveeva[1], V. Soloviev[1], K. Wallmann[2], A. Obzhirov[3], N. Biebow[4], J. Poort[5], A. Salomatin[3] and H. Shoji[6]

[1] All-Russian Research Institute for Geology and Mineral Resources of the Ocean (VNIIOkeangeologia), 1, Angliyskiy Avenue, 190121 Saint-Petersburg, Russia [tv_matveeva@mail.ru]
[2] GEOMAR, Research Center for Marine Geosciences, Wischhofstrasse, 1-3, D-24148, Kiel, Germany
[3] Pacific Oceanological Institute, Far East Brunch of Russian Academy of Sciences, 43, Baltiyskaya Street, 690041, Vladivostok, Russia
[4] Tethys Geoconsulting Gmbh, Wischhofstrasse, 1-3, D-24148, Kiel, Germany
[5] Renard Center of Marine Geology, University of Gent, Krijgslaan 281 S8, 9000 Ghent, Belgium
[6] Kitami Institute of Technology, New Energy Resources Research Center, 165 Koen-cho, Kitami 090-8507, Japan

Methane hydrate occurrences related to an active gas vents in the Sea of Okhotsk are known from offshore Paramushir Island and offshore northeast Sakhalin Island (Zonenshayn, 1987; Ginsburg et al., 1993; Soloviev et al., 1994). Location of the gas seepage sites has been detected using echo sounding and was determined by high methane concentrations in the water column (Obzhirov, 1992). The gas venting plumes at the water column were observed on echo sounder records as "flare" type anomalies. Recent studies of the gas vent area during repeated expeditions in the framework of Russian-German KOMEX Project (Kurile-Okhotsk Marine EXperiment) have revealed up to 150 additional locations with features typical for gas emission within the area (Biebow and Hutten, 1999; Biebow, 2000; Biebow, in press). Occurrence of the gas seepage sites on the continental slope northeast off Sakhalin Island within a 20 km wide zone that extends about 130 km from north to south and coring results suggested that this region is a large gas-hydrate-bearing province (Soloviev and Ginsburg, 1997).

The gas hydrate occurrence discovered by Ginsburg et al. (1993) had been cored during the 28-th cruise onboard RV Akademik Lavrentyev (Biebow and Hutten, 1999) and in the 1-th cruise of MV Marshal Gelovany (Biebow et al., 2000). The gas vent footprint of which bounds hydrate accumulation offshore NE Sakhalin was named "Obzhirov flare" during the KOMEX expeditions.

29-th cruise onboard RV Akademik Lavrentev was latest in the framework of KOMEX Project. Two areas characterizing by different geological and geochemical environments have been studied during the cruise. Gas hydrates were recovered within methane gas vent offshore NE Sakhalin and some indirect indications of gas hydrate presence were documented within

barite build-ups in the Derugin Basin. The location of anomalous barite-contained fluid discharge was established in previous KOMEX expeditions (Biebow et al., 2000). Among the aims of 29-th cruise of RV Akademik Lavrentyev performed from June to August 2002 were observation of gas hydrates, their indirect indications onboard of the vessel, and pore water geochemical and isotope studies onland. In order to conduct the gas hydrate studies, wet sediment subsamples have been collected for chemical (major elements composition) and isotope analyses (oxygen and hydrogen) of interstitial waters and water content measurements.

Gas hydrate occurrence offshore NE Sakhalin.

Sampling points on the continental slope offshore NE Sakhalin were assigned by deep-sea ELAC echo sounder with the frequency of 12 kHz. The Obzhirov flare area is characterized by multiple gas seepage manifestations clearly visible on the echosounding images. Two cores LV29-46-1 and LV29-50-1 were obtained at the Obzhirov flare at water depth of 684-695 m.

Gas hydrates were recovered in the bottom interval of 405-410 cmbsf and in the core catcher of core 50-1. According to data presented in Biebow et al. (2000), two sediment cores contained gas hydrates had been taken at the same location during Marshall Gelovany cruise. The top of gas hydrate layer was sampled in these cores at 300 cmbsf. Ginsburg et al. (1993) found the gas hydrate top at significantly shallower subbottom depth of 30-120 cm. The fact that gas hydrates through 10 years since they first discovery have been recovered on a greater subbottom depth than it was before probably suggests temporary fluctuations in the gas vent activity. Hydrates were observed as an ice like sub-horizontal thin layers with the thickness from 1 to 7 mm represents bedded structure sub-parallel to the sea floor. The observed gas hydrate-forming structure was similar to that described by Ginsburg with co-authors (1993). The hydrate amount in the hydrate-bearing interval was visually estimated as much as 1-3% from the sediment volume.

Obtained within Obzhirov flare area water chemistry data suggest the presence of an upward infiltration of fluid with enhanced dissolved species concentrations as respect to seawater and background concentrations. The pore water from the ascending fluid and the surrounding seawater differ in the chemical composition but has similar isotopic composition. According to the segregation model of gas hydrate formation proposed in Soloviev and Ginsburg (1997), diffusion is the main mechanism of gas transfer to the hydrate formation front. In that case, gas hydrates form due to upward methane diffusion while pore water moves in the opposite direction to the front of the reaction. However, obtained data testified a more complex scenario. The existence of the compositional variability in pore water with increased depth and in separate units implies that both advective and diffusional mixing is responsible for elevated concentrations of dissolved species. Most likely, this variability reflects interaction of pore water and ascending fluid along with pore water segregation in opposite direction. In such

hydrogeochemical environment, a mix of seawater and water of ascending fluid likely represent hydrate-forming fluid.

A good agreement between oxygen and hydrogen isotope composition suggests that changes in the water isotopic composition are due to isotope fractionation during hydrate formation. The driven forces for the fluid flow are probably gravitational consolidation of sediment accumulated at very high rates and tectonic compression. The fractures and faults widespread within study area may serve as upward gas and fluid migration pathways.

On the other hand, this upward fluid migration can create condition favorable for hydrate formation on the periphery of the gas vent acting as a heat-carrying agent. Horizontal temperature gradient from vent center to its periphery apparently induces gas hydrate precipitation due to decrease of solubility of dissolved gas and equilibrium pressure of hydrate formation.

Barite build-ups in the Derugin Basin

At the Derugin Basin for cores were obtained. Cores LV29-53-1 and LV29-56-1 were taken within barite build-ups area, and cores LV29-59-1 and LV29-63-1 were taken at some distance from barite "mounds" where abundant biogenic community were observed through the underwater television system.

Sediments obtained within barite mounds contained anomalous high gas amount. In core LV29-53-1, in the interval from 300 cm downcore gas expansion cracks were observed and "crackle" sound was heard as gas released. At the level of ~ 300 cmbsf, numerous barite-carbonate concretions were found. Core LV29-56-1 contained gas pockets in sediments from approximately 100 cm subbottom depth downcore. Most gaseous and fluidized sediments in this core were documented in the interval from 140 cm to 360cm subbottom depth. Water content and temperature measurements data shown a good agreement with these observations: water content becomes higher in the interval from 142 to 367 cm where decreasing of core temperature was documented. Hydrate dissociation leads to fluidization of the host sediments may explain that. Negative temperature anomaly might be result from hydrate dissociation was registered in the same interval. Pore water and isotope data obtained at this area are support onboard observations. According to hydrochemical data, anomalies in $\delta 18O$ and δD occur in the interval of most gaseous and wet sediments and are accompanied by decreasing chlorinity values that suggest possible hydrate presence in the sediments recovered within barite-rich fluid discharege area.

Summarizing the above mention features one can conclude the following:

Gas hydrates were recovered at the previously investigated hydrate occurrence situated within

NE Sakhalin slope on the greater subbottom depth, than they were recovered earlier. The obtained hydrochemical data testify the presence of upward fluid infiltration within gas hydrate accumulation associated to Obzhirov flare that together with the gas seepage creates specific conditions for hydrate formation within the area.

Sediment cores obtained within barite "mounds" revealed indirect indications of gas hydrate presence such as anomalous high amount of gas in sediments, strong H2S odor, and fluidizations of sediments. The onboard observations supported by hydrochemical data and suggest possible gas hydrate presence in this location.

This work has been supported partly by the Russian Foundation for Basic Research (grants 02-05-64346 and 02-05-06321). We also would like to acknowledge administration of Kitami Institute of Technology (Japan) for the financial support of this work.

REFERENCES

Biebow N and Hutten E (Ed.) (1999) Cruise Report KOMEX I and II: RV Professor Gagarinsky Cruise 22, RV Akademik Lavrentyev Cruise 28.GEOMAR Report 82, 188 pp

Biebow N, Ludmann T, Karp B, and Kulinich R (Ed.) (2000) Cruise Report KOMEX V and VI: RV Professor Gagarinsky Cruise 26, MV Marshal Gelovany Cruise1.GEOMAR Report 88, 296 pp

Ginsburg GD, Soloviev VA, Cranston RE, Lorenson TD, Kvenvolden KA (1993) Gas hydrates from the continental slope, offshore Sakhalin Island, Okhotsk Sea. Geo-Marine Letters 13: 41-48

Obzhirov AI (1992) Gas-geochemical manifestations of gas-hydrates in the Sea of Okhotsk. Alaska Geology 21 (7): 1-7

Soloviev VA,Ginsburg GD, Duglas VK, Cranston R, Lorenson T, Alekseev IA, Baranova NS, Ivanova GA, Kazazaev VP, Lobkov VA, Mashirov YuG, Natorkhin MI, Obzhirov AI, Titaev BF (1994) Gas hydrates of the Okhotsk Sea. Otechestvennaya Geologya 2: 10-16 (in Russian)

Soloviev VA, Ginsburg GD (1997) Water segregation in the course of gas hydrate formation and accumulation in submarine gas-seepage fields. Marine Geology 137: 59-68

Zonenshayn LP, Murdmaa IO, Baranov V, Kuznetsov AP, Kuzmin MI, Avdeiko GP, Stunzhas PA, Lukashin VN, Barash MS, Valyashko GM, and Dyomina LL (1987) An underwater gas source in the Sea of Okhotsk. Oceanology 27 (5): 598-602

The 10th Seoul International Symposium on Polar Sciences
October 21-22, 2003, Incheon, Korea

HIGH-RESOLUTION ECHO FACIES ANALYSIS OF GLACIAL-MARINE DEPOSITS IN THE BRANSFIELD BASIN , ANTARCTICA

S.H. Yoon[1], H.I. Yoon[2] and J. Howe[3]

[1] Faculty of Ocean Sciences, Cheju National University, Jeju 690-756, Korea [shyoon@cheju.ac.kr]
[2] Polar Research Center, Korea Ocean Research and Development Institute, Ansan P.O. Box 29, Seoul 425-600, Korea
[3] Dunstaffnage Marine Laboratory, P.O. Box 3, Oban, Argyll, PA34 4AD, Scotland

INTRODUCTION

The Bransfield Basin, between the South Shetland Islands and the western margin of the northern Antarctic Peninsula, is a NE-SW trending, deep asymmetric trough characterized by a steep gradient on the South Shetland Islands margin and a broad, gentle slope in the Antarctic Peninsula margin (Fig. 1). During the Last Glacial Maximum, most of the present shelf platforms were overridden by ice extending from the Antarctic continent, and the basin received large amounts of terrigenous sediments from the extensively glaciated basin margins (Banfield and Anderson, 1995; Yoon et al., 2002). This study presents the acoustic character and morphology of the late Quaternary glacial-marine deposits using high-resolution (3.5 kHz)

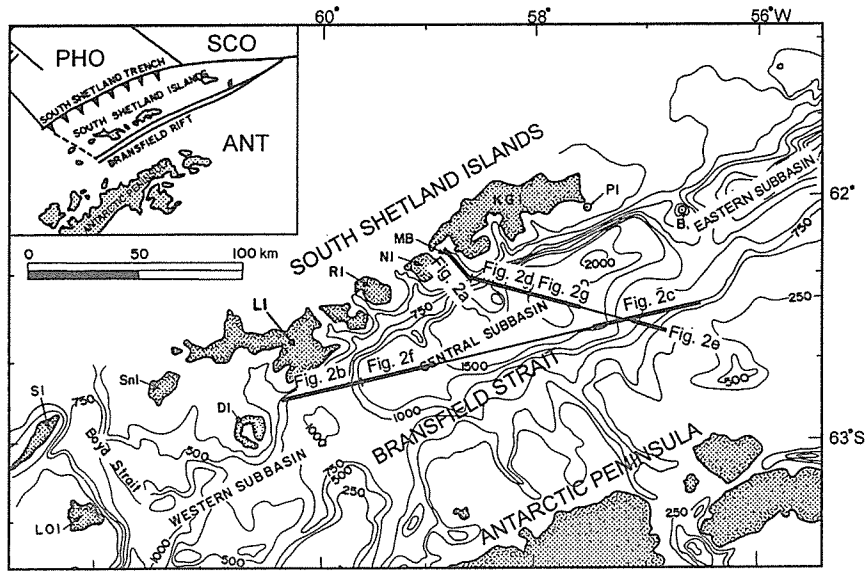

Figure 1. Bathymetric map of Bransfield Strait showing 3.5 kHz tracklines. Inset shows a regional tectonic setting.

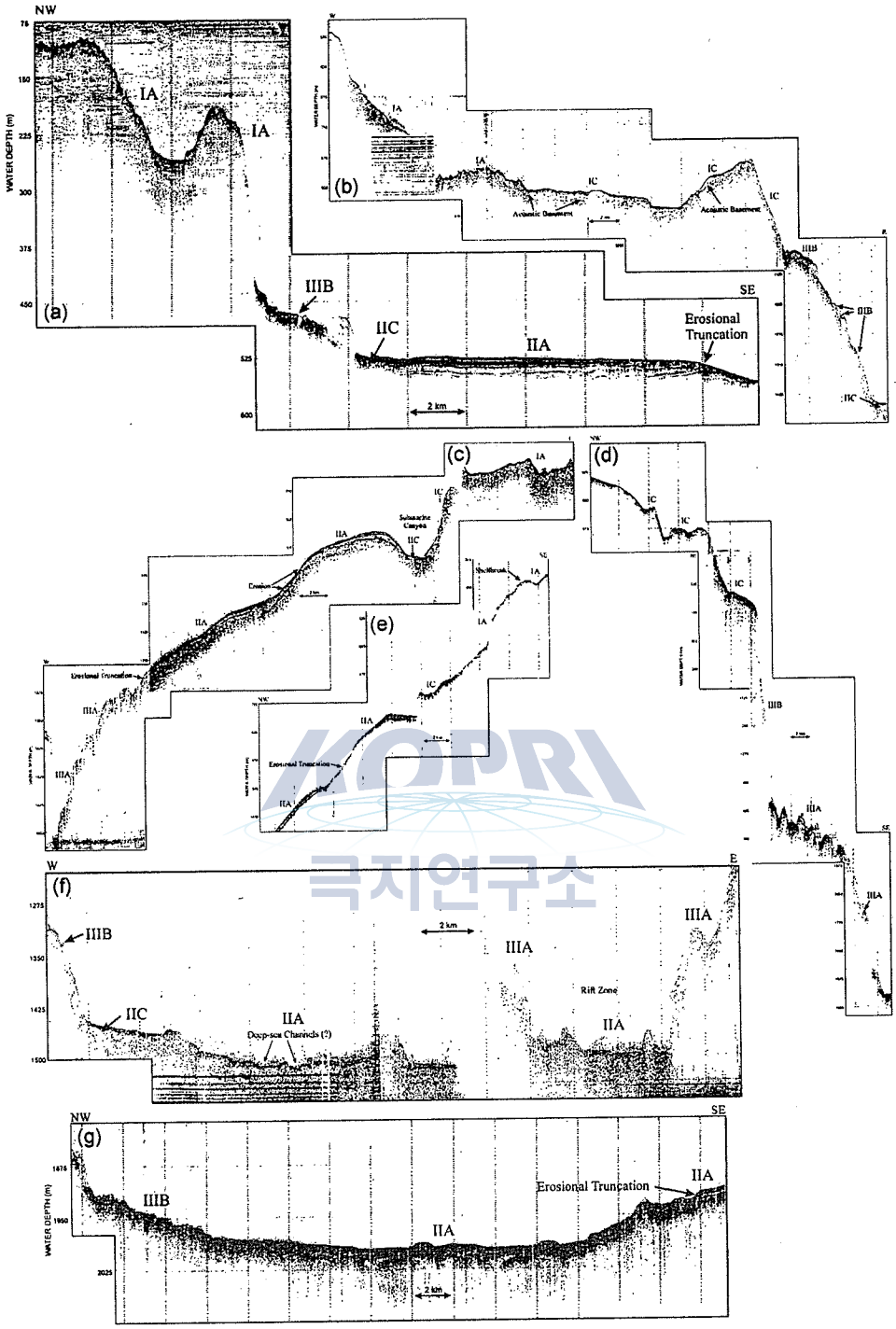

Figure 2. High-resolution seismic profiles from Bransfield Strait. Capital codes represent type of echo facies. For locations see figure 1.

seismic profiles (Fig. 1) and depicts the sedimentation pattern during the Last Glacial Maximum and subsequent deglaciation period.

ECHO FACIES

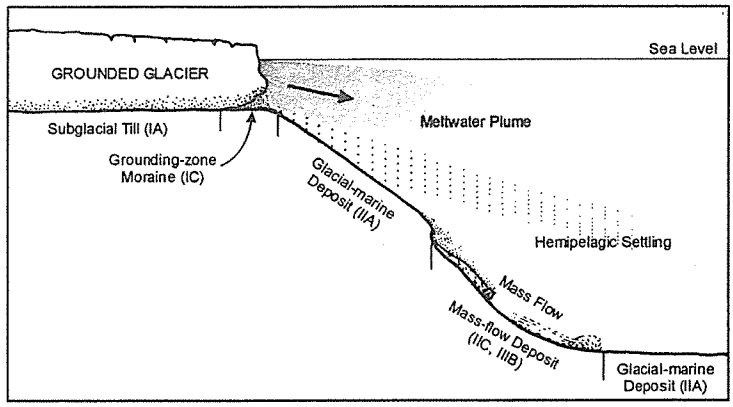

Figure 3. Schematic diagram of sedimentation pattern and associated echo facies distribution during the last glacial maximum.

The high-resolution echo characters were classified into 6 echo facies on the basis of clarity, continuity, and shape of bottom and subbottom echoes together with seafloor topography. In the shelf and the upper continental slope, **echo facies IA** is characterized by relatively distinct, sharp bottom echoes without subbottom reflectors, showing hummocky seafloor topography less than a few meters high (Fig. 2a, b, c, e). Based on extremely unsorted core samples and hummocky topography, the origin of echo facies IA is interpreted as coarse-grained tills deposited directly from glaciers coming from the South Shetland Islands and Antarctic Peninsula (Holtedahl and Sellevoll, 1972; Yoon et al., 2000). **Echo facies IC** is mainly recorded from the upper slope, where it is characterized by mounded or ridged, sharp continuous bottom echoes and acoustically transparent internal reflection (Fig. 2b, c, d). This echo is interpreted to represent grounding-zone moraines (Damuth, 1978). The deep basin floor of Bransfield Strait and the middle to lower slope of Antarctic Peninsula are dominated by **echo facies IIA** which shows semi-prolonged bottom and several parallel subbottom echoes (Fig. 2). This echo suggests a combined effect of hemipelagic settling and turbidity currents or meltwater turbid plumes (Yoon et al., 1991). **Echo facies IIC** recorded from restricted areas of the base of slope is associated with lens-shaped sediment masses without internal reflectors (Fig. 2f). The transparent acoustic character is generally accepted characteristics of debris flow deposits (Embley, 1976; Chough et al., 1985). In the western margin of Central Subbasin, **echo facies IIIA** is characterized by very prolonged bottom echoes and irregular, overlapping hyperbolae with significantly varying vertex elevations (tens to hundreds of meters). This echo indicates hard rock basement or irregular volcanic edifices (Damuth, 1980). **Echo facies IIIB**, mainly recorded from the base of slope areas of Maxwell Bay and Central Subbasin, is characterized by regular, overlapping hyperbolae with slightly varying vertex elevations (< 30 m) and slightly prolonged subbottom reflection. This echo is interpreted to indicate deposits of slump/slide and debris flow (Embley, 1976; Yoon et al., 1991).

SEDIMENTATION PATTERN

The contour-parallel zonal distribution of echo facies suggests that the Bransfield Basin received large amounts of sediments from the grounded glaciers extended to the upper slope during the last glacial maximum (Fig. 3). Unsorted basal debris was accumulated as subglacial tills beneath the grounded glaciers (IA) and grounding-zone moraines in front of the grounding line (IC); suspended fine sediments released from the glacial margin were further transported basinward by meltwater plumes and accumulated as distal glacial-marine deposits together with hemipelagic sediments (IIA). On the steep mid-to-lower slope, glacial deposits were reworked and transported downslope by mass flows including slide, slump and debris flow (IIC, IIIB). In some places of the lower continental slope, irregular volcanic edifices and faulted basement are exposed recording echo facies IIIA.

REFERENCES

Banfield, L.A. and Anderson, J.B., 1995, Seismic facies investigation of the late Quaternary glacial history of Bransfield Basin, Antarctica. Antarctic Research Series, 68, 123-140.

Chough, S.K., Mosher, D.C. and Srivastava, S.P., 1985, Ocean Drilling Program (ODP) site survey (Hudson 84-30) in the Labrador Sea: 3.5 kHz profiles. Geological Survey of Canada, Paper, 85-1B, 33-41.

Damuth, J.E., 1978, Echo character of the Norwegian-Greenland Sea: relationship to Quaternary sedimentation. Marine Geology, 28, 1-36.

Damuth, J.E., 1980, Use of high-frequency (3.5-12 kHz) echograms in the study of near-bottom sedimentation processes in the deep-sea: a review. Marine Geology, 38, 51-75.

Embley, R.W., 1976, New evidence for occurrence of debris flow deposits in the deep sea. Geology, 4, 371-374.

Holtedahl, H. and Sellevoll, M., 1972, Notes on the influence of glaciation on the Norwegian continental shelf bordering on the Norwegian Sea. Ambio Special Report, 2, 31-38.

Yoon, H.I., Park, B.K., Kim, Y. and Kim, D., 2000, Glaciomarine sedimentation and its paleoceanographic implications along the fjord margins in the South Shetland Islands, Antarctica during the last 6000 years. Palaeogeography, palaeoclimatology, Palaeoecology, 157, 189-211.

Yoon, H.I., Park, B-K, Kim, Y. and Kang, C.Y., 2002, Glaciomarine sedimentation and its paleoclimatic implications on the Antarctic Peninsula shelf over the last 15000 years. Palaeogeography, Palaeoclimatology, Palaeoecology, 185, 235-254.

Yoon, S.H., Chough, S.K., Thiede, J. and Werner, F., 1991, Late Pleistocene sedimentation on the Norwegian continental slope between 67° N and 71° N. Marine Geology, 99, 187-207.

The 10th Seoul International Symposium on Polar Sciences
October 21-22, 2003, Incheon, Korea

CHARACTERISTICS OF BEACH SANDS, KING GEORGE ISLAND, WEST ANTARCTICA

Tae Jin Choi[1], Yong Il Lee[1] and Ho Il Yoon[2]

[1] School of Earth and Environmental Science, Seoul National University, Seoul 151-747 Korea [taejin99@snu.ac.kr]
[2] Korea Polar Research Institute, Korea Ocean Research and Development Institute Ansan, P.O.Box 29, 425-600, Korea

INTRODUCTION

King George Island, South Shetland Islands, is a volcanic island associated with subduction of the oceanic plate during the late Mesozoic to early Cenozoic (Smellie et al., 1984). The Barton peninsula is located at 62°12'S-62°42'S and 58°42'W-58°49'W in the southwestern part of the island, composed of lower volcaniclastic rocks (Sejong Formation), upper mafic-intermediate volcanic rocks and plutonic rocks (Lee et al., 2002).

Rocky coasts with gravel beaches exist around the peninsula, but a few sandy beaches also exist. Because the rounded gravels of these beaches are supposed to be the one piece of evidence for the uplift of the Barton Peninsula after the last deglaciation, (Koh et al., 1993) previously the beach gravels have been studied, but no study has been done yet on beach sands. This study intends to describe the depositional environment, geochemistry and depositional mechanism of beach sands of the Barton Peninsula.

GENERAL GEOLOGY

The lowermost lithostratigraphic unit in the Barton peninsula is the Sejong Formation (Fig. 1, Yoo et al., 2001), which is distributed in the southern-southeastern part of the peninsula. The formation is mainly composed of volcaniclastic sediments have a gentle slope to south-southwest, Late Paleocene to Eocene in age (Chun et al. 1994). Mafic to intermediate volcanic lavas are overlying the Sejong Formation and distributed in wide area of the Barton Peninsula. Several units of thick-bedded lapilli tuffs are intercalated within lava flows. A granodioritic stock of Eocene age with minor fine-grained diorite occurs in the northern Barton Peninsula (Kim et al., 2000). Rocks of the Barton Peninsula were experienced hydrothermal alterations (Hur et al., 2001). Although it is difficult to divide the alteration zones, generally rocks in the

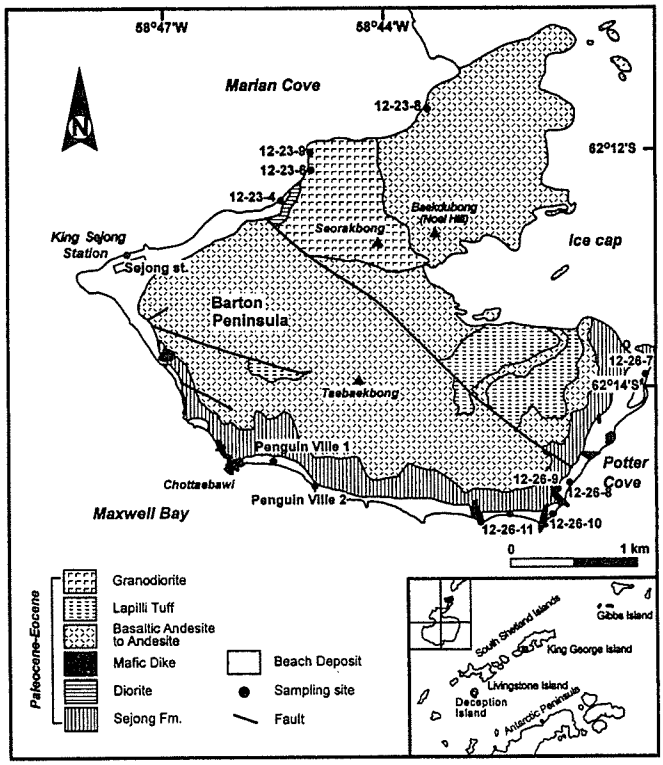

Figure 1. The geological map of the Barton Peninsula, and sampling locations.

north of the granodiorite stock are more altered than those in the south.

METHODS

A total of 12 beach sands (5 from NW coast and 7 from SE coast) were collected along the pocket beaches of the Barton peninsula (Fig. 1). The samples were dry-sieved and grain-size parameters were determined according to Folk and Ward (1957). Samples were also impregnated and thin-sectioned for modal analysis (300 points per slide). Chemical compositions of the samples are analyzed by a XRF at the Korea Basic Science Institute.

RESULTS

Most of beach sands are well sorted and relatively coarse grained. The mean grain size ranges 0 ~ 1Φ. The cumulative curves have three inflection points and four linear segments, each point being located at -1Φ, 0Φ and 1Φ.

Sands are composed of mostly volcanic fragments, with the rest being plutonic and sedimentary rock fragments and heavy minerals. Plutonic rock fragments occur mostly in the NW coast (10 ~ 30%), whereas very minor amount (<5% by volume) is also observed in sands of the SE coast. A significant amount of altered grain (alterite) is found in all samples: SE coast (average 38.9%) has more alterites than NW coast (average 28.3%). Altered grains have feldspars containing sericite and/or silicified quartz. Parts of some plagioclase crystal, laths of volcanic rock fragment and its matrix were replaced by K-feldspar. Grains have low sphericity and are poorly rounded.

SiO_2 content of beach sands of SE coast (55 ~ 65 wt.%) has wider range than those of NW coast. Major elements except for K_2O and Na_2O show negative correlation with SiO_2. Except for MgO, CaO and Na_2O contents, major element contents are quite different in beach sands between two coasts. Sands in the SE coast contain lesser amount of Al_2O_3 and K_2O, but higher amount of Fe_2O_3, MnO, P_2O_5 and TiO_2 than those in the NW coast.

DISCUSSION

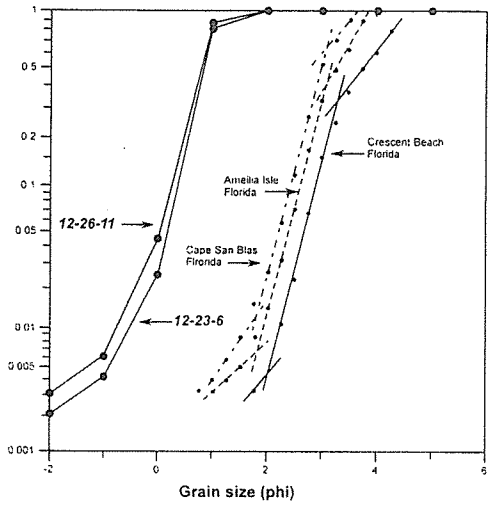

Figure 2. Cumulative curves of grain size distributions, comparing beach sands of the Barton Peninsula, West Antarctica with those of Florida (Visher, 1969), North America. 12-26-11 represents SE coast, and 12-23-6 NW coast.

When comparing the beach sand samples of the Barton Peninsula with those of lower latitudes (e.g., Visher, 1969), the Barton Peninsular beach sands are characterized by coarser grain size. This suggests transport of sands by more powerful energy than usual beach environments in the lower latitudes (Fig. 2). Three inflection points in the cumulative curves indicate that the Barton Peninsula beach sands are currently being deposited by waves, and that they are not the reworked lag deposits derived from nearby rocky coasts.

The alterite in the beach sand is interpreted as hydrothermally altered parent rocks mostly of volcanic rock fragments. The presence of abundant plutonic rock fragment in the NW coast was derived from the nearby granodiorite. A small amount of plutonic rock fragment as well as very minor, quartz grain, and plagioclase grain is found in SE coast sand samples. However, there is no crystalline parent rock closer to the SE coast (Fig. 1). They must have come through the sea because a strong candidate, the granodiorite in the NW Barton Peninsula, could not supply sediments directly due to the presence of topographic barrier. Two transport mechanism can be invoked; long-shore current or ice rafting. The long-shore current, however, is not a good carrier since it can transport relatively smaller particles and it is hard to pass protruding parts between the NW coast and the SE coast with sediments, considering possible flow direction. The second and more probable transport medium is the iceberg, which can carry larger grains from Marian Cove and pass the protruding parts. Thus, crystalline rock fragments in the SE coast might have been transported by the iceberg.

CIA, A-CN-K (Al_2O_3-(CaO^*+Na_2O)- K_2O) diagram and A-CNK-FM (Al_2O_3-(CaO^*+Na_2O+K_2O)-(Fe_2O_3+MgO) diagram of the Barton Peninsula are presented in Fig. 3, their parent rock data marked with them. CIA (Chemical Index of Alteration; Nesbitt and Young, 1989.) of the Barton Peninsula beach sands ranges from 48.1 to 63.7 with an average of 52.0. These values are lower than the average CIA value of the Barton Peninsula soil (53.3~68.6, average 59.6) and rock fragments separated from soil (51.3 ~ 64.2, average 57.9) (Lee, 2003).

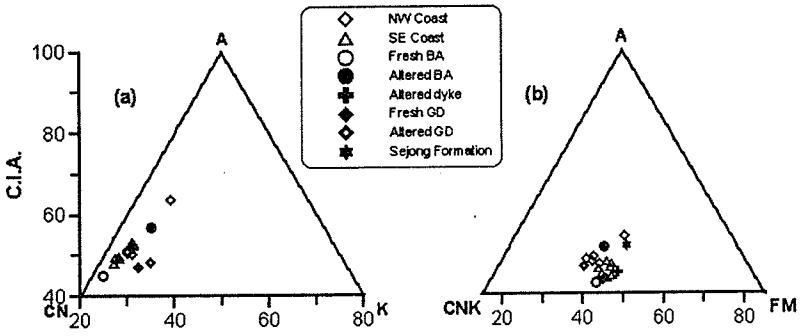

Figure 3. (a)A-CN-K diagram and (b) A-CNK-FM diagram of the Barton Peninsula beach sands and their parent rocks. Basaltic andesite and granodiorite are subdivided into fresh or altered ones.

This indicates direct delivery from parent rocks into the coasts without chemical weathering. Although hydraulic sorting may cause lower CIA values in coarse-grained sediments, CIA values between fresh and hydrothermally altered rocks indicate insignificant chemical weathering.

CONCLUSION

Beach sand characteristics of the Barton Peninsula were studied in terms of textural and chemical compositions. In the Barton Peninsula, beach sediments are composed of well-sorted coarse sands and were supplied from adjacent parent rocks directly without undergone chemical weathering. This textural feature is consistent with chemical composition. The beach sands represent the product of current wave regime in the Barton Peninsula. The presence of a small amount of plutonic rock fragments originated from the granodiorite in northwestern part of the peninsula indicates that some sand grains in the SE beach sands were transported probably by iceberg.

ACKNOWLEDGEMENT: This study was supported by the Project for Paleoclimate and Paleoceanography of Antarctica (PP03106) from the Korea Ocean Research and Development Institute.

REFERENCES

Chun, H.Y., Chang, S.K. and Lee, J.I., 1994, Biostratigraphic study on the plant fossils from the Barton peninsula and adjacent area, Journal of the Paleontological Society of Korea, 10, 69-84.

Folk, R.L. and Ward, W.C., 1957, Brazos river bar: A study in the significance of grain size parameters. Journal of Sedimentary Petrology, 27, 3-27.

Hur, S.D., Lee, J.I., Hwang, J. and Choe, M.Y., 2001, K-Ar age and geochemistry of hydrothermal alteration in the Barton Peninsula, King George Island, Antarctica. Ocean and Polar Research, 23, 11-21.

Kim, H., Lee, J.I., Choe, M.Y., Cho, M., Zheng, X., Sang, H. and Qin, J., 2000, Geochronologic evidence

for Early Cretaceous volcanic activity on Barton Peninsula, King George Island, Antarctica. Polar Research, 19, 251-260.

Koh, Y.-Y., Park, Y.-A., and Choe, M.Y., 1993, Analysis of beach gravels in Barton and Weaver Peninsulas, King George Island, Antarctica. Ocean and Polar Research, 4, 39-52.

Lee, J.I., Hur, S.D., Yoo, C.M., Yeo, J.P., Kim, H., Hwang, J., Choe, M.Y., Nam, S.H., Kim, Y., Park, B.K., Zheng, X. and Lopez-Martinez, J., 2002, Explanatory text of the geological map of Barton and Weaver peninsulas, King George Island, Antarctica(1:10,000). Polar Sciences Laboratory, KORDI, Ansan, 30p.

Lee, Y.I., 2003, The provenance of dusts and their influence on Holocene continental shelf sediments in West Antarctica. Paleoceanography and Paleoclimate Study in the Antarctic for the Preparation of Global Climate Change Agreement in the 21st Century, 385-394.

Nesbitt, H.W. and Young, G.M., 1989, Formation and diagenesis of weathering profiles. The Journal of Geology, 97, 129-147.

Smellie, J.L., Pankhurst, R.J., Thomson, M.R.A. and Davies, R.E.S., 1984, The geology of the South Shetland islands:VI. Stratigraphy, Geochemistry and Evolution. British Antarctic Survey Scientific Reports 87, 85p.

Visher, G.S., 1969, Grain size distributions and depositional processes. Journal of Sedimentary Petrology, 39, 1074-1106.

Yoo, C.M., Choe, M.Y., Jo, H.R., Kim, Y.D., Kim, K.H., 2001, Volcaniclastic sedimentation of the Sejong Formation(Late Paleocene-Eocene), Barton Peninsula, King George Island, Antarctica. Ocean and Polar Research, 23, 97-107.

The 10th Seoul International Symposium on Polar Sciences
October 21-22, 2003, Incheon, Korea

TRANSITION FROM DEBRIS FLOW TO HYPERCONCENTRATED FLOW IN A SUBMARINE CHANNEL (THE CRETACEOUS CERRO TORO FORMATION, SOUTHERN CHILE)

Y.K. Sohn[1], M.Y. Choe[2] and H.R. Jo[2]

[1] Department of Earth and Environmental Sciences, Gyeongsang National University, Chinju 660-701, Korea [yksohn@nongae.gsnu.ac.kr]
[2] Polar Sciences Laboratory, Korea Ocean Research and Development Institute, PO Box 29, Ansan 425-600, Korea

It is important to understand the exact process whereby very large amounts of sediment are transported. This paper reports peculiar conglomerate beds reflecting the transition of submarine debris flows into hyperconcentrated flows, something that has been well documented only in subaerial debris-flow events until now. Voluminous debris flows generated along a Cretaceous submarine channel, southern Chile, transformed immediately into multiphase flows. Their deposits overlie fluted or grooved surfaces and comprise a lower division of clast-supported and imbricated pebble-cobble conglomerate with basal inverse grading and an upper division of clast- to matrix-supported, disorganized conglomerate with abundant intraformational clasts. The conglomerate beds suggest temporal succession of turbidity current, gravelly hyperconcentrated flow, and mud-rich debris flow phases. The multiphase flows resulted from progressive dilution of gravelly but cohesive debris flows that could hydroplane, in contrast to the flow transitions in subaerial environments, which involve mostly noncohesive debris flows. This finding has significant implications for the definition, classification, and hazard assessment of submarine mass-movement processes and characterization of submarine reservoir rocks.

The 10th Seoul International Symposium on Polar Sciences
October 21-22, 2003, Incheon, Korea

CHEMICAL WEATHERING OF GLACIAL DEBRIS AND VOLCANIC ASH IN KING GEORGE ISLAND, ANTARCTICA

Gi Young Jeong and Bong Ho Lee

Department of Earth and Environmental Sciences, Andong National University,
Andong 760-749, Korea [jearth@andong.ac.kr]

King George island, Antarctica, is mostly covered by ice sheet and glaciers, but the land area is locally exposed for several thousand years after deglaciation. For a mineralogical study of chemical weathering in the polar environment, glacial debris was sampled at the well-developed patterned ground which was formed by long periglacial process. As fresh equivalents, recently exposed tills were sampled at the base of ice cliff of outlet glaciers and at the melting margin of ice cap together with fresh bedrock samples.

Fresh tills are mostly composed of quartz, plagioclase, chlorite, and illite, but those derived from hydrothermal alteration zone contain smectite and illite-smectite. In bedrocks, chlorite was the major clay minerals in most samples with minor illite near hydrothermal alteration zone and interstratified chlorite-smectite in some samples. Smectite closely associated with eolian volcanic glass was assigned to alteration in their source region. Blocks with rough surface due to chemical disintegration showed weathering rinds of several millimeter thick. Comparision between inner fresh and outer altered zones did not show notable change in clay mineralogy except dissolution of calcite and some plagioclase. Most significant weathering was observed in the biotite flakes, eolian volcanic glass, sulfides, and carbonates in the debris. Biotite flakes derived from granodiorite were altered to hydrobiotite and vermiculite of yellow brown color. Minor epitactic kaolinite and gibbsite were formed in the cleaved flakes of weathered biotite. Pyrite was replaced by iron oxides. Calcite was congruently dissolved. Volcanic glass of basaltic andesite composition showed alteration rim of several micrometer thick or completely dissolved leaving mesh of plagioclase laths. In the alteration rim, Si, Na, Mg, and Ca were depleted, whereas Al, Ti, and Fe were relatively enriched. Mineralization of lichen and moss debris is of much interest. They are rich of Al and Si roughly in the ratio of 2:1 to 3:1 typical of allophane. In some case, Fe and Ti are enriched in addition to Al and Si. Transmission electron microscopy of the samples rich of volcanic glass showed abundant amorphous aluminosilicates, which are interpreted as allophane.

Chemical weathering in the King George Island is dominated by the leaching of primary phyllosilicates, eolian volcanic glass, and minor sulfides. Authigenesis of clay minerals is less active. Allophane in the debris implicates Si-poor solution environment resulting from the significant leaching of Si and alkalis. Smectite formation is likely impossible under conditions of allophane formation. Since we did not have still a positive evidence of significant formation of supergene smectite, its contribution to the clay mineralogy of marine sediments are doutful even near the maritime Antarctica undergoing a more rapid and intenser chemical weathering under more humid and milder climate than other regions of Antarctica.

The 10th Seoul International Symposium on Polar Sciences
October 21-22, 2003, Incheon, Korea

THE CENOZOIC SEDIMENTARY RECORDS FOUND IN THE GROVE MOUNTAINS, EAST ANTARCTICA AND THEIR CLIMATIC IMPLICATIONS

Aimin Fang[1], Xiaohan Liu[1], Xiaoli Li[1], Jong Ik Lee[2], Yitai Ju[1] and Feixin Huang [1]

[1] Laboratory of lithosphere Tectonic Evolution, Institute of Geology and Geophysics, Chinese Academy of Science, Beijing 100029, China [xhliu@public3.bta.net.cn]

[2] Polar Science Laboratory, Korea Ocean Research and development Institute, Ansan P.O. Box 29, Seoul 425-600, Korea

The Grove Mountains, located about 450km inland from the coast line of Prydz Bay, consists of 64 nunataks exposed as 5 island chains extending from NNE to SSW in the East Antarctic Ice Sheet (EAIS) within an area of about 3200km^2. From 1998, the Chinese National Antarctic Research Expedition (CHINARE) has surveyed this area several times, and three kinds of Cenozoic sedimentary records have been found during our field works, so far.

The first one is the debris of sedimentary rocks found in the moraine banks on the surface of blue ice near one of the nunataks- Mont Harding in the center area of Grove Mountains, which can be subdivided into two kinds: one is well to half cemented hard rocks, the other is loosely aggregated deposits. All of them are of the characteristics of glaciogenic diamicton sediments.

Characteristics of the textures and structures of the sedimentary rocks, the grain size distributions, quartz grains and their surface textures and features, together with the geo-chemical data all demonstrated that these sedimentary rocks are a kind of subglacial lodgement tills formed in the ice-sheet frontal area by the reactions of glacial movements together melt water. By comparison, the glacigenic sediments are correspondent with such Pliocene Strata as the Sirius Group in Trans-Antarctica Mountains, the Sørsdal Formation in the neighboring area of the Northern Prince Charles Mountains, and the Pangodromal Formation in Riiser-Larsen Hills and Vestfold Hills. Furthermore, these sedimentary rocks contain some Late Tertiary pollen assemblages. Thus, we considered these sedimentary rocks were formed in the Pliocene.

The second one is the soils found in several small depressions in the southern slope of Harding Mts. According to the characteristics of its colors, weathering degree of the surface rocks, vertical and horizontal differentiation of the salts in the soils and soil depth, the soils are formed during 0.5 Ma to 3.5 Ma, which also present a warm climatic event in this area.

The third is the subglacial tillites found in the bottom of ice-sheet, which are loosely aggregated sediments, and mainly composed of fine clay particles formed by the shear

movements of the glacier. The age dating by thermoluminescence shows that the subglacial tillites in this area are formed during the Last Glacial Maximum.

Each of these sedimentary recorders may reflect different glacial evolutionary events of the east Antarctic ice-sheet.

The sedimentary rock clasts found in Grove Mts. and its pollen assemblage contain some climatic and environmental information about its upstream or up-glacier source rock area. So far we can draw such basic conclusions as follows from these sedimentary clasts found in Grove Mts.

(1) the sedimentary clasts and erratics found in Grove Mountains is a kind of glacigenic sediments whose depositional environment should be ice-sheet frontal areas, and their sedimentary environment should be located in local or upstream areas (the interior region from Grove Mts.), i.e. the east Antarctic ice-sheet frontal should have ever retreated at least to Grove Mts. area, which certainly represent a warm event;

(2) the pollen assemblage in these glacigenic sedimentary rock clasts is not in-situ, which reflects that some former sedimentary basins must have existed in Grove Mts. region or its upstream area (the interior part of east Antarctica), and the spore and pollen contained in the mixed assemblage also provide some climatic and environmental information of these former sedimentary basins which may also represent another warm event (earlier than the one present by these sedimentary rocks themselves);

(3) after the deposit of this glacigenic sedimentary rocks, there are at least one cold glacial event happened, which leads to a large scale of ice-sheet developed in this area, eroding the glacigenic sedimentary strata and transporting some of its clasts to Grove Mts. region as they are recovered today. We also find some evidence in the field survey that the maximum elevation of the ice-sheet surface in Grove Mts. should be more than 50 meters higher than the present one. So the ice-sheet fluctuation in east Antarctica should be more extensive and continuous than it used to be thought.

In general, the glacigenic sedimentary rock clasts found in Grove Mts. involves at least three ice-sheet evolutionary events in east Antarctica. It also contains a lot of environmental and climatic information of three positions: the former interior sedimentary basins in which the spore and pollen deposit; the ice-sheet frontal area in which the glacigenic sedimentary rocks deposit; and the current Grove Mts. region in which these clasts finally are recovered. If we can make out the relationships between these events and positions, we will have a clear understanding upon the ice-sheet evolutionary history in east Antarctica.

Thus, they provide a kind of new evidence for the glacial retreat event in Grove Mountains, east Antarctica.

Key words: the Grove Mountains, east Antarctica, Cenozoic sedimentary recorders, glacial history.

The 10th Seoul International Symposium on Polar Sciences
October 21-22, 2003, Incheon, Korea

THE POLLEN ASSEMBLAGES FOUND IN THE CENOZOIC SEDIMENTARY ROCKS IN GROVE MOUNTAINS, EAST ANTARCTICA

Aimin Fang[1], Xiaohan Liu[1], Xiaoli Li[1], Yitai Ju[1] and Weimin Wang[2]

[1] Laboratory of lithosphere Tectonic Evolution, Institute of Geology and Geophysics, Chinese Academy of Science, Beijing 100029, China [xhliu@public3.bta.net.cn]
[2] Institute of Geology and Paleontology, Chinese Academy of Science, Nanjing 210008, China

During the field works of the 1998-1999's and 1999-2000's Chinese National Antarctic Research Expedition (CHINARE), glacigenic sedimentary rocks have been found in moraine banks of Grove Mountains, east Antarctica, which is about 450km inland from the Prydz Bay coast line. Most of these sedimentary rocks are a kind of lodgment tillites which was formed in glacial frontal environments. From their textural and consolidation characteristics, they can be correlated well with the Cenozoic sedimentary strata of the Pagodroma Group found in the Charles Mountain area and the Sorsdal Formation in Vest Fold Hills.

Four samples were chosen to study their micro-fossil assemblages. Although no diatom were found in all of these sedimentary rocks, these sedimentary clasts contain sparsely Late Tertiary pollen assemblages (table 1). By analysis, in all the 4 samples, 60 particles of pollen of different species were totally found, including: *Toroisporis* Lygodiaceae, *Osmundacidites Osmunda, Granulatisporites* Pteridaceae?, Polypodiaceae, *Podocarpidites Podocarpus*, Araucariaceae, *Rhoipites Rhus*, *Nothofagidites Nothofagus*, *Proteacidites* Proteaceae, *Quercoidites Quercus*, *Fraxinoipollenites* Oleaceae, *Operculumpollis*, *Tricolpopollenites, Atemisiaepollenites Atemisia,* Chenopodiaceae, *Oleoidearumpollenites* Oleaceae, and so on. Among which, *Podocarpidites Podocarpus* is the most abundant, while *Nothofagidites Nothofagus* is the most common. Although the small quantity of the pollen particles found in the sedimentary rocks are not enough to reconstruct their original flora, the existing of *Nothofagidites Nothofagus* in all the samples provides some useful evidence to infer their age and paleoclimate. As identified from the Pliocene sedimentary rocks of the Sirius Group found in the Transantarctic Mountains, *Nothofagus* was considered to exist in some extreme conditions during the Pliocene in Antarctic area, with a minimum temperature of 5 degree and supplies of liquid water in the summer. Thus, they provide a kind of new evidence for the glacial retreat and climate warm event in Grove Mountains, east Antarctica.

The preservation features of most of the spore and pollen shows they have experienced

deformations to some extend, indicating that they are not in situ buried assemblages, and may have been transported by the East Antarctic Ice-Sheet (EAIS) before they finally deposited in these glacigenic sedimentary rocks. However, the pollen and spore assemblages may also represent a local flora during the Pliocene time in the Grove Mountains region or in the nearby upstream inland of the east Antarctica.

The absence of diatoms may indicate that there are no marine strata, but only terrestrial deposits in the interior of east Antarctica beyond the Grove Mountains during the Pliocene warmth, which can fit well with the distribution of the sedimentary facies of the Pliocene strata exposed along the section from the Prydz Bay to the inland basins.

Table 1. Results of the pollen analysis of the 4 sedimentary rocks in Grove Mts.

Samples	S1501		S1507		S1509		S1514		Totall	
	Nu	%	Nur	%	Nu	%	Nu	%	Nur	%
Total spore-pollen	33	100	6	100	17	10	4	100	60	100
Lygodiaceae *Toroisporis*	4	12.1			1	5.8			5	8.3
Osmunda Osmundacidites	5	15.1	1	16.6	4	23			*10*	16.
Pteridaceae? *Granulatisporites*	1	3.03			1	5.8			2	3.3
Polypodiaceae	1	3.03							1	1.7
Podocarpus Podocarpidites	9	27.2			3	17	1	25	*13*	21.
Araucariaceae	3	9.09	1	16.6	2				6	10.
Rhus Rhoipites	2	6.06							*2*	3.3
Nothofagus Nothofagidites	2	6.06	1	16.6	1	5.8	1	25	5	8.3
Proteaceae *Proteacidites*	1	3.03							1	1.7
Quercus Quercoidites	1	3.03	1	16.6					2	3.3
Oleaceae *Fraxinoipollenites*	2	6.06							2	3.3
Operculumpollis	1	3.03							1	1.7
Tricolpopollenites	1	3.03							1	1.7
Atemisia Atemisiaepollenites			2	33.3	2	11			4	6.7
Chenopodiaceae					2	11	2	50	4	6.7
Oleaceae *Oleoidearumpollenites*					1	5.8			1	1.7

Nothofagus fossils in the Sirius Group, Transantarctic Mountains: Leaves and pollen and their climatic implications

Robert S. Hill & E. M. Truswell (1993)

Korea Polar Research Institute,
KORDI
Ansan P.O.Box 29, Seoul 425-600,
KOREA
Tel. : +82-31-400-6400
Homepage : www.polar.re.kr